

VOLUME 26

OCTOBER, 1938

NUMBER 10

PROCEEDINGS  
*of*  
The Institute of Radio  
Engineers



Application Blank for Associate Membership on Page XIII

---

# Institute of Radio Engineers Forthcoming Meetings

---

## ROCHESTER FALL MEETING

Rochester, N. Y.

November 14, 15, and 16, 1938

---

## CLEVELAND SECTION

October 27, 1938

---

## DETROIT SECTION

October 21, 1938

---

## LOS ANGELES SECTION

October 18, 1938

---

## NEW YORK MEETING

November 2, 1938

---

## PHILADELPHIA SECTION

October 6, 1938

November 3, 1938

---

## PITTSBURGH SECTION

October 18, 1938

---

## WASHINGTON SECTION

October 10, 1938

---





ERNEST T. FISK  
Vice President of the Institute, 1938

Ernest T. Fisk was born on August 8, 1886, at Sunbury-on-Thames, England. He was educated privately and at United Kingdom College in London.

He entered the Marconi Company School in 1906 and during the next few years was active in the erection and operation of several stations in the Arctic and North America. In 1913 he assisted in the formation of Amalgamated Wireless (Australasia), Ltd., becoming general manager. He became managing director in 1917 and chairman of the board in 1932. During the war he continued his work in Australia at the request of the Australian Naval Board.

In 1918 he received the first direct signals from Carnarvon, Wales, and as a result of this and his later efforts direct commercial communication with Great Britain was established. In 1924, his experiments with beam radio circuits to Poldhu, in association with Marconi, demonstrated their effectiveness and led to commercial radiotelegraph and radiotelephone service to England in 1927 and to Canada in 1928.

The first demonstration of broadcasting in Australia was given by him in 1920 and regular service was inaugurated the next year. In 1920 he installed the first large-scale public-address system in the Parliament House at Melbourne.

Sir Ernest was made a Knight Bachelor at the coronation of King George VI in 1937, received the Cross of the Crown of Italy in 1933, and the Jubilee and Coronation medals in 1935 and 1937. He is active in numerous organizations and served as president of the Institution of Radio Engineers, Australia for a number of years. He became a Member of the Institute in 1915 and a Fellow in 1926.

## INSTITUTE NEWS AND RADIO NOTES

### World Radio Convention

Sydney, Australia

Last January, as president of the I.R.E., I received an invitation to attend as an official guest, a World Radio Convention to be held at Sydney by the Institution of Radio Engineers of Australia, from April 4 to 14, 1938.

This convention was organized as one of the events associated with the 150th anniversary celebration of the founding of Australia, which was the occasion of great festivities for three months this past spring.

Leaving New York on January 15 I attended the International Radio and Telegraph Conferences held during February and March at Cairo, Egypt, in behalf of the Mackay Radio and Telegraph Company. Because of insufficient time for steamer travel, Mrs. Pratt and I journeyed from Egypt to Australia via Imperial Airways and Quantas Imperial Airways.

This voyage of about 10,500 miles was made in nine days, going by way of Palestine, Iraq, Iran, Northern India, Burma, Siam, Straits Settlements, Dutch East Indies, and 2000 miles over Northeastern Australia from Darwin to Brisbane. The weather was flawless and the accommodations comfortable, the equipment being a large four-motored all-metal flying boat as far as Singapore and a four-motored De Haviland "28" land plane beyond that point. Hot meals, promenade deck, and smoking room were features of the flying boat. Overnight stops were made each day for dinner and rest at good hotels in the principal cities en route.

A welcoming committee from the local section of the Institution and the representative of Standard Telephones and Cables Ltd., Pty., met us at the Brisbane airport and conducted us to our hotel. Many radio engineers and business men of the city visited us and all were anxious to hear about radio matters abroad and particularly about the Cairo Conference. That evening I spoke for about fifteen minutes on radio communication over broadcast station 4BC.

Two days later, on April 2, we arrived at Sydney and were welcomed at the depot by the Institution's General Secretary, Mr. O. A. Mingay, and by Mr. H. C. Trenam, Manager of Standard Telephones and Cables, Ltd., Pty. On the following day, your Vice President, Sir Ernest Fisk, President of the Institution of Radio Engineers of Aus-

tralia, and President of the World Radio Convention, entertained us, together with other overseas guests and members of the Council of the Institution, at a garden party held at his home amid rural settings in the beautiful suburban countryside near Sydney.

An important highlight of the convention was the official banquet Monday evening at the Australia Hotel. The Governor of New South Wales, Lord Wakehurst, Lady Wakehurst, the Premier, and other prominent officials were present as were all the officers of the Institution, their guests, and ladies. This gala affair was excellently organized and most ably managed by Sir Ernest Fisk, the toastmaster. His welcome of your President to the convention was most cordial, mention being made by Sir Ernest of the remarkable occasion whereby the President and Vice President of your Institute met for the first time during the year of their incumbancy, under such unusual circumstances. In reply I invited Sir Ernest to join with me in extending greetings and good wishes from our Institute for a successful convention.

Another bright spot was an official reception by Lord and Lady Wakehurst at Government House, Sydney, attended by Australian officialdom and convention overseas visitors.

The many technical sessions held in the Great Hall of the University of Sydney, were well attended. Nearly fifty interesting papers were given, followed by discussions. The members of the Institution have learned the value of good discussions and conduct their sessions with seriousness and care. Through the courtesy of Mr. Mingay, who was a most efficient and hard-working Convention Manager, copies of the papers which were given in Sydney have been made available for the Institute's archives.

At the evening session on April 12, I presented a paper entitled "Problems of the Radio Engineer," in which there was emphasized the need for radio engineers to expand their interests beyond the restricted fields of detailed design and construction problems and to assist in creating a more orderly management of radio communication development through furnishing a more substantial basis to guide administrating officials in their increasingly difficult tasks of planning and allocating services. Such a basis requires the co-ordinated efforts of engineers implemented with fundamental scientific factual data.

On April 14, the closing day, we joined with the other overseas guests in giving a luncheon at the Australia Hotel for our Australian hosts in appreciation for their many courtesies and attentions. Several of them came to the dock that afternoon to bid us bon voyage on the *S.S. Niagara*.

Our return home was by way of New Zealand, the Fiji Islands, Canton Island, and Honolulu. On this trip we had the pleasure of the company of Dr. Balth. van der Pol, past vice president of your Institute, and Dr. J. D. McGee of England. The ocean voyage terminated at San Francisco May 10.

The Convention Committee, under the chairmanship of Sir Ernest Fisk, was comprised of L. P. R. Bean, N. S. Gilmour, L. A. Hooke, J. Malone, D. G. Wyles, P. S. Parker, C. H. Norville, and O. F. Min-gay. Delegates were present from the Adelaide, Brisbane, Melbourne, Perth, and Victorian Divisions of the Institution.

Among the overseas guests and visitors were General J. G. Harbord, Chairman of the Radio Corporation of America, F. S. Hayburn, Director and foreign envoy of the Marconi Companies, J. L. Baird, Joint Managing Director of Baird Television, Ltd., of London, R. M. Ellis, Vice President, Radio Manufacturers Association, England, Joint Managing Director, Pye Radio Ltd., London, E. S. Colling, Public Relations Officer, Radio Corporation of America, Dr. J. D. McGee, Television Engineer, Research Department, Electric and Musical Industries Ltd., Hayes, England, Dr. van der Pol, Director of Research Laboratories, Philips Radio, Holland, and J. Sanders, Department of Radio and Telegraph Technics, Dutch East Indies.

HARADEN PRATT  
President, 1938

### Rochester Fall Meeting

November 14, 15, and 16 are the dates for the Fall Meeting to be held in Rochester, New York, with headquarters at the Sagamore Hotel. A list of the technical papers to be presented follows:

#### Monday, November 14

9:30 A.M.

- "Frequency Modulation," by C. B. Fisher, Northern Electric Company.
- "Television Radio-Frequency Input Circuits," by H. T. Lyman, General Electric Company.
- "Loud-Speaker Considerations in Feedback Amplifiers," by H. S. Knowles, Jensen Radio Manufacturing Company.

2:00 P.M.

- "The Overvoltage Timer and an Example of its Application to the Measurement of Radio Interference," by C. M. Burrill and E. T. Dickey, RCA Manufacturing Company, Inc., RCA Victor Division.
- "Measurement of Radio Interference," by C. J. Franks, Ferris Instrument Corporation.

7:45 P.M.

"Image Amplifier Pickup Tubes," by P. T. Farnsworth and B. C. Gardner, Farnsworth Television, Inc.

**Tuesday, November 15**

9:30 A.M.

"Standardized Intermediate Frequency," by J. E. Brown, Zenith Radio Corporation.

"Recent Developments in Tube Design," by R. M. Wise, Hygrade Sylvania Corporation.

2:00 P.M.

"Cathode Neutralization in Intermediate-Frequency Amplifiers," by J. A. Worcester and C. S. Root, General Electric Company.

"Gamma and Range in Television," by I. G. Maloff, RCA Manufacturing Company, RCA Victor Division.

**Wednesday, November 16**

9:30 A.M.

"The Interpretation of Amplitude and Phase Distortion in Terms of Paired Echoes," by H. A. Wheeler, Hazeltine Service Corporation.

"New High-Transconductance Ultra-High-Frequency Tubes," by A. P. Kauzmann, RCA Manufacturing Company, RCA Radiotron Division.

"The Use of Die Castings in Radio Applications," by W. W. Broughton, The New Jersey Zinc Company.

2:00 P.M.

"Principles and Methods in Television Laboratory Technique," by S. W. Seeley and D. E. Foster, RCA License Laboratory.

"Production of Image-Dissector Tubes for Motion-Picture Pickup," by C. Larson and B. C. Gardner, Farnsworth Television, Inc.

An exhibition of parts, measuring equipment, and manufacturing aids will be held as in the past. The tenth anniversary dinner will be held on Tuesday evening, November 15. Advance registration for hotel accommodations should be forwarded early to the Hotel Sagamore.

---

**Pacific Coast Convention**

The Pacific Coast Convention held in Portland, Oregon, on August 10 and 11, had a total registration of 121 men and 23 women. All of the technical sessions were well attended and nineteen papers were presented as scheduled. The joint session with the American Institute of Electrical Engineers was attended by about 175.

**Committee Work****ADMISSIONS COMMITTEE**

A meeting of the Admissions Committee was held in the Institute office on September 7 and attended by F. W. Cunningham, chairman; J. F. Farrington, R. A. Heising, L. C. F. Horle, A. F. Van Dyck, and H. P. Westman, secretary.

One application for transfer to Fellow, three for transfer to Member, and four for admission to Member grade were approved. One application for admission to Member grade was denied.

**NEW YORK PROGRAM COMMITTEE**

The New York Program Committee met in the Institute office on September 2. Those present were Austin Bailey, chairman; I. S. Coggeshall, Keith Henney, J. D. Parker (representing A. B. Chamberlain), and H. P. Westman, secretary. The meeting was devoted to the preparation of a list of papers to be presented during the next few Institute meetings in New York City.

**TECHNICAL COMMITTEE ON RADIO RECEIVERS****Sectional Committee on Radio**

A meeting of the Technical Committee on Radio Receivers, operating under the Sectional Committee on Radio of the American Standards Association, was held in the Institute office and attended by H. P. Westman, acting chairman and secretary; J. D. Crawford (guest), D. E. Foster, C. J. Franks, J. W. Fulmer, F. A. Polkinghorn, and Gordon Thompson. The report of the Institute Standards Committee on Radio Receivers was approved with minor modifications for submission to the American Standards Association.

---

**Institute Meetings****ATLANTA SECTION**

The Atlanta Section met on June 23 in the Atlanta Athletic Club with C. F. Daugherty, chairman, presiding. There were forty-six present.

A paper on "Crystal Band filters, Magnetic Generation of Harmonics, Stabilized Feed-Back Amplifiers, and Their Uses in Wide-Band Carrier Telephone Systems" was presented by H. H. Joyner, technical employee of the American Telephone and Telegraph Company. There was first presented a brief review of the fundamental principals of carrier telephony. The problems encountered in extending

the carrier-frequency limit were enumerated and the advantages of stabilized feed-back amplifiers in improved response and gain were mentioned. The use of an electromechanical bridge to compensate for the effects of temperature on the transmission characteristics of the circuit was described. There was then presented a description of equipment used in a main repeater station. Copper-oxide modulators, crystal filters, and magnetic harmonic generators were discussed. There was then presented a detailed discussion of stabilized feed-back amplifiers. This was followed by a consideration of a typical crystal filter network used for wide-band-pass circuits. Piezoelectric phenomena were then considered. The paper was concluded with a description of a copper-oxide modulator and its operation.

#### DETROIT SECTION

The June 24 meeting of the Detroit Section was held in the Detroit News Conference Room and presided over by E. H. Lee, chairman. There were sixty-five present.

Carl Wesser, chief engineer of W8XWJ, described the problems encountered in the construction and operation of the ultra-high-frequency transmitter at W8XWJ. A number of airplane flights have been made to check the vertical field intensity and the results of these measurements were presented.

The antenna is located on top of a tall building surrounded by similar structures and it was found that a strong signal could be obtained directly above it. This is probably caused by reflections from surrounding buildings. A recent change from 100 to 500 watts and from 31 to 41 megacycles has resulted in fewer reports from foreign countries and a substantial increase in local signal strength.

After adjournment, the group visited the studio and transmitter. A facsimile scanner and printer were available at the studio for inspection.

#### PITTSBURGH SECTION

The May 17 meeting of the Pittsburgh Section was held at Carnegie Institute of Technology. W. P. Place, vice chairman, presided and there were thirty-five present.

The two papers presented were by students and introduced by Professor Williamson of Carnegie Institute. L. L. Davenport, graduate student of the University of Pittsburgh, presented a paper on "An Electrical Method of Solving Secular Determinants." This paper which was purely mathematical was introduced with a historical outline of methods used to solve secular determinants and concluded with explanations of the author's experimental work on the problem.

The second paper by S. L. Stine, a student in the physics department of Carnegie Institute of Technology, was on "An Accurately Square-Law Tube Voltmeter." It covered detailed descriptions of square-law voltmeters and the errors encountered in their use. Various methods of obtaining a meter which would hold calibration for a fairly long period of time were discussed.

The first June meeting of the section was held on the 6th at Carnegie Institute of Technology and was presided over by R. T. Gabler, chairman. There were thirty-five present.

F. E. Terman, head of the electrical engineering department of Stanford University, presented his paper on "Detectors—Distortionless and Otherwise." This was summarized on page 923 of the August, 1938, PROCEEDINGS.

On June 21st, the annual dinner meeting and election of officers was held at Carlo's Villa De Estes in Pittsburgh, and was presided over by R. T. Gabler, chairman. There were sixteen present.

In the election of officers, W. P. Place, Union Switch and Signal Company, was named chairman; J. E. Bandino, vice chairman; and R. E. Stark, Federal Metals Corporation, secretary-treasurer.

Finn Ronnie of the Westinghouse Electric and Manufacturing Company, gave a talk on Admiral Byrd's Second Antarctic Expedition in which he participated.

#### ROCHESTER SECTION

On March 3, a joint meeting of the Rochester Section, the local group of the American Institute of Electrical Engineers, and the Rochester Engineering Society was held at the University of Rochester. It was presided over by B. M. Werly and attended by 420.

"Adventures in Electricity" was the subject of a popular demonstration-lecture presented by Phillips Thomas, director of research of the Westinghouse Electric and Manufacturing Company.

The demonstration included the operation of the Precipitron, dry insulation, Pol-Lite, Sterilamp, card sorter, atom smasher, and thermionic relay. Nearly all of the apparatus utilized some application of radio amplifiers or parts familiar to the radio engineer.

On May 26 Lee DuBridge, chairman, presided at a meeting of the Rochester Section held at the Sagamore Hotel.

R. M. Wise, chief engineer of Hygrade-Sylvania Corporation, presented a paper on "A High-Frequency Amplifier Pentode of New Design." This tube is especially designed for television purposes in the

medium high-frequency band from 15 to 150 megacycles. Its design results in improved shielding of tube elements, low interelectrode capacitance, and short connecting leads to the elements.

This was the annual meeting of the section and in the election of officers, H. J. Klumb, Rochester Gas and Electric Company, was designated chairman; E. C. Karker, Mechanics Institute, was named vice chairman; and H. C. Sheve, Stromberg-Carlson Telephone Manufacturing Company, was named secretary-treasurer.

---

### Personal Mention

D. C. Beard, Lieutenant, U.S.N., has been transferred to the U.S.S. *Boise*, basing at Newport News, Va.

R. W. Bowers, Lieutenant, U.S.N., has been transferred to the U.S.S. *Sirius*, basing at New York City.

C. W. Finnigan, previously with Philco Radio and Television Corporation, is now with RCA License Laboratories, New York City.

Fritz Gleim, Lieutenant, U.S.N., has been transferred to the U.S.S. *Phelps*, basing at San Diego, Calif.

Formerly with Hygrade-Sylvania Corporation, F. M. Hager, Jr., is now with E. F. Johnson Company at Waseca, Minn.

G. P. Harnwell is now at the University of Pennsylvania, having formerly been at Princeton University.

T. L. Herdman has left Pye Radio, Ltd., to enter the experimental department of the wireless telegraph section of the Metropolitan Police Engineering Department in London, England.

T. D. Humphreys has left Ultra Electric, Ltd., to become a senior engineer for A. C. Cossor, Ltd., in London, England.

M. W. Kenney has been appointed chief engineer of both the J. P. Seeburg Corporation and the Seeburg Radio Corporation of Chicago.

B. S. Longfellow of the Federal Communications Commission inspection staff has been transferred from New York City to Boston.

R. P. Lyman, Captain, U.S.A., has been transferred to Fort Monmouth, N. J.

A. W. Marriner, Major, U. S. Air Corps, has been transferred to the Army Industrial College, Washington, D.C.

C. A. Martin of RCA Communications, has been transferred from Rocky Point, New York, to LeRoy, Ind.

W. H. Murphy, Major, U.S.A., has been transferred to Patterson Field, Fairfield, Ohio.

J. S. Reese, Lieutenant, U.S.N., has been transferred to the Brooklyn Navy Yard.

## TECHNICAL PAPERS

### REPORT OF COMMITTEE ON RADIO WAVE PROPAGATION\*

#### INTRODUCTION

AT THE fourth meeting of the International Radio Consulting Committee (C.C.I.R.) held at Bucharest, Rumania, in May and June, 1937, one of the committees considered the subject of wave propagation. A large number of valuable contributions to the subject had been made in the documents submitted by the various administrations and companies. It transpired that it was not possible in the time available at Bucharest to prepare a technical report. In Opinion No. 87, the Conference expressed the opinion that the question of wave propagation should be retained for continued study, and also recommended that the Centralizing Administration should undertake the preparation of a general report on this subject. It was decided that this report should be distributed by the Bureau of the Union before the Cairo Conference. The British Administration, as Centralizing Administration, therefore called a special meeting in London on 23-25 November, 1937, of experts on radio wave propagation under the chairmanship of Doctor van der Pol.

The delegates were welcomed by Colonel Angwin, who had been head of the British delegation at the Bucharest Conference. Those present were as follows:

L. S. Angwin	Great Britain	B. van der Pol	The
L. Eckersley		H. Bremmer	Netherlands
J. Gill		J. H. Dellinger	United
W. Hayes		J. C. Schelleng	States
F. Millington		R. Braillard	Union Internationale de Radiodiffusion
L. Smith-Rose			
J. Stevenson			

Professor Gutton and Doctor Le Corbeiller who had expected to attend the meeting were unfortunately detained.

Besides the documents on wave propagation which had been submitted to the Bucharest Conference a number of new documents were furnished to the Committee by those who attended and also by the

\* Decimal classification: R113. Original manuscript received by the Institute, March 23, 1938.

Laboratoire National de Radioelectricite, Paris. These new documents are listed in the Appendix. The Committee thus had before it material which brought knowledge of the facts of radio wave propagation up to date. The Committee understood that its function was to prepare a report summarizing the principal facts of radio wave propagation throughout the radio spectrum in as concise a form as would be useful to the practical radio engineer having to do with the allocation of frequencies and with the operation of radio stations carrying on national and international services. The following report is offered by the Committee in the hope that it is reasonably in accord with this objective.

As may be seen from the headings of the following parts of the report, the Committee considered it to be useful to divide the information into four parts as follows:

- A. Medium Frequencies, Ground Wave,
- B. Medium Frequencies, Sky Wave,
- C. High Frequencies, and
- D. Ultra-High Frequencies,

It is recognized that the terminology of these headings is not entirely scientific, since there may be some debate as to where one of these provinces ends and another begins. In a broad, general way, Parts A and B are considered as including the range of frequencies from approximately 150 to 1500 kilocycles (2000 to 200 meters). Part C covers from approximately 1500 to 30,000 kilocycles (200 to 10 meters); and Part D covers frequencies above 30,000 kilocycles (below 10 meters).

In surveying the material available to it and the results it has been able to present, the Committee is impressed by the valuable work now in progress on the part of many laboratories and radio stations. It is strongly recommended that such work be extended and published as widely as possible. The intelligent allocation and use of radio frequencies will be greatly facilitated by the extension of quantitative records of radio reception and of ionosphere observations at as many latitudes as possible.

#### **A. MEDIUM FREQUENCIES—GROUND WAVE**

The curves for day propagation as prepared in Madrid and modified in Lisbon were based on an interpretation of two theories; viz., (a) valid for a plane earth only and (b) valid for a spherical earth but for great distances between sender and receiver.

The curves now presented have been calculated to a higher pre-

cision with the aid of two additional theories, the first<sup>1</sup> being based on an exact solution of the Maxwellian equations with proper boundary conditions and the second<sup>2</sup> on the phase-integral method.

In most of the practical cases the numerical results obtained by means of these two additional theories are in good agreement, so that they are presented with complete confidence. They are represented in Figs. 1 and 2 giving the field on the surface of the earth as a function of the distance between sender and receiver. The sender is assumed to be situated on the surface of the earth, and the results are given in terms of a radiated power of 1 kilowatt. For a sender of  $P$  kilowatts, the value of the field given should be multiplied by  $\sqrt{P}$ .

Fig. 1 refers to propagation over sea water ( $\sigma = 4 \times 10^{-11}$  electromagnetic units), while Fig. 2 refers to  $\sigma = 10^{-13}$  electromagnetic units (average ground conductivity). In both figures the following frequencies have been considered:

150 kc	(2000 m)	1000 kc	(300 m)
200 kc	(1500 m)	1500 kc	(200 m)
300 kc	(1000 m)	2000 kc	(150 m)
500 kc	(600 m)	5000 kc	(60 m)

These figures are intended to replace the Madrid and Lisbon ground-wave curves.

In conclusion it may be of interest to point out that theory shows that for a given frequency there exists an optimum conductivity corresponding to the greatest field at great distances. Thus for a frequency of 1500 kilocycles (200 meters), this optimum conductivity is that of sea water ( $\sigma = 4 \times 10^{-11}$  electromagnetic units), while for 300 kilocycles (1000 meters) it is  $\sigma = 2.2 \times 10^{-12}$  electromagnetic units, and for 50 kilocycles (6000 meters) it is  $\sigma = 10^{-13}$  electromagnetic units which corresponds to average ground. It should, however, be noted that this optimum condition is not very critical.

## B. MEDIUM FREQUENCIES—SKY WAVE

During the night, the sky-wave radiation reaches values which are much greater than day values at the same point. For this reason, the ground wave ceases to be predominant at a much shorter distance from the sender.

In order to take account of the problematic character of the resulting night field, the Madrid Conference introduced the notions of

<sup>1</sup> B. van der Pol and H. Bremmer, *Phil. Mag.*, vol. 24, pp. 141-176, July; p. 826-864; November, (1937); *Hochfrequenz. und Elektroakustik*, vol. 51, pp. 81-188; June, (1938).

<sup>2</sup> T. L. Eckersley, *Proc. Roy. Soc. ser. A*, vol. 136, pp. 499-527; June 1 1932). (See also supplementary paper, to be published.)

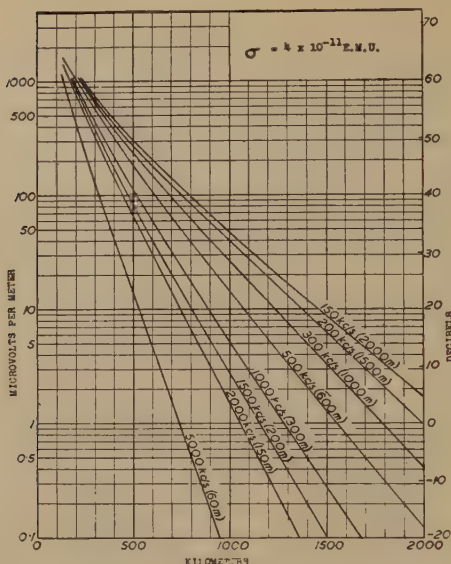


Fig. 1—Field intensity of ground wave at various distances over sea water ( $\sigma = 4 \times 10^{-11}$  electromagnetic units) for a radiated power of 1 kilowatt.

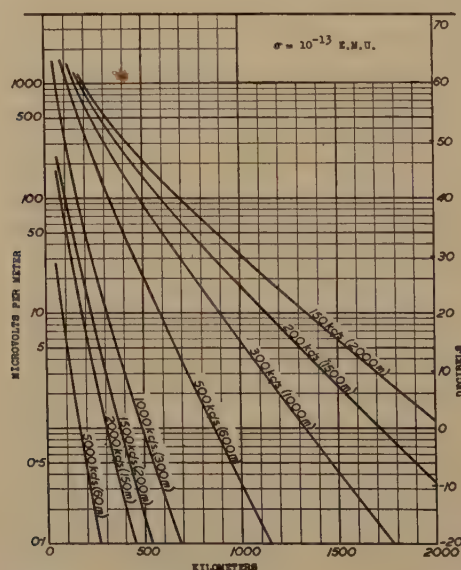


Fig. 2—Field intensity of ground wave at various distances over land ( $\sigma = 10^{-13}$  electromagnetic units) for a radiated power of 1 kilowatt.

"median" and "quasi-maximum" values of the field—magnitudes exceeded by the instantaneous value during 50 and 5 per cent of the time, respectively.

The curves of Figs. 3, 4, and 5, correspond to the quasi-maximum value for 1 kilowatt radiated, in terms of distance. The median value is about 0.35 of this quasi-maximum value. Fig. 3 gives the quasi-maximum value of the field up to 12,000 kilometers for a complete night path throughout the whole distance traversed. The curves have been plotted from the results of very numerous tests carried out during

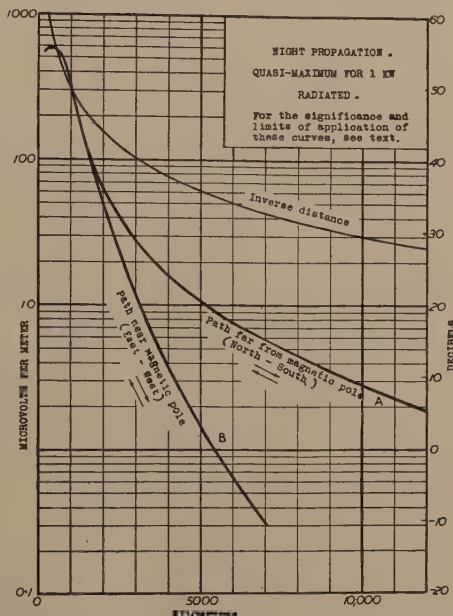


Fig. 3—Quasi-maximum field intensity at great distances for propagation at night for a radiated power of 1 kilowatt.  
Curve A relates to a propagation path far away from the magnetic pole.  
Curve B relates to a propagation path passing near the magnetic pole.

a period of more than four years. They show, moreover, very good agreement with the results of theoretical studies respecting multiple reflections.

The long-distance field measured varies greatly according as the path followed approaches more or less the earth's magnetic pole. Curve A relates to paths of which all the points are very far away from the magnetic pole, which generally corresponds to a North-South or South-North path, e.g., between North America and South America, Europe and Central America, Europe and South America.

Curve *B* relates to paths which approach the earth's magnetic pole; this generally corresponds in the northern hemisphere to an East-West or West-East path, e.g., between Northern United States and Northern and Central Europe or between Northern and Central Europe and Siberia.

In the present state of experimental work, curves *A* and *B* appear to indicate the limiting observed values as a function of the distance separating the magnetic pole from the portion of the path which is

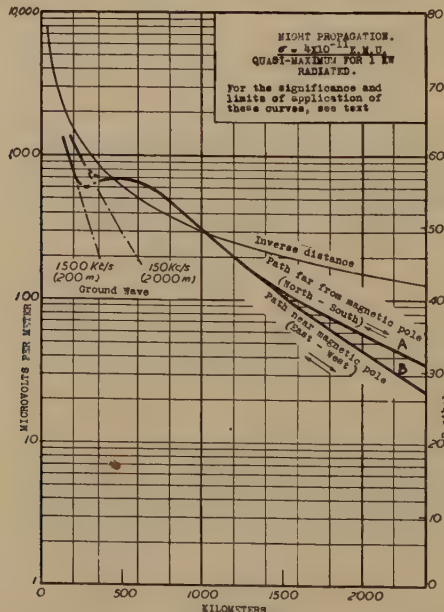


Fig. 4—Quasi-maximum field intensity at various distances for propagation at night over sea water ( $\sigma = 4 \times 10^{-11}$  electromagnetic units) for a radiated power of 1 kilowatt.

Curve *A* relates to a propagation path far away from the magnetic pole.  
Curve *B* relates to a propagation path passing near the magnetic pole.

nearest to it. Sufficient experimental results are not yet available so far as concerns the paths which touch the magnetic pole or are situated in the southern hemisphere.

Figs. 4 and 5 give the quasi-maximum value of the field up to distances of 2400 kilometers, for conductivities of  $4 \cdot 10^{-11}$  and  $10^{-13}$  electromagnetic units, respectively, and for frequencies of 150 kilocycles (2000 meters) and 1500 kilocycles (200 meters).

At the point where the ground wave ceases to be preponderant, the value of the resulting field depends on numerous factors which

may modify it considerably: frequency, form of aerial, and conductivity of ground. The curves of Figs. 4 and 5 give only (by a dotted line) a very approximate average value and it is desirable that each particular case should be studied on its merits.

### C. HIGH FREQUENCIES

Radio transmission at high frequencies is governed by factors quite different from those at medium and lower frequencies. The de-

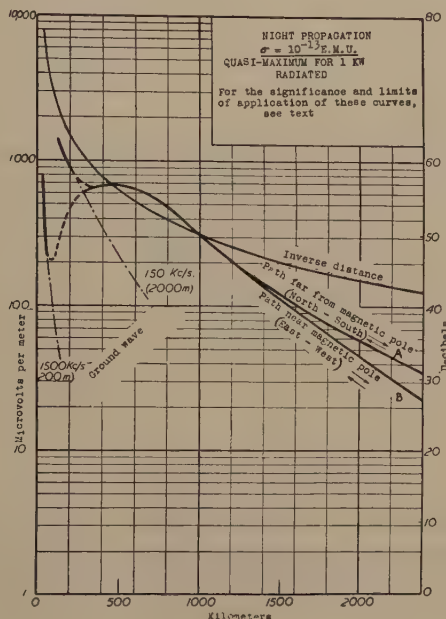


Fig. 5—Quasi-maximum field intensity at various distances for propagation at night over land ( $\sigma = 10^{-13}$  electromagnetic units) for a radiated power of 1 kilowatt.

Curve A relates to a propagation path far away from the magnetic pole. Curve B relates to a propagation path passing near the magnetic pole.

termining factors are simpler, on the one hand, because the ground wave is negligibly small in comparison with the sky wave, and on the other hand are more complicated in that there are more complex variations in the ionosphere layers which determine the transmission. The complexity of these variations precludes the comprehensive presentation of the facts of high-frequency transmission in any small number of graphs or charts.

If ionospheric data were completely known all over the earth's surface at all seasons, it would be possible, though difficult, to calculate

the communication conditions. A knowledge of conditions in the ionosphere is most comprehensively expressed in terms of data which relate the virtual height of the layer and the frequency. These data are of a relatively high order of accuracy for any particular time and place.

Normal-incidence results have, so far, only been obtained in a few places and are, therefore, inadequate as a survey of the ionosphere all over the earth. Extensions of such measurements and prompt publication would be highly desirable.

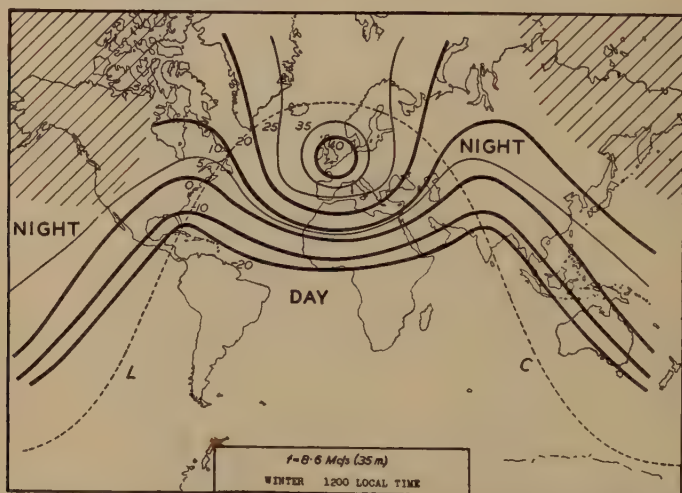


Fig. 6—Field-intensity contour chart for a wave of 8.6 megacycles (35 meters).  
 ——— lines of equal field intensity in decibels above 1 microvolt per meter,  
 - - - - - sunrise (L) to sunset (C) locus,  
 // / / / skip region of zero field intensity.

Recent developments of the theory of transmission through the ionosphere have focused attention on a very significant method<sup>3</sup> according to which the conditions of long-distance transmission can be completely specified in terms of normal-incidence virtual-height measurements at varying frequency. In the light of these considerations, there are two methods open for the specification of long-distance transmission:

(1) Accurate, but at present limited, results may be given from the normal-incidence equivalent-height frequency curves.

<sup>3</sup> The determination of critical frequencies at oblique-incidence from normal-incidence critical frequencies is definitely calculable. A method of doing this is given by N. Smith, "Extension of normal-incidence ionosphere measurements to oblique-incidence radio transmission," *Nat. Bur. Stand. Jour. Res.*, vol. 19, pp. 89-94; July, (1937) (RP 1013). A more exact method is given in papers C5 and C7 listed in the Appendix hereof.

(2) The extensive knowledge of the transmission of radio waves over the earth's surface may be used to construct a more comprehensive, but less accurate, chart of the ionosphere.

### 1. Field-Intensity Contour Charts

Field-intensity contour charts have been given in the Lisbon documents. To simplify the use of these charts, some examples of the working out of the results are given here. Contour maps are attached for a wave of 8.6 megacycles (35 meters) (Figs. 6 to 14) and for a wave of

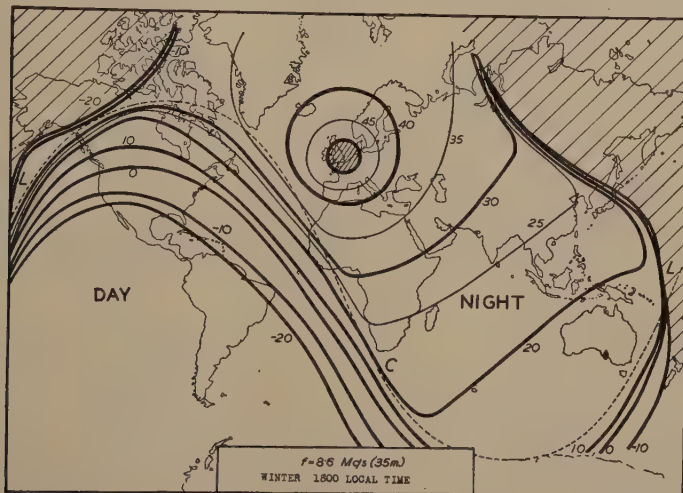


Fig. 7—Field-intensity contour chart for a wave of 8.6 megacycles (35 meters).  
 ——— lines of equal field intensity in decibels above 1 microvolt per meter,  
 - - - - - sunrise (*L*) to sunset (*C*) locus,  
 // / / / skip region of zero field intensity.

18.8 megacycles (16 meters) (Figs. 15 to 23). The charts have been given for winter, equinox, and summer conditions each at 1200, 1800, 2400, G.M.T., at the sender.

Since the ionosphere conditions may alter significantly for times of the day differing by an hour or less, the times chosen, 1200, 1800, and 2400, G.M.T., do not give an adequate account of the variation of the transmission characteristics throughout the day. To make maps for every hour would require a prohibitive amount of labor. For times not given, the original charts must be used.

The maps are centered on a latitude 50 degrees north; that is, the sender is supposed to be situated at this latitude. The contours give the quasi-maximum field intensity  $f$  for a sender supplying 1 kilowatt to a half-wave aerial. The field intensities are shown in decibels above

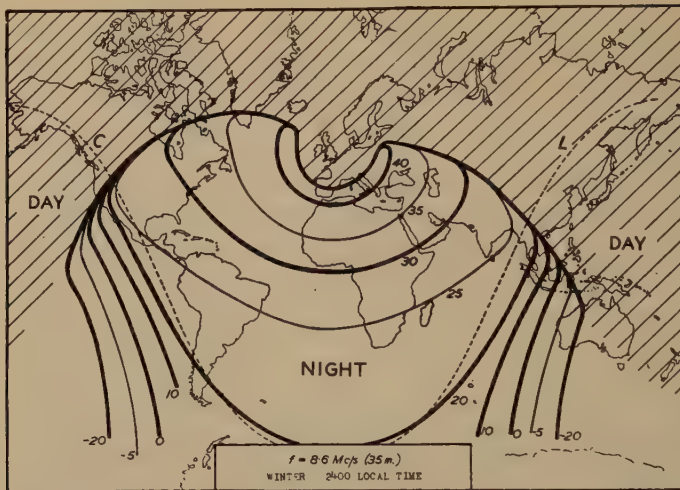


Fig. 8—Field-intensity contour chart for a wave of 8.6 megacycles (35 meters).  
 — lines of equal field intensity in decibels above 1 microvolt per meter,  
 - - - sunrise ( $L$ ) to sunset ( $C$ ) locus,  
 ////////////// skip region of zero field intensity.

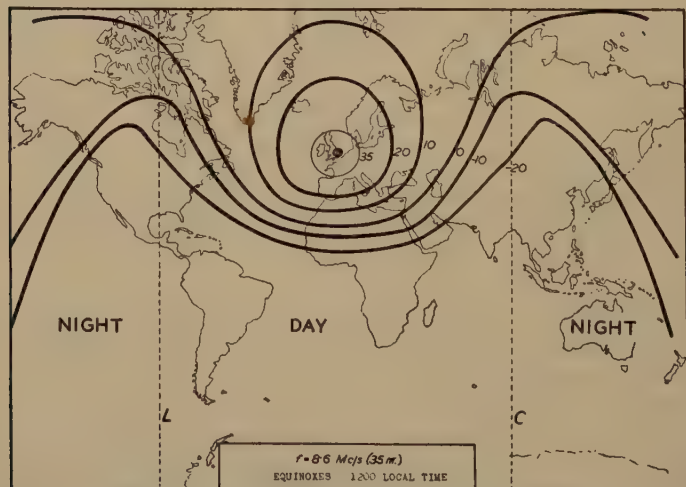


Fig. 9—Field-intensity contour chart for a wave of 8.6 megacycles (35 meters).  
 — lines of equal field intensity in decibels above 1 microvolt per meter,  
 - - - sunrise ( $L$ ) to sunset ( $C$ ) locus,  
 ////////////// skip region of zero field intensity.

1 microvolt per meter. Although the maps are given for a transmitter at longitude 0 degrees they refer equally well to any longitude  $\theta$  degrees, if instead of G.M.T. the local solar time corresponding to this longitude

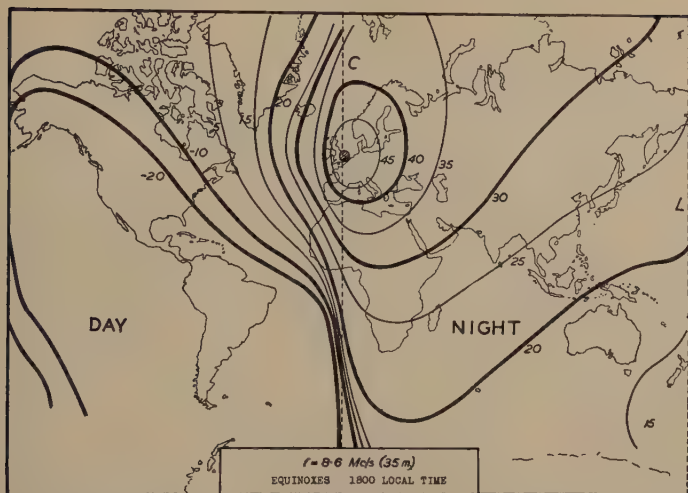


Fig. 10—Field-intensity contour chart for a wave of 8.6 megacycles (35 meters).  
 — lines of equal field intensity in decibels above 1 microvolt per meter,  
 - - - sunrise ( $L$ ) to sunset ( $C$ ) locus,  
 ////////////// skip region of zero field intensity.

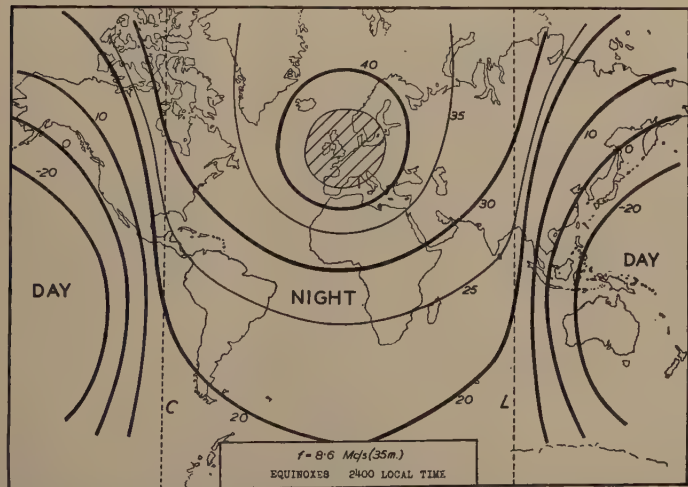


Fig. 11—Field-intensity contour chart for a wave of 8.6 megacycles (35 meters).  
 — lines of equal field intensity in decibels above 1 microvolt per meter,  
 - - - sunrise ( $L$ ) to sunset ( $C$ ) locus,  
 ////////////// skip region of zero field intensity.

is taken, and the charts are moved relative to a map in longitude. This is most simply effected by having the contours on tracing paper which can be slid over a fixed map.

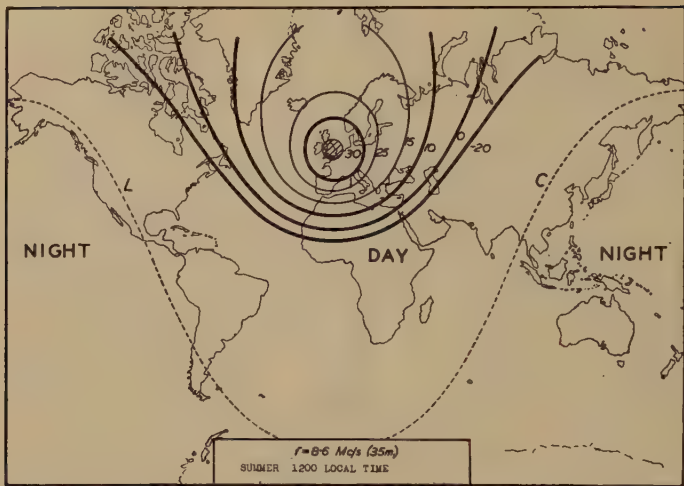


Fig. 12—Field-intensity contour chart for a wave of 8.6 megacycles (35 meters).  
 — lines of equal field intensity in decibels above 1 microvolt per meter,  
 - - - sunrise (*L*) to sunset (*C*) locus,  
 ////////////// skip region of zero field intensity.

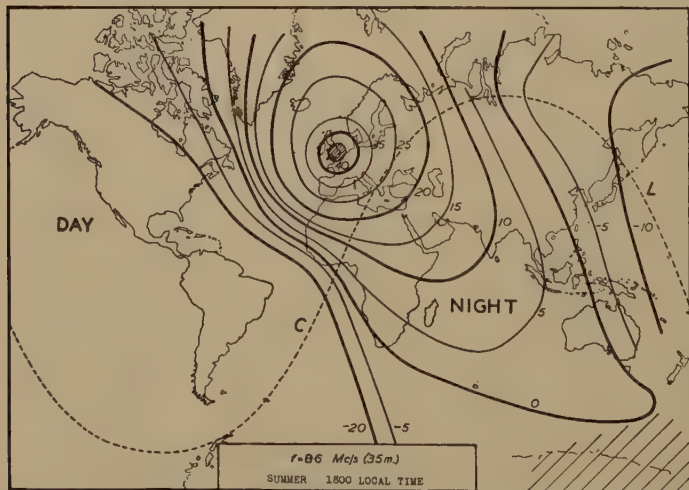


Fig. 13—Field-intensity contour chart for a wave of 8.6 megacycles (35 meters).  
 — lines of equal field intensity in decibels above 1 microvolt per meter,  
 - - - sunrise (*L*) to sunset (*C*) locus,  
 ////////////// skip region of zero field intensity.

It was assumed in constructing these charts that reciprocal conditions are, on the average, satisfied so that the rôles of the sender and the receiver may be interchanged. The maps therefore give the

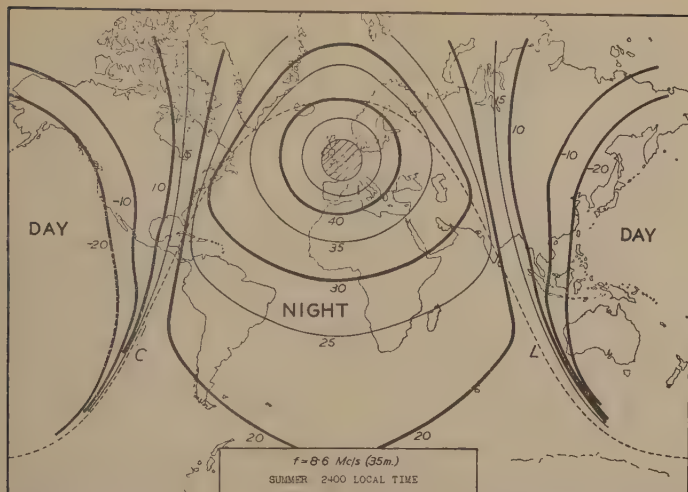


Fig. 14—Field-intensity contour chart for a wave of 8.6 megacycles (35 meters).  
 — lines of equal field intensity in decibels above 1 microvolt per meter,  
 - - - sunrise (L) to sunset (C) locus,  
 ////////////// skip region of zero field intensity.

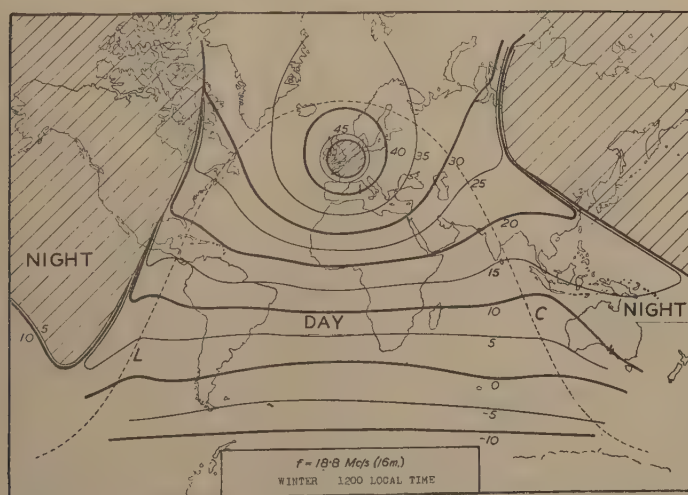


Fig. 15—Field-intensity contour chart for a wave of 18.8 megacycles (16 meters).  
 — lines of equal intensity in decibels above 1 microvolt per meter,  
 - - - sunrise (L) to sunset (C) locus,  
 ////////////// skip region of zero field intensity.

transmission conditions, at the specified time, of a sender situated anywhere on the earth and a receiver at the origin. The dotted lines on the contour map give the sunrise and sunset locus, and the shaded

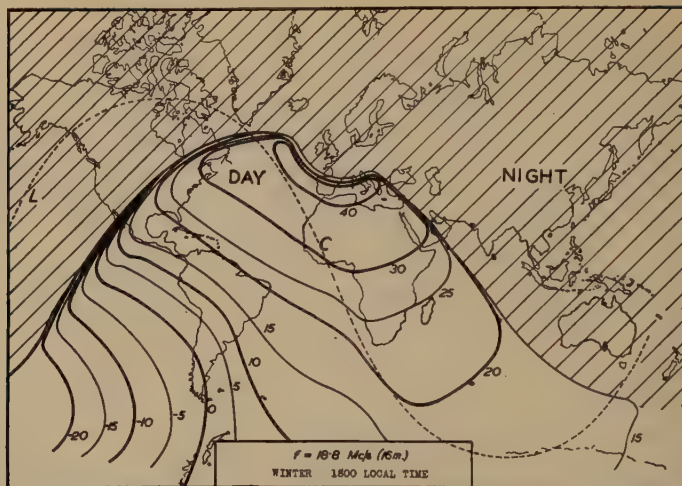


Fig. 16—Field-intensity contour chart for a wave of 18.8 megacycles (16 meters).  
 ——— lines of equal intensity in decibels above 1 microvolt per meter,  
 - - - - - sunrise (L) to sunset (C) locus,  
 // / / / / skip region of zero field intensity.

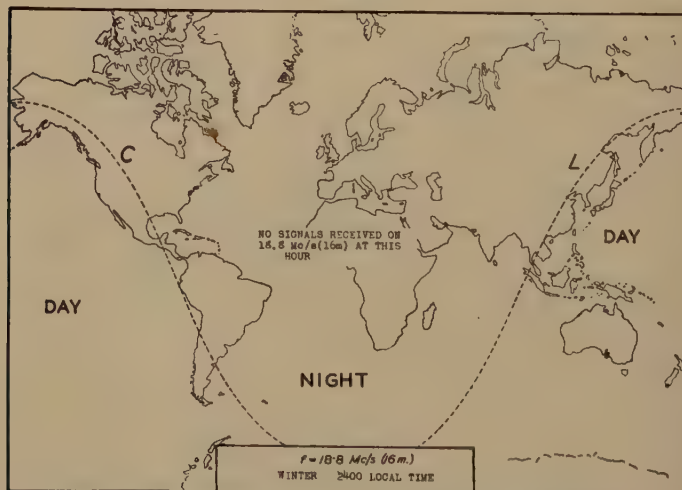


Fig. 17—Field-intensity contour chart for a wave of 18.8 megacycles (16 meters).  
 ——— lines of equal intensity in decibels above 1 microvolt per meter,  
 - - - - - sunrise (L) to sunset (C) locus,  
 // / / / / skip region of zero field intensity.

portion is the skip region where, on account of electron limitation, the waves penetrate the ionosphere and no signals (except perhaps scattered signals which are, in general, of such poor quality as to be un-

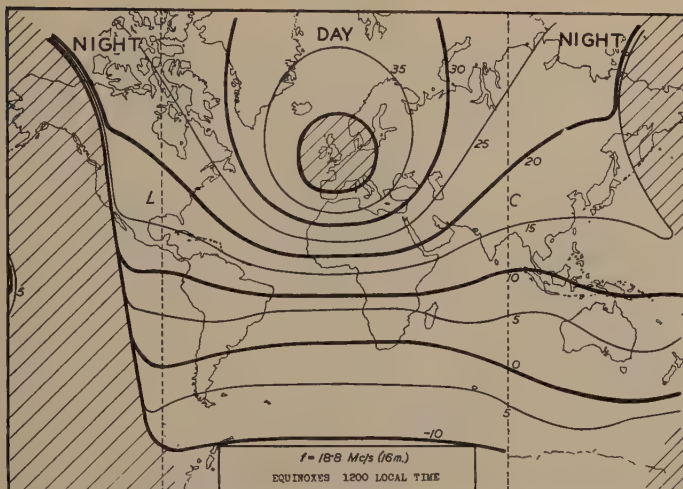


Fig. 18—Field-intensity contour chart for a wave of 18.8 megacycles (16 meters).  
 — lines of equal intensity in decibels above 1 microvolt per meter,  
 - - - sunrise (*L*) to sunset (*C*) locus,  
 // / / skip region of zero field intensity.

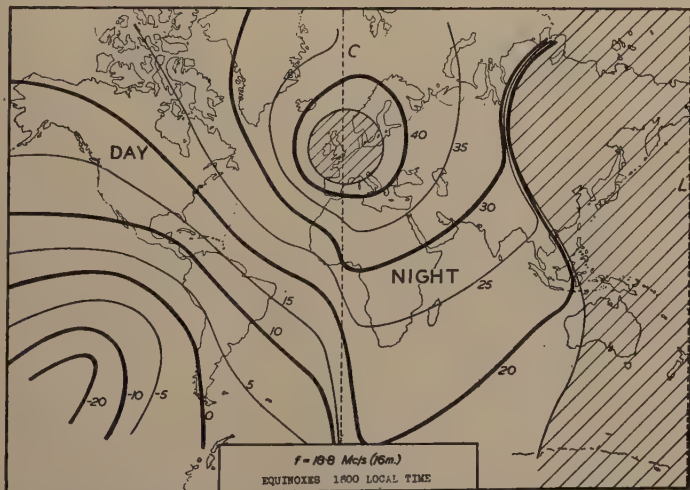


Fig. 19—Field-intensity contour chart for a wave of 18.8 megacycles (16 meters).  
 — lines of equal intensity in decibels above 1 microvolt per meter,  
 - - - sunrise (*L*) to sunset (*C*) locus,  
 // / / skip region of zero field intensity.

usable) are received. The maps are drawn for the epoch 1929 to 1932.

The field-intensity contour charts are for long distances only. They do not take account of possible differences between the northern and

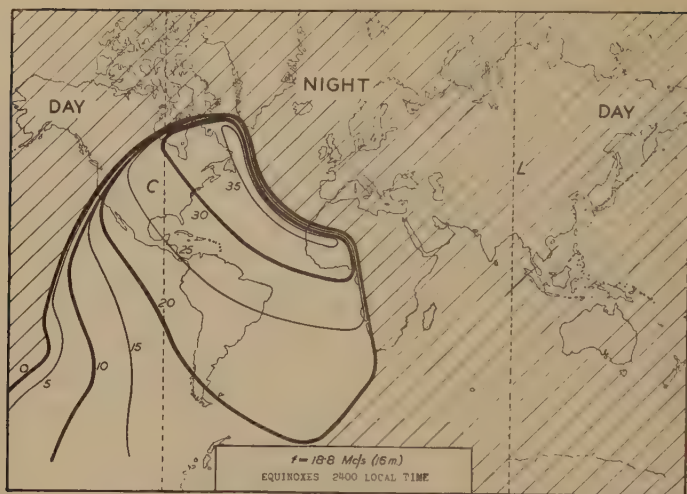


Fig. 20—Field-intensity contour chart for a wave of 18.8 megacycles (16 meters).  
 — lines of equal intensity in decibels above 1 microvolt per meter,  
 - - - sunrise ( $L$ ) to sunset ( $C$ ) locus,  
 / / / / skip region of zero field intensity.

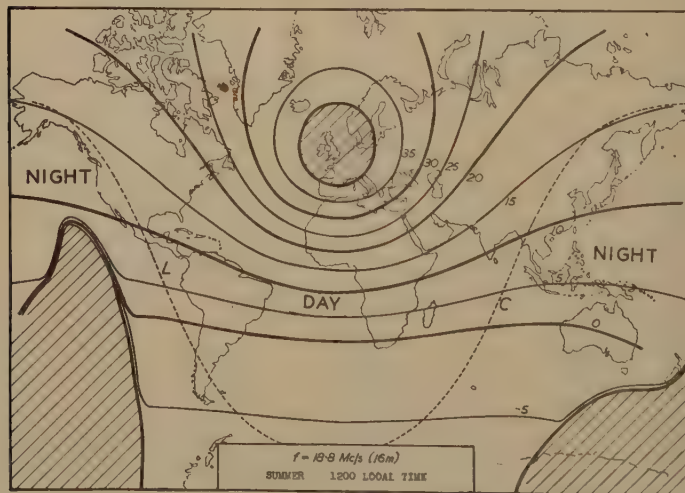


Fig. 21—Field-intensity contour chart for a wave of 18.8 megacycles (16 meters).  
 — lines of equal intensity in decibels above 1 microvolt per meter,  
 - - - sunrise ( $L$ ) to sunset ( $C$ ) locus,  
 / / / / skip region of zero field intensity.

southern hemispheres nor of effects due to proximity to the magnetic pole.

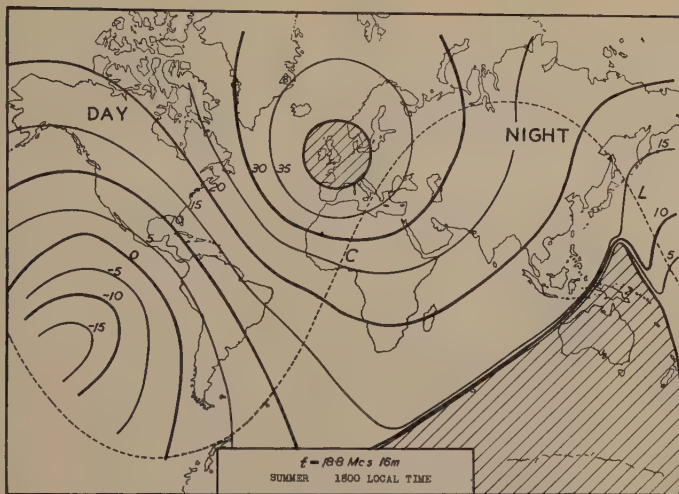


Fig. 22—Field-intensity contour chart for a wave of 18.8 megacycles (16 meters).  
 ——— lines of equal intensity in decibels above 1 microvolt per meter,  
 - - - - - sunrise (L) to sunset (C) locus,  
 // / / / / skip region of zero field intensity.

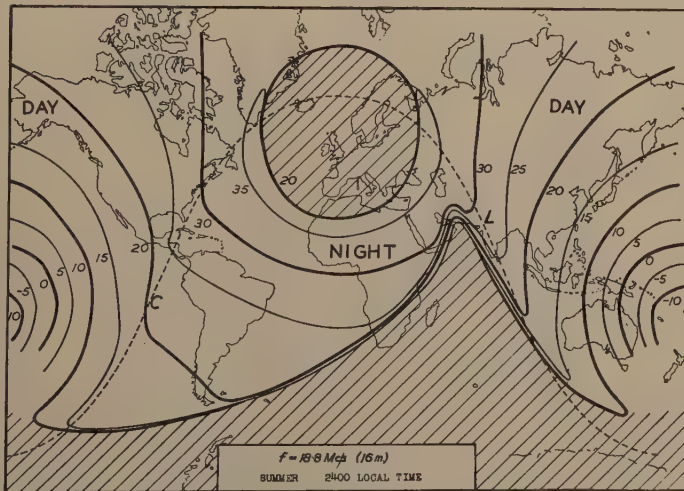


Fig. 23—Field-intensity contour chart for a wave of 18.8 megacycles (16 meters).  
 ——— lines of equal intensity in decibels above 1 microvolt per meter,  
 - - - - - sunrise (L) to sunset (C) locus,  
 // / / / / skip region of zero field intensity.

## 2. Graphs of Maximum Usable Frequencies

To give the facts of transmission for all frequencies, times, etc., would be impossible by any form of presentation, but the series of

simple linear graphs attached (Figs. 24 to 39) give considerable information desired for wide ranges of time, frequency, distance, etc. In determining the utility of a given radio frequency for a given time and path, a complete specification would include data on the wave absorption.

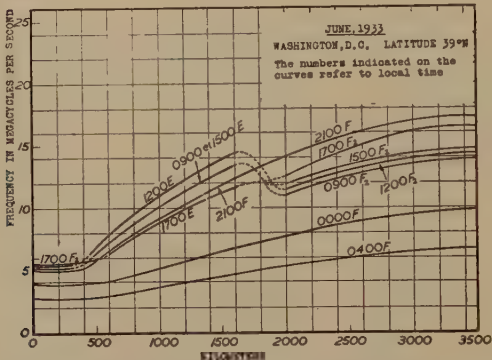


Fig. 24—Maximum usable frequencies for various distances of transmission, based on measurements on the ionosphere at normal incidence.

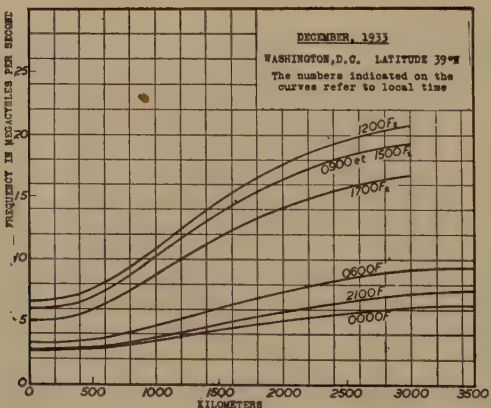


Fig. 25—Maximum usable frequencies for various distances of transmission, based on measurements on the ionosphere at normal incidence.

However, received intensities in general increase with the frequency nearly up to the critical frequency, i.e., the upper limit of frequency which can be transmitted. For practical radio operation, therefore, it is of special value to know the highest frequency which can be transmitted, at the time and over the distance desired; this will be called the maximum usable frequency. This frequency is of particular interest in that it is definitely determinable, and is known as a result of

ionosphere observations. It should be noted that sometimes waves are transmissible at higher frequencies, proceeding by way of sporadic-E reflection or scattered reflections.

The maximum usable frequency is different for different distances of transmission, latitude (possibly different in northern and southern

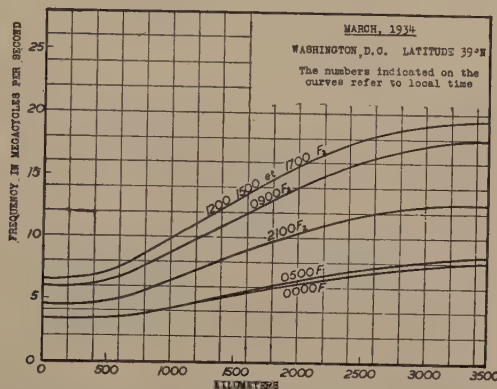


Fig. 26—Maximum usable frequencies for various distances of transmission, based on measurements on the ionosphere at normal incidence.

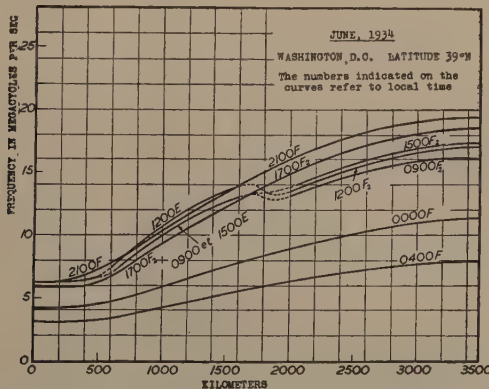


Fig. 27—Maximum usable frequencies for various distances of transmission, based on measurements on the ionosphere at normal incidence.

hemispheres), time of day (and therefore longitude), season, and year. Information on maximum usable frequencies under all these various conditions is given in the attached graph sheets, Figs. 24 to 39. These data are based on ionosphere measurements (i.e., measurement of ionosphere layer heights and critical frequencies for normal incidence).

In the figures, the data are given up to a distance of 3500 kilometers, which is sufficient. The values given for 3500 kilometers are

approximately correct for all greater distances also, as 3500 kilometers is the limit of distance practically attainable in transmission by one reflection from the ionosphere; greater distances are attained by multiple reflections, in which no increase in frequency is possible. The letters on each curve indicate the region of the ionosphere which propagates the waves at the time concerned.

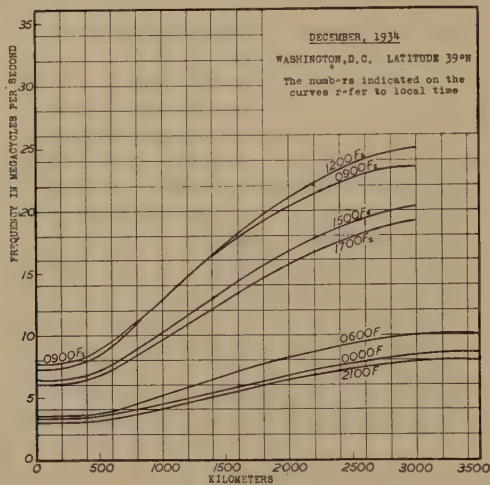


Fig. 28—Maximum usable frequencies for various distances of transmission, based on measurements on the ionosphere at normal incidence.

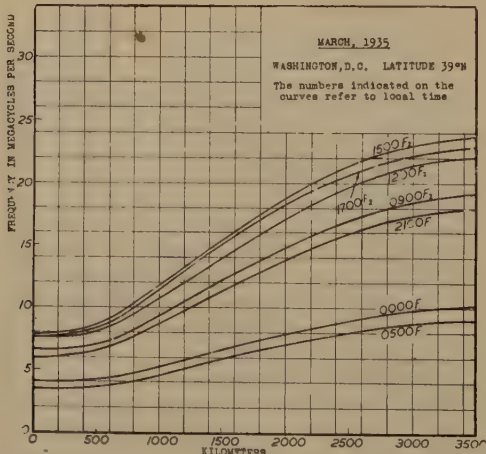


Fig. 29—Maximum usable frequencies for various distances of transmission, based on measurements on the ionosphere at normal incidence.

multiple reflections, in which no increase in frequency is possible. The letters on each curve indicate the region of the ionosphere which propagates the waves at the time concerned.

Almost all the data are for latitude 39 degrees north, based on ionosphere measurements at Washington, D. C. For this latitude the

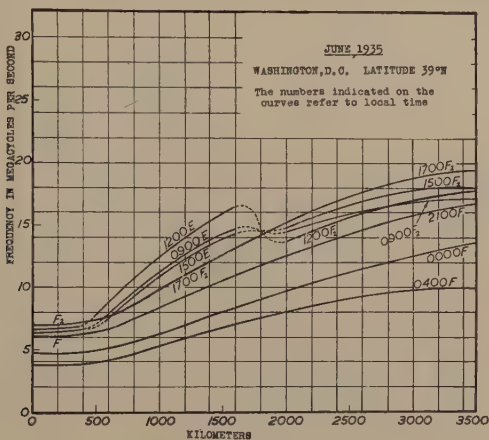


Fig. 30—Maximum usable frequencies for various distances of transmission, based on measurements on the ionosphere at normal incidence.

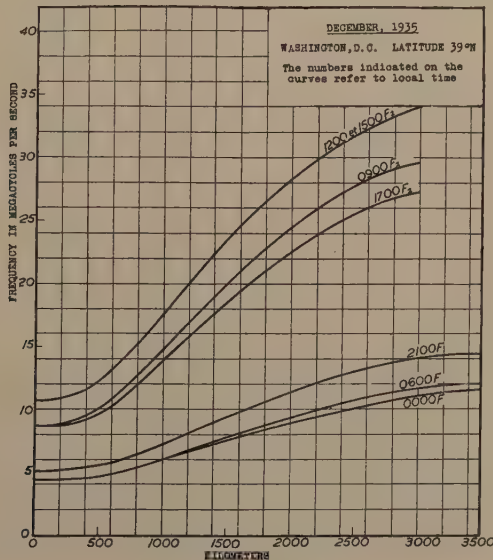


Fig. 31—Maximum usable frequencies for various distances of transmission, based on measurements on the ionosphere at normal incidence.

data are given for the period from June, 1933, to December, 1937, inclusive, and thus extend over a substantial portion of the 11-year cycle of solar activity.

A limited idea of the variation with latitude and with hemisphere is given in the data shown for latitude 30 degrees south. As in the field-intensity contour charts above, no information is included on the effect of proximity of the magnetic pole.

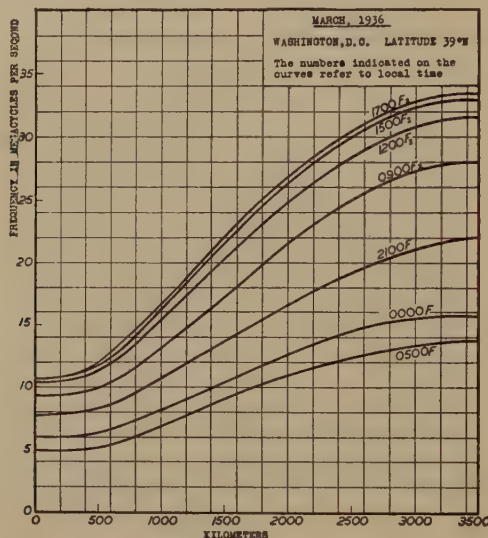


Fig. 32—Maximum usable frequencies for various distances of transmission, based on measurements on the ionosphere at normal incidence.

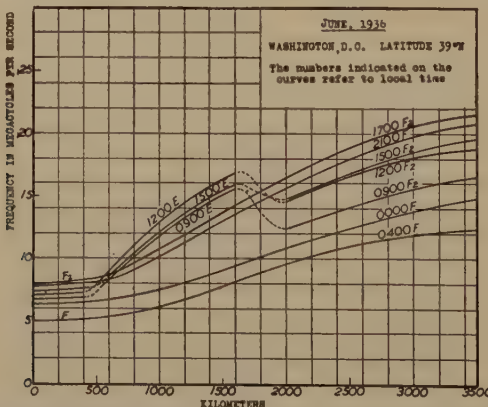


Fig. 33—Maximum usable frequencies for various distances of transmission, based on measurements on the ionosphere at normal incidence.

Each figure indicates the effects of time of day, while the variations with season and from year to year are shown throughout the different figures. Data are shown only for three times of year, i.e., for summer,

winter, and vernal equinox. The conditions at the autumnal equinox are practically the same as at the vernal equinox. Summer and winter conditions in the ionosphere center on the solstices, and thus the ionospheric seasons do not coincide with the seasons of weather.

In each graph, the data given are averages for the month. Variations from day to day are generally within 15 per cent of the values given, except for disturbed periods, which may be called ionosphere

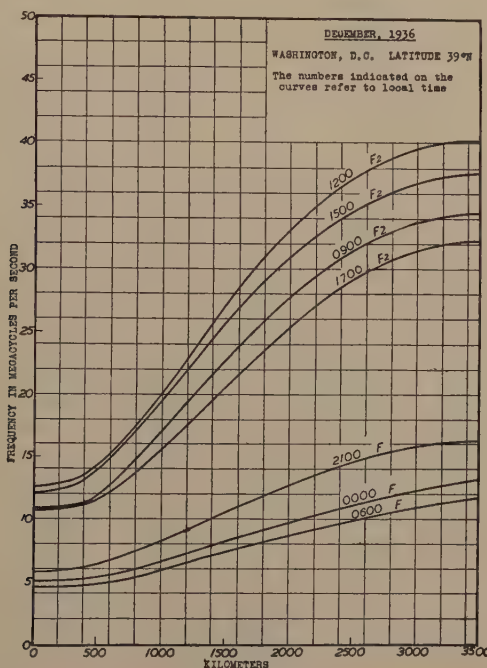


Fig. 34—Maximum usable frequencies for various distances of transmission, based on measurements on the ionosphere at normal incidence.

storms, during which field intensities are abnormally low and the maximum usable frequencies are less than the values shown, and except also for times of sudden ionosphere disturbance during which transmission may be interrupted completely for periods of a few minutes to an hour.

As an example of the use of the graphs, reference is made to those for June, 1936 (Fig. 33). At noon (1200) the average normal-incidence critical frequency for the F<sub>2</sub> region was about 7150 kilocycles (42 meters). This means that 7150 kilocycles (42 meters) was the highest frequency for which the ionosphere would return signals to the emit-

ting point. This corresponds to zero distance on the chart. For a distance of 400 kilometers the  $F_2$  region determined the maximum usable frequency of 7320 kilocycles (41 meters). At about 450 kilometers the E region began to be effective as shown by a dotted portion of the graph. Beyond 1600 kilometers the effectiveness of the E region decreased rapidly because of the high angle of incidence of the waves. At 1600 kilometers the maximum usable frequency was 17,000 kilo-

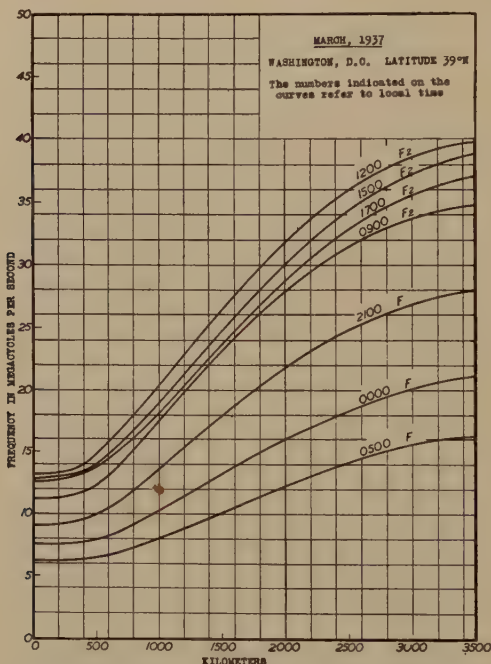


Fig. 35—Maximum usable frequencies for various distances of transmission, based on measurements on the ionosphere at normal incidence.

cycles (17.6 meters) determined by the E region and at 2000 kilometers it was 14,600 kilocycles (20.6 meters) determined by the  $F_2$  region. Between 1600 and 2000 kilometers the graphs are dotted to indicate the transition from E to  $F_2$  transmission. Beyond 2000 kilometers the maximum usable frequencies were determined by the  $F_2$  region. At 3500 kilometers the maximum usable frequency was 18,800 kilocycles (16 meters). At all greater distances the maximum usable frequency may be expected to be only slightly greater than that for 3500 kilometers. This is about the limit for single-reflection transmission by way of the  $F_2$  region; at greater distances transmission is by multiple reflections.

The geographical part of the ionosphere which controls long-distance high-frequency propagation is that at which the wave in the useful direction strikes the reflecting region. Therefore the times given in the graphs are local times for the geographical part of the ionosphere at which the waves are reflected. Because of large differences in local time and latitude encountered in long transmission paths, involving more than one reflection from the ionosphere, widely different condi-

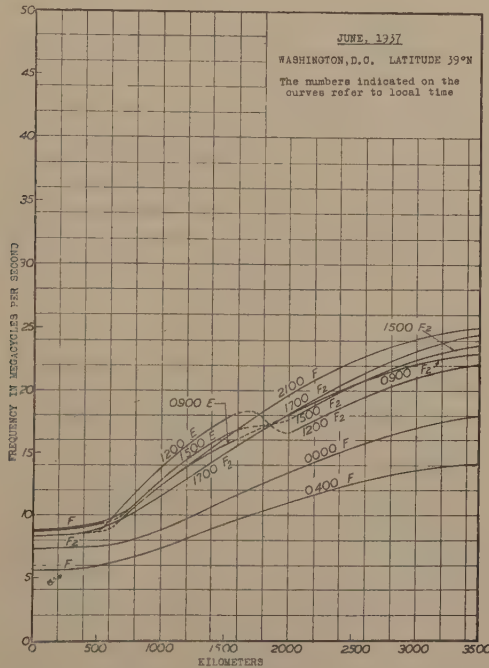


Fig. 36—Maximum usable frequencies for various distances of transmission, based on measurements on the ionosphere at normal incidence.

tions sometimes prevail over different parts of these paths. In such cases, that transmission frequency will have to be used which corresponds to the part of the path in which the maximum usable frequency is the lowest.

### *3. Directivity of Aerials*

In the course of the year 1937, numerous measurements were carried out in North and South America and in Europe in order to appraise the practical efficiency of directional emitting aerials used by broadcast stations on short waves (9.5 to 21.5 megacycles) (31.6 to 14 meters).

The field measurements were made immediately before and after the change of aerial used at the sender and they showed the effect either of transferring from a nondirectional aerial to a directional aerial or vice versa, or of changing the direction of the beam.

From the whole of the 1500 results collected and analyzed, which confirm observation previously made in the fixed services, the following practical conclusions may be deduced, without prejudice to the pro-

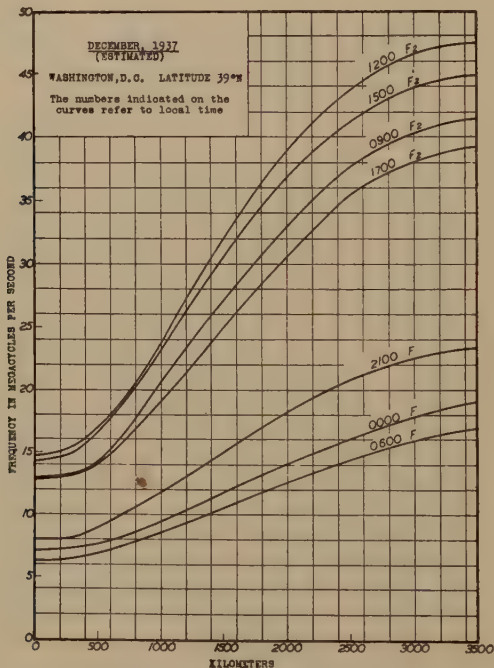


Fig. 37—Maximum usable frequencies for various distances of transmission, based on measurements on the ionosphere at normal incidence.

*Note:* Data from the National Bureau of Standards since this report was prepared, show that the December values were lower than the estimated values in this figure (prepared before December); T. R. Gilliland, S. S. Kirby, N. Smith, and S. E. Reymer, "Maximum usable frequencies for radio sky-wave transmission, 1933-1937," PROC. I.R.E., to be published, November, (1938).

ress which may be effected later so far as the efficiency of directional aerials is concerned.

The gain observed for a directional aerial in the desired direction, compared with a nondirectional aerial, is approximately 10 decibels. The reduction of field in the undesired direction when transfer is made from a nondirectional to a directional aerial is from 5 to 15 decibels.

The result is, therefore, that when directional aerials of a very efficient modern type are employed, the protection which can be hoped for is 15 to 25 decibels on the average, in regions outside the

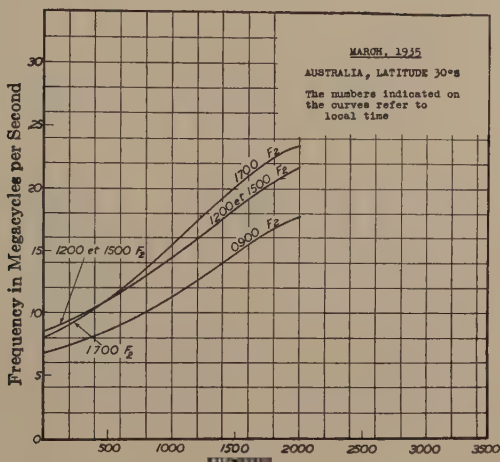


Fig. 38—Maximum usable frequencies for various distances of transmission, based on measurements on the ionosphere at normal incidence.

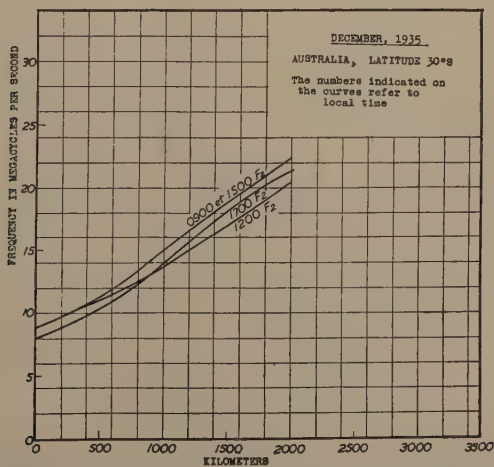


Fig. 39—Maximum usable frequencies for various distances of transmission, based on measurements on the ionosphere at normal incidence.

directional beam. The highest values correspond to the highest frequencies.

These results relate exclusively to broadcast services on short waves

in which the beams are relatively wide at the sender, no directional aerials being employed at the receiver.

It is quite evident that higher coefficients of protection may be obtained in point-to-point services, in which directional aerials, with beams which are narrow both at the sender and the receiver, are employed.

## D. ULTRA-HIGH FREQUENCIES

### 1. Introduction

Waves of frequencies above 30 megacycles (wavelengths below 10 meters) are now usually termed ultra-high-frequency waves. Such waves may be propagated (a) by diffraction around the earth's surface, (b) by refraction in the lower portions of the atmosphere, and (c), in rare cases, by transmission through the ionosphere. Except for very long distance transmission, it is now well known from experience that, to a first approximation, the ionosphere has no effect on the propagation of electromagnetic waves of frequencies greater than about 30 megacycles (wavelengths below 10 meters) particularly when the range of transmission is restricted to moderate distances of a few hundred kilometers. The actual limiting frequency above which such immunity obtains is subject to variation with time and with the condition of solar activity, over a range of 25 to 50 megacycles (12 to 6 meters), but it is customary to take the frequency of 30 megacycles (wavelength, 10 meters) as the transition value.

Further, it is now a well-established experimental fact that the range of transmission of these ultra-high-frequency waves is not by any means limited to the horizon distance or optical line of sight from the sender. Such extended transmission ranges can be accounted for by a diffraction of the waves around the curved surface of the earth, or by a refraction of the waves in the lower regions of the atmosphere due to a variation of density of the air with height above the ground. In general, it is evident that the field at a distance will be due to both diffraction and refraction effects.

### 2. Diffraction

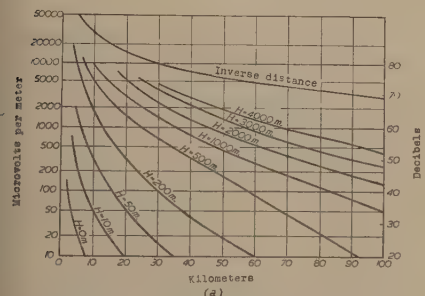
During recent years, extensive theoretical investigations,<sup>4,5,6</sup> of the diffraction problem have been carried out for the case of the bending of

<sup>4</sup> T. L. Eckersley, "Ultra short wave refraction and diffraction," *Jour. I.E.E.* (London), vol. 80, pp. 286-304; March, (1937).

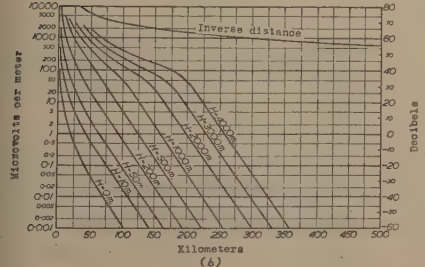
<sup>5</sup> B. van der Pol and H. Bremmer, "The diffraction of electromagnetic waves from an electrical point source round a finitely conducting sphere," *Phil. Mag.*, vol. 24, pp. 141-176, July; and 826-864; Nov., (1937).

<sup>6</sup> B. van der Pol and H. Bremmer, *Hochfrequenztechnik und Elektroakustik*, vol. 51, pp. 181-188, June, (1938).

waves round an ideally smooth spherical earth of finite conductivity. The results of some of these calculations have been provided in a series of graphs, which are convenient for the determination of the field to be expected at various distances for given values of radiated power, frequency, height of sender and receiver, and electrical constants of the ground. Figs. 40 to 59 provide data for five frequencies between 30 and 150 megacycles (wavelengths between 10 and 2 meters) inclusive; for ranges of transmission up to 400 kilometers, and for two sets of



(a)



(b)

Fig. 40

Fig. 40—Field intensity at various distances of diffracted wave over land for various heights of sender and receiver and for a radiated power of 1 kilowatt.

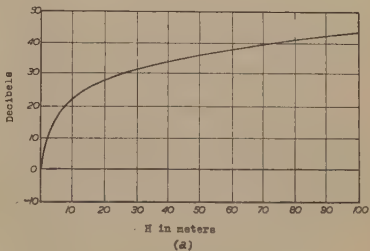
$$f = 150 \text{ megacycles (2 meters)}$$

land  $\epsilon = 5$ ,  $\sigma = 10^{-13}$  electromagnetic units.

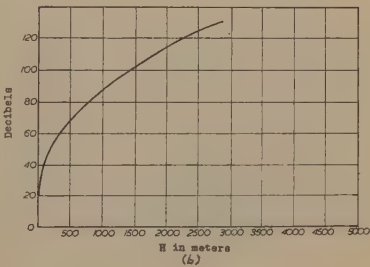
Fig. 41—Gain in field intensity due to elevation of sender or receiver to a height  $H$  above the earth (to be applied to the field intensity values obtained from Fig. 40).

$$f = 150 \text{ megacycles (2 meters)}$$

land  $\epsilon = 5$ ,  $\sigma = 10^{-13}$  electromagnetic units.



(a)

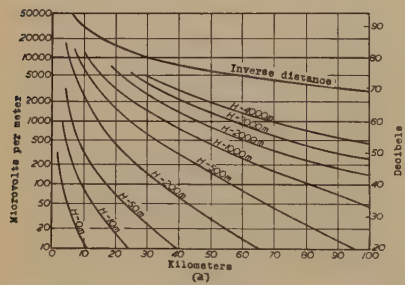


(b)

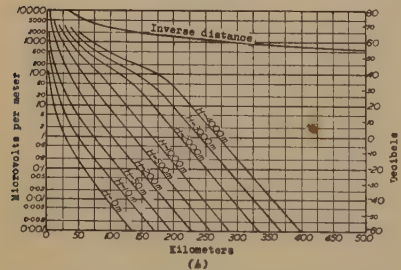
Fig. 41

electrical constants corresponding to average values for land and sea respectively. The field values given as ordinates of the curves refer to reception from a small vertical doublet as transmitting aerial, situated on the earth's surface, and radiating a power of 1 kilowatt. When, as is frequently the case in practice, the sender is raised above the earth's surface, it is assumed that the power supplied to the sender is adjusted so that the current in the aerial remains constant.

The individual curves on each graph refer to the conditions in which either the transmitting or the receiving aerial is raised above the ground by various amounts up to 4000 meters. In this connection it should be mentioned that the principle of reciprocity may be applied to this case of radio communication. Thus the curves illustrated will give either the value of the field at the ground when the sender is raised to various heights, or the field at various heights when the sender is located at the earth's surface. When both the sender and re-



(a)



(b)

Fig. 42—Field intensity at various distances of diffracted wave over land for various heights of sender and receiver and for a radiated power of 1 kilowatt.

$$f = 75 \text{ megacycles (4 meters)}$$

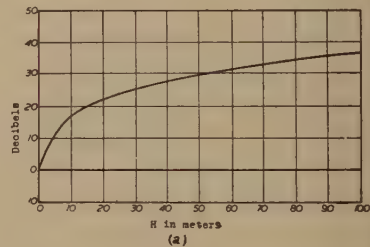
$$\text{land } \epsilon = 5, \sigma = 10^{-13} \text{ electromagnetic units.}$$

Fig. 43—Gain in field intensity due to elevation of sender or receiver to a height  $H$  above the earth (to be applied to the field-intensity values obtained from Fig. 42).

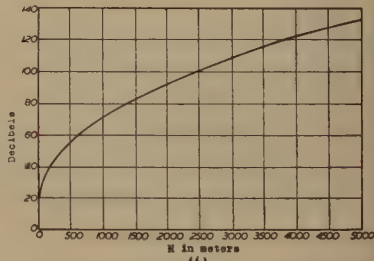
$$f = 75 \text{ megacycles (4 meters)}$$

$$\text{land } \epsilon = 5, \sigma = 10^{-13} \text{ electromagnetic units.}$$

ceiver are elevated, it is necessary to increase the value of the field appropriate to a zero height at one end, by a gain value which is obtained from the series of graphs giving the gain in decibels in relation to the height in meters for which the correction is required. These curves, which are applicable to distances beyond the horizon and which give the relation between height and the resulting gain, are based upon the fact which is implicit in the analysis that, above a certain height



(a)



(b)

Fig. 43

which is only a slowly varying function of the wavelength, the gain in field strength with height is to a high degree of approximation, independent of the earth constants.

As an example of the application of these graphs, we may calculate the field intensity received at a distance of 200 kilometers over land, when the sender is at a height of 100 meters and the receiver at 2000 meters, the frequency employed being 150 megacycles (2 meters). If the transmitter were at the earth's surface and radiating 1 kilowatt, the

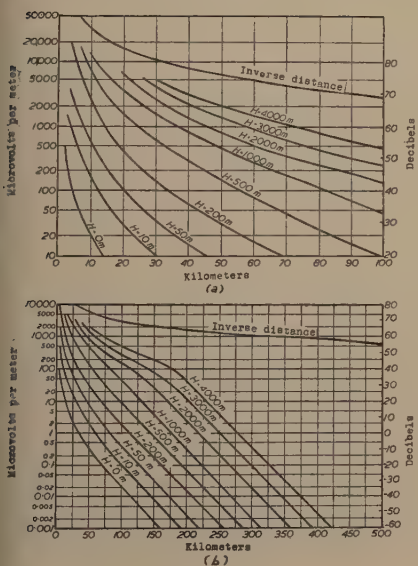


Fig. 44

Fig. 44—Field intensity at various distances of diffracted wave overland for various heights of sender and receiver and for a radiated power of 1 kilowatt.  
 $f = 50$  megacycles (6 meters)  
 land  $\epsilon = 5$ ,  $\sigma = 10^{-13}$  electromagnetic units.

Fig. 45—Gain in field intensity due to elevation of sender or receiver to a height  $H$  above the earth (to be applied to the field-intensity values obtained from Fig. 44).  
 $f = 50$  megacycles (6 meters)  
 land  $\epsilon = 5$ ,  $\sigma = 10^{-13}$  electromagnetic units.

field at the receiver is seen from Fig. 40 (b) to be about 1.0 microvolt per meter. The effect of raising the sender from ground level to a height of 100 meters is seen from Fig. 41 to result in a gain of received field of 43 decibels, equal to a ratio of about 140 to 1. Thus the received field under the conditions stated will be 140 microvolt per meter.

In a more extended analysis of the diffraction problem carried out by an independent method, results have been obtained which represent

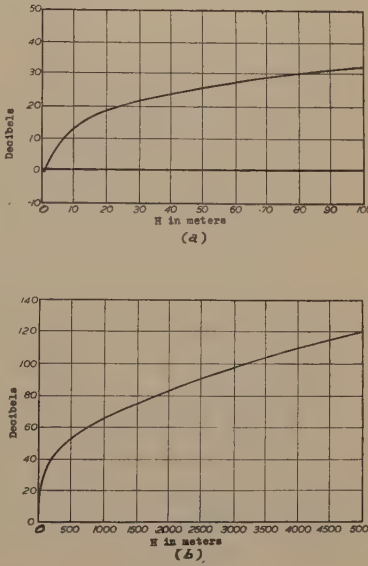


Fig. 45

the actual received fields to a higher accuracy. Examples of the results of these calculations are given in Figs. 60 to 64. Figs. 60 and 61 give graphs of the same type as those considered above showing the relation of field strength to distance for a frequency of 43 megacycles and for electrical constants,  $\sigma = \infty$ ;  $\sigma = 10^{-11}$  electromagnetic units,  $\epsilon = 80$  (sea water); and  $\sigma = 10^{-13}$  electromagnetic units,  $\epsilon = 4$  (average soil). In Fig. 60 the dotted curves refer to a plane earth whereas the full curves correspond to the spherical earth. These curves clearly show

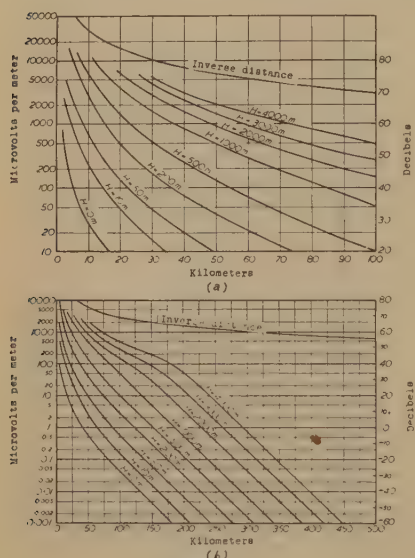
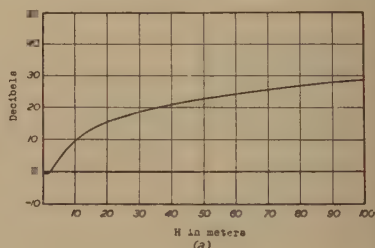
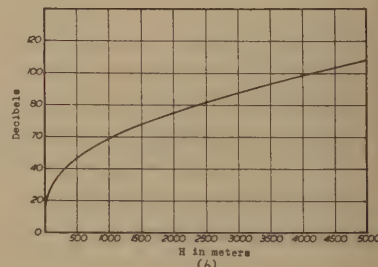


Fig. 46



(a)



(b)

Fig. 46—Field intensity at various distances of diffracted wave over land for various heights of sender and receiver and for a radiated power of 1 kilowatt.  
 $f = 37.5$  megacycles (8 meters)  
 land  $\epsilon = 5$ ,  $\sigma = 10^{-13}$  electromagnetic units.

Fig. 47—Gain in field intensity due to elevation of sender or receiver to a height  $H$  above the earth (to be applied to the field-intensity values obtained from Fig. 46).

$$f = 37.5 \text{ megacycles (8 meters)} \\ \text{land } \epsilon = 5, \sigma = 10^{-13} \text{ electromagnetic units.}$$

that for practical distances the attenuation due to absorption is preponderant compared with the influence of curvature.

Further, Fig. 61 shows the influence of raising the sender to a height  $h_1 = 100$  meters, the receiver being supposed at the surface of the earth ( $h_2 = 0$ ). This figure shows the reduction of the absorption due to the raising of the sender.

Whereas Figs. 60 and 61 give the received field directly, Figs. 62,

63, and 64 represent the attenuation factor by which the field which would obtain in the absence of the earth is to be multiplied. This method of presenting the results demonstrates the nature of the change in the rate of attenuation of the field which occurs as the place of reception passes beyond the horizon.

It is clearly shown that for the case of an earth of infinitely great conductivity, only for frequencies of about 30,000 megacycles or higher (wavelengths of the order of 1 centimeter or less), does there exist a clearly defined shadow effect.

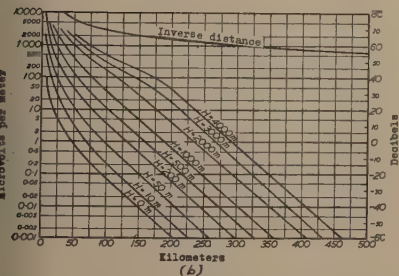
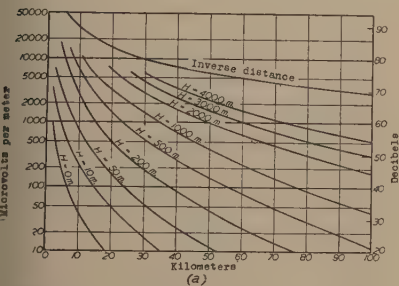


Fig. 48

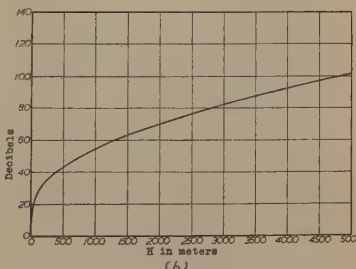
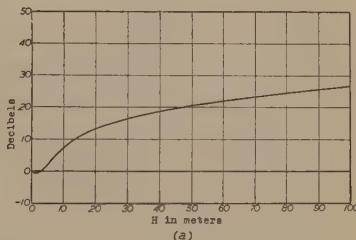


Fig. 49

Fig. 48—Field intensity at various distances of diffracted wave over land for various heights of sender and receiver and for a radiated power of 1 kilowatt.

$f = 30$  megacycles (10 meters)

land  $\epsilon = 5$ ,  $\sigma = 10^{-13}$  electromagnetic units.

Fig. 49—Gain in field intensity due to elevation of sender or receiver to a height  $H$  above the earth (to be applied to the field-intensity values obtained from Fig. 48).

$f = 30$  megacycles (10 meters)

land  $\epsilon = 5$ ,  $\sigma = 10^{-13}$  electromagnetic units.

For all cases encountered in the practical use of ultra-high frequencies at the present time, therefore, no marked shadow effect is to be expected as the distance of the receiver from the sender passes beyond the optical horizon, when either the sender or the receiver is on the ground. On this point, the theory is well confirmed by practical experience. This provides evidence that the decrease in amplitude of

the received field beyond the horizon is still controlled by the absorption effect resulting from the finite conductivity of the ground.

The reliability of the theoretical curves presented above in Figs. 40 to 59 has been checked as far as possible by comparison with such experimental data as have so far become available. These data cover various frequencies between 31 and 400 megacycles (8.8 and 0.733 meters), heights of sender or receiver up to about 1000 meters, and distances ranging up to 200 kilometers. On the whole, the agreement

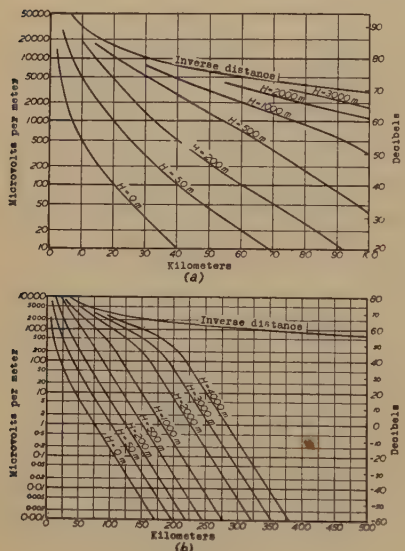


Fig. 50

Fig. 50—Field intensity at various distances of diffracted wave over land for various heights of sender and receiver and for a radiated power of 1 kilowatt.  
 $f = 150$  megacycles (2 meters)  
 $\text{sea } \epsilon = 80, \sigma = 4 \times 10^{-11}$  electromagnetic units.

Fig. 51—Gain in field intensity due to elevation of sender or receiver to a height  $H$  above the earth (to be applied to the field-intensity values obtained from Fig. 50).

$$f = 150 \text{ megacycles (2 meters)} \\ \text{sea } \epsilon = 80, \sigma = 4 \times 10^{-11} \text{ electromagnetic units.}$$

between theoretical and experimental results is moderately good, especially in view of the difficulties of carrying out measurements of the absolute values of field intensities at ultra-high frequencies. Until, therefore, the results of further detailed experimental investigations become available, the theoretical curves provided above form a basis for predicting the signal to be expected without refraction effects over any practical radio-communication circuit operating on ultra-high

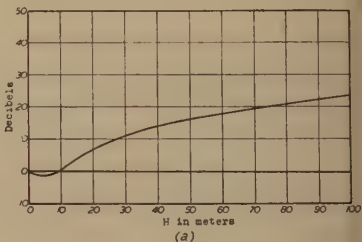
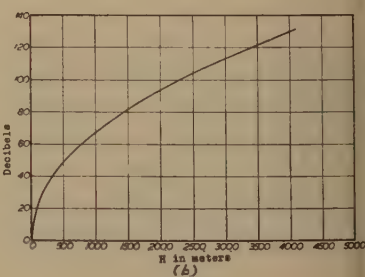


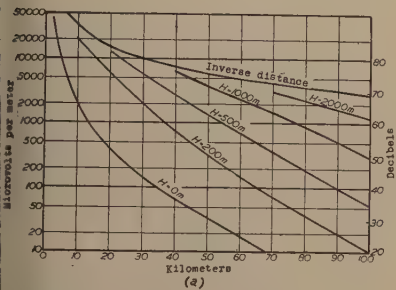
Fig. 51



frequencies up to distances of 400 kilometers. It should be noted that these results are not applicable to cases in which irregularities on the surface of the earth introduce serious departures from the ideal conditions assumed.

### 3. Refraction

When the range of reception on ultra-high frequencies exceeds a few kilometers, the transmitted waves become subject to an appreciable



(a)

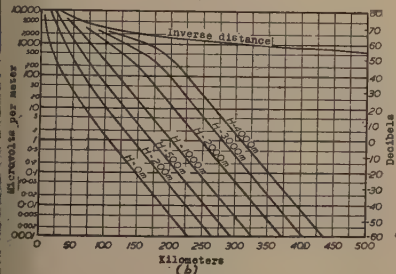
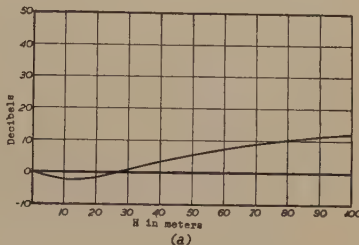


Fig. 52



(a)

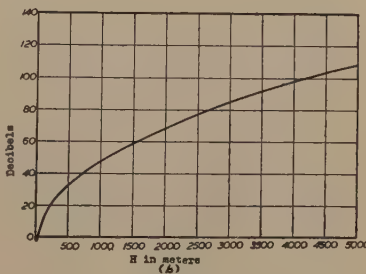


Fig. 53

Fig. 52—Field intensity at various distances of diffracted wave over land for various heights of sender and receiver and for a radiated power of 1 kilowatt.

$$f = 75 \text{ megacycles (4 meters)}$$

$$\text{sea } \epsilon = 80, \sigma = 4 \times 10^{-11} \text{ electromagnetic units.}$$

Fig. 53—Gain in field intensity due to elevation of sender or receiver to a height  $H$  above the earth (to be applied to the field-intensity values obtained from Fig. 52).

$$f = 75 \text{ megacycles (4 meters)}$$

$$\text{sea } \epsilon = 80, \sigma = 4 \times 10^{-11} \text{ electromagnetic units.}$$

able refraction in the atmosphere due to the density gradient which normally prevails for small heights above the earth's surface. This refraction results first in an increase in the field intensity at the receiver, as the rays will become concave towards the earth's surface, and, second, in a variation in the field, due to variations in the atmospheric density gradient. The total field at the receiver is thus the

resultant effect of the diffraction and refraction of the waves in their passage from sender to receiver.

The increase in the steady component of the field which results from refraction can be calculated for a given uniform gradient of refractive index of the air, as has been shown.<sup>1</sup> Theoretically, the phenomenon may be taken account of by increasing the value of the effective radius of the earth used in the diffraction formula. The result is that the slope of the straight portions of the graphs in Figs. 40 (b)

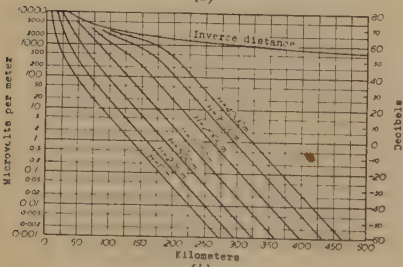
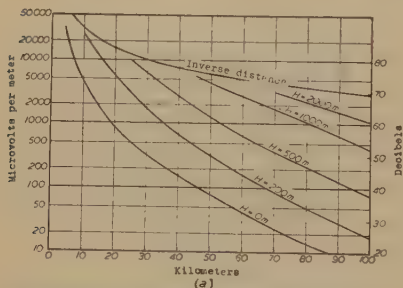


Fig. 54

Fig. 54—Field intensity at various distances of diffracted wave over land for various heights of sender and receiver and for a radiated power of 1 kilowatt  
 $f = 50$  megacycles (6 meters)  
 sea  $\epsilon = 80$ ,  $\sigma = 4 \times 10^{-11}$  electromagnetic units.

Fig. 55—Gain in field intensity due to elevation of sender or receiver to a height  $H$  above the earth (to be applied to the field-intensity values obtained from Fig. 54).  
 $f = 50$  megacycles (6 meters)  
 sea  $\epsilon = 80$ ,  $\sigma = 4 \times 10^{-11}$  electromagnetic units.

42 (b) to 58 (b), is decreased in the ratio  $(R_0/R_1)^{2/3}$  where  $R_0$  is the actual radius of the earth and  $R_1$  is the effective radius.

If the refractive index  $\mu$  as a function of the height  $h$  can be expressed in the form  $\mu = \mu_0 - ah$ , where  $\mu_0$  is the value at the ground and  $a$  is a constant, then

$$R_1 = \frac{R_0}{1 - aR_0}$$

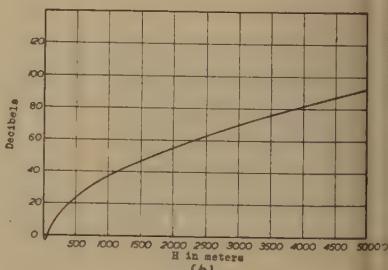
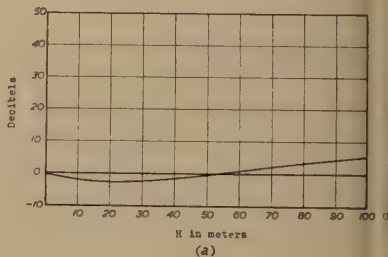


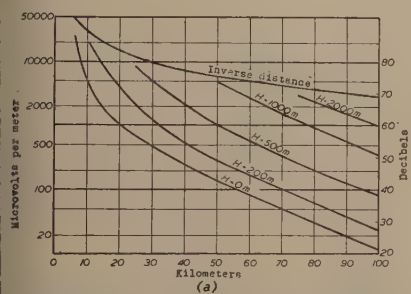
Fig. 55

whence

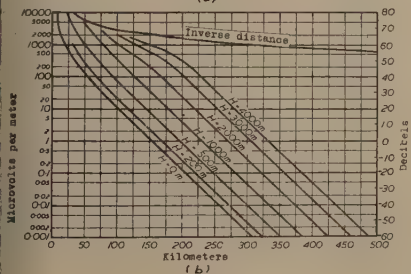
$$\left(\frac{R_0}{R_1}\right)^{2/3} = (1 - aR_0)^{2/3}$$

in which  $R_0$  must be measured in the same units as  $h$ .

Thus the effect of refraction under these ideal circumstances can be accounted for by reducing the slope of the straight portion of the appropriate diffraction curve by the factor  $(1 - aR_0)^{2/3}$ , in which the value of  $a$  can be obtained from meteorological data.<sup>7,8</sup>



(a)



(b)

Fig. 56

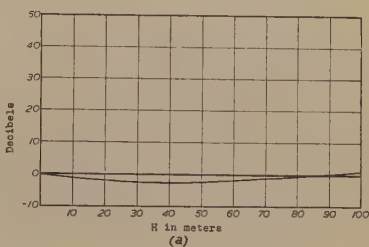
Fig. 56—Field intensity at various distances of diffracted wave over land for various heights of sender and receiver and for a radiated power of 1 kilowatt.  
 $f = 37.5$  megacycles (8 meters)  
 $\text{sea } \epsilon = 80, \sigma = 4 \times 10^{-11}$  electromagnetic units.

Fig. 57—Gain in field intensity due to elevation of sender or receiver to a height  $H$  above the earth (to be applied to the field-intensity values obtained from Fig. 56).  
 $f = 37.5$  megacycles (8 meters)  
 $\text{sea } \epsilon = 80, \sigma = 4 \times 10^{-11}$  electromagnetic units.

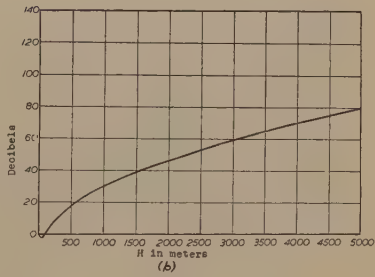
Experimental measurements on the transmission of ultra-high frequencies using frequencies between 32 and 150 megacycles (9.4 to 2

<sup>7</sup> R. L. Smith-Rose and J. S. McPetrie, "Ultra short waves: refraction in the lower atmosphere," *Wireless Eng. and Exp. Wireless*, vol. 11, pp. 3-11; January, (1934).

<sup>8</sup> C. R. Englund, A. B. Crawford, and W. W. Mumford, "Further results of study of ultra-short-wave transmission phenomena," *Bell Sys. Tech. Jour.*, vol. 14, pp. 369-387; July, (1935).



(a)



(b)

Fig. 57

meters) have shown that the fading effects due to refraction in the lower atmosphere become imperceptible at distances of the order of 20 kilometers, if the heights of sender and receiver are not greater than about 100 meters. Under such conditions, the fading appears to be of a slow type and has an amplitude range of only one or two decibels relative to the steady field.

As the distance of transmission is increased, the fading becomes more rapid and increases up to the order of 10 decibels; occasionally

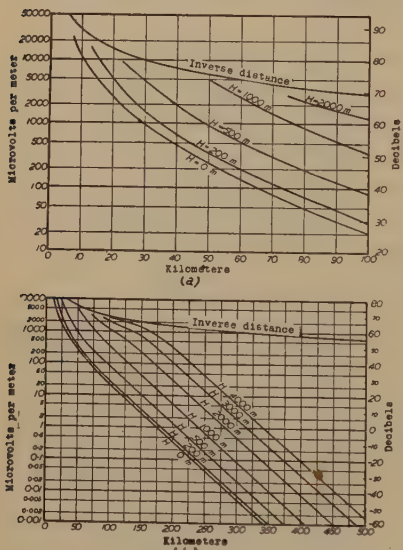


Fig. 58

Fig. 58—Field intensity at various distances of diffracted wave over land for various heights of sender and receiver and for a radiated power of 1 kilowatt.  
 $f = 30$  megacycles (10 meters)  
 $\text{sea } \epsilon = 80, \sigma = 4 \times 10^{-11}$  electromagnetic units.

Fig. 59—Gain in field intensity due to elevation of sender or receiver to a height  $H$  above the earth (to be applied to the field-intensity values obtained from Fig. 58).

$f = 30$  megacycles (10 meters)  
 $\text{sea } \epsilon = 80, \sigma = 4 \times 10^{-11}$  electromagnetic units.

however, the fading may be much more serious. Over ranges of about 120 kilometers, the mean value of the received field has been found to be considerably higher in summer than in winter, while at night the fading is greater and the mean field higher<sup>9</sup> than the corresponding day values. These results must, however, only be taken tentatively as an-

<sup>9</sup> This word was, through an error, given as "lower" ("plus faible" in the French text) in the original.

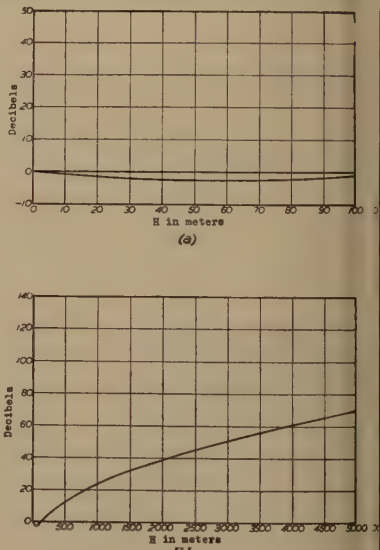


Fig. 59

indication of the type of phenomena observed in miscellaneous experiments on ultra-high frequencies. It will be necessary to obtain the results of many further systematic experimental investigations of this

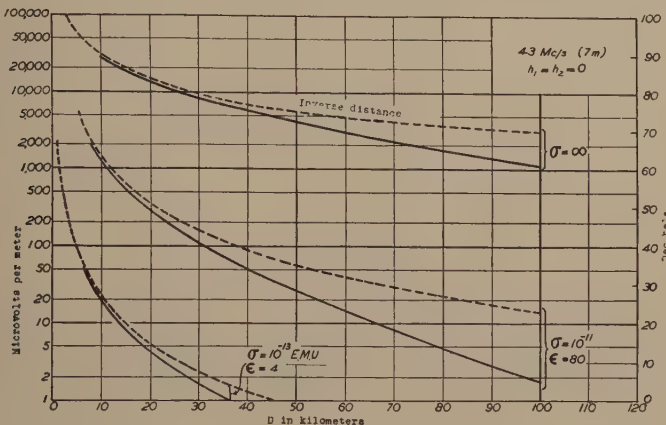


Fig. 60—Influence of the curvature of the earth on the field of the ground wave for  $\sigma = \infty$ ;  $\sigma = 10^{-11}$ ,  $\epsilon = 80$ ; and  $\sigma = 10^{-13}$ ,  $\epsilon = 4$ . Radiation: one kilowatt at 43 megacycles (7 meters). The dotted lines refer to a plane earth, the full lines to a spherical earth. Both the transmitter and the receiver are situated on the ground.

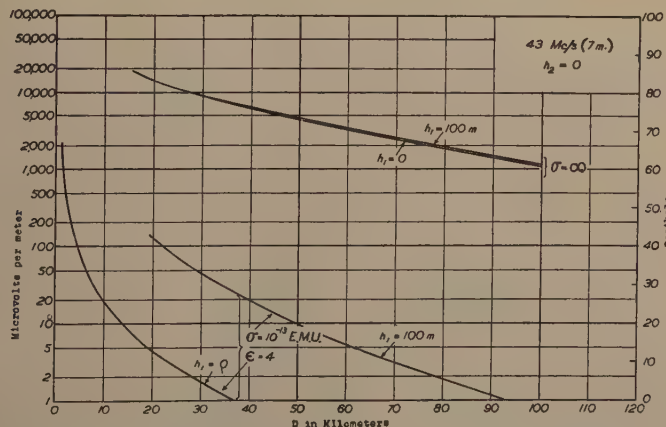


Fig. 61—Effect of raising the sender from ground level to a height of 100 meters on the field at a receiver on the ground at various distances. Radiation: 1 kilowatt at 43 megacycles (7 meters).

phenomenon before any more definite statement can be made as to the effect of refraction in the propagation of ultra-high frequencies. Such data will need to be correlated with the corresponding meteorological data relating to the same conditions and place of observation.

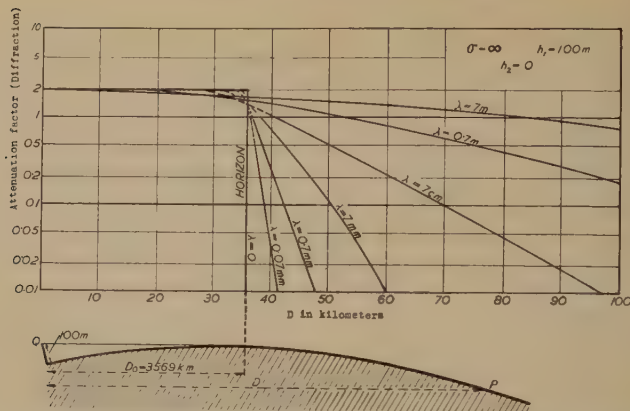


Fig. 62—Diffraction attenuation factor ( $F_{\text{diff}}$ ) of the field at the surface of an infinitely conducting spherical earth for a sender at a height of 100 meters. A sender which would radiate  $P$  kilowatts, in the absence of the earth, actually produces, therefore, the field  $= 150/D_{\text{km}} \cdot \sqrt{P_{\text{kW}}} \cdot F_{\text{diff}}$ .

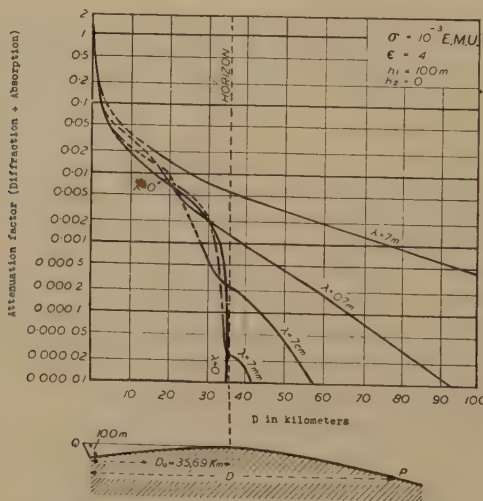


Fig. 63—Attenuation factor ( $F_{\text{diff+abs}}$ ) due to both diffraction (spherical earth) and absorption ( $\sigma = 10^{-13}$ ,  $\epsilon = 4$ ). A sender at a height of 100 meters produces, therefore, at the surface of the earth a field  $= 150/D_{\text{km}} \cdot \sqrt{P_{\text{kW}}} \cdot F_{\text{diff+abs}}$ .

## APPENDIX

### List of Unpublished Documents

#### A. Medium-Frequency Ground-Wave Propagation

- Document No. A. 1. Comparison of the Existing Theories of Wave Propagation over a Spherical, Finitely Conducting Earth (Holland.)

**B. Medium-Frequency Sky-Wave Propagation**

- Document No. B. 1. Allocation Survey. (United States of America.)  
 Document No. B. 2. Supplementary Report on Wave Propagation for the C.C.I.R. (United States of America.)  
 Document No. B. 3. Étude des Courbes de Propagation des Ondes. (U.I.R.)

**C. High-Frequency Propagation.**

- Document No. C. 1. Note on Translantic Frequency—Use Charts. (U.S.A.)  
 Document No. C. 2. Comment on Eckersley's Short-Wave Transmission Charts. (U.S.A.)

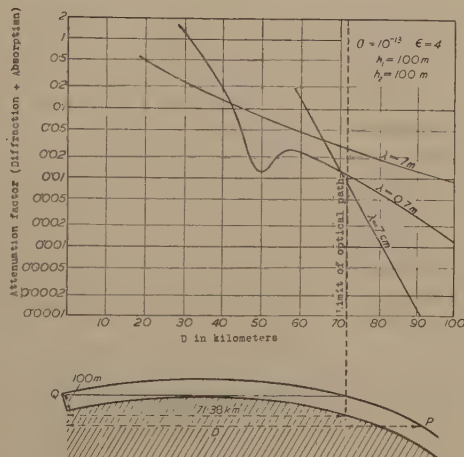


Fig. 64.—Attenuation factor ( $F_{\text{diff+abs}}$ ) due to both diffraction (spherical earth) and absorption ( $\sigma = 10^{-13}$ ,  $\epsilon = 4$ ), when both sender and receiver are raised to a height of 100 meters. The field in this case would therefore be  $150/D_{km} \cdot \sqrt{P_{kw}} \cdot F_{\text{diff+ab}}$ .

Document No. C. 3. Discussion of Eckersley's High-Frequency Transmission Curves. (U.S.A.)

Document No. C. 4. Field-Intensity Contour Charts. (Great Britain.)

Document No. C. 5. Skip Distance Analysis. (Great Britain.)

Document No. C. 6. Graphs of Maximum Usable Frequencies. (U.S.A.)

Document No. C. 7. Method of deriving Maximum Usable Frequencies from Normal Incidence Ionosphere Measurements. (U.S.A.)

Document No. C. 8. Specimen Weekly Broadcasts of Ionosphere Data. (U.S.A.)

Document No. C. 9. Characteristics of the Ionosphere at Washington. (U.S.A.)

Document No. C. 10. Rapport Relatif à la Propagation des Ondes Décamétriques. (France.)

Document No. C. 11. Note on Reciprocity in Radio Propagation. (U.S.A.)

Document No. C. 12. Essais sur la Directivité des Antennes d'Emission: Ondes Courtes. (U.I.R.)

*D. Ultra-High-Frequency Propagation.*

- Document No. D. 1. Comparison between Theory and Experimental Data for Ultra-Short (Metric) Wave Propagation. (Wave-lengths below 10 meters; Frequencies above 30 Megacycles per Second). (Great Britain.)
- Document No. D. 2. Report on Reception of Signals from London Television Station. (Great Britain.)
- Document No. D. 3. Stability of Two-Meter Waves. (U.S.A.)
- Document No. D. 4. Fading in Ultra-High-Frequency Transmission. (U.S.A.)

## A METHOD FOR THE INVESTIGATION OF UPPER-AIR PHENOMENA AND ITS APPLICATION TO RADIO METEOROGRAPHY\*

By

HARRY DIAMOND, WILBUR S. HINMAN, JR., AND F. W. DUNMORE  
(National Bureau of Standards, Washington, D. C.)

**Summary**—Experimental work conducted for the United States Navy Department on the development of a radio meteorograph for sending down from unmanned balloons information on upper-air pressures, temperatures, and humidities, has led to radio methods applicable to the study of a large class of upper-air phenomena. The miniature transmitter sent aloft on the small balloon employs an ultra-high-frequency oscillator and a modulating oscillator; the frequency of the latter is controlled by resistors connected in its grid circuit. These may be ordinary resistors mechanically varied by instruments responding to the phenomena being investigated, or special devices, the electrical resistances of which vary with the phenomena. The modulation frequency is thus a measure of the phenomenon studied. Several phenomena may be measured successively, the corresponding resistors being switched into circuit in sequence by an air-pressure-driven switching unit. This unit also serves for indicating the balloon altitude. At the ground receiving station, a graphical frequency recorder, connected in the receiving-set output, provides an automatic chart of the variation of the phenomena with altitude. The availability of a modulated carrier wave during the complete ascent allows of tracking the balloon for determining its azimuthal direction and distance from the receiving station, data required in measuring the direction and velocity of winds in the upper air.

### I. INTRODUCTION

THE USE of special radio equipment carried aloft in unmanned balloons for the investigation of upper-air phenomena has attracted the attention of a number of scientific workers during recent years. A large class of phenomena may be conveniently studied by such methods at relatively low cost. Examples of such phenomena include meteorological elements, such as barometric pressure, air temperature, humidity, wind velocity, cloud height and vertical thickness, radio wave propagation, light intensity in various parts of the light spectrum, electrical conductivity and voltage gradient, cosmic-ray intensities, etc. Measurements of these phenomena may be carried out at predetermined fixed altitudes or as a function of altitude. In general, besides providing means for translating the variation of the phenomenon to be measured into radio signals which may be interpreted on the ground, the apparatus carried aloft must also trans-

\* Decimal classification: R539.1. Original manuscript received by the Institute, January 6, 1938. Published in *Nat. Bur. Stand. Jour. Res.*, vol. 20, p. 369; June, (1938). Publication approved by the Director of the National Bureau of Standards of the U. S. Department of Commerce.

mit information on the altitude of the balloon. In several of the applications, such as the determination of upper-air wind velocities and radio propagation studies, it is also necessary to know the distance to the balloon, which may be determined by radio direction-finding methods. It is thus desirable that the type of radio emission employed on the balloon be continuous in order to facilitate direction finding.

This paper describes a radio method which fulfills the three requirements just outlined and appears particularly adaptable for the study of certain of the phenomena enumerated. The principal objective of our experiments has been the development of a radio-meteorograph system for use in the aerological service of the Navy Department, at the request of that department. However, as will appear from a description of the method and apparatus evolved, its properties permit of a considerably broader field of application.

## II. CLASSIFICATION OF PRIOR AND CONTEMPORARY DEVELOPMENTS

In general, most upper-air phenomena may be measured in terms of the deflection of mechanical instruments or of changes in the properties of electrical devices. To transmit these measurements by radio to a receiving station on the ground it is necessary to convert the mechanical deflection or the change in electrical properties into an interpretable characteristic of the radio emission. Means for accomplishing this conversion may be divided into three general classifications according to their operation. In one class, the angular deflections from fixed references of the pointers of one or more mechanical instruments are interpreted in terms of time intervals. The various arrangements of the Olland-type radio meteorograph developed in this country and abroad<sup>1,2,3,4,5,6,7,8</sup> are representative of this class. A rotating

<sup>1</sup> P. Moltchanoff, "Zur Technik der Erforschung der Atmosphäre," *Beiträge zur Physik der freien Atmosphäre*, vol. 14, pp. 45-77, (1928). In this paper Moltchanoff proposed adoption of the telemeteorographic principle of Olland to radio meteorography. His first working model was however based on a different principle.

<sup>2</sup> L. Heck and G. Sudeck, "Neue Meteographen für drahtlose Fernübertragung," *Gerlands Beiträge*, vol. 31, pp. 291-314, (1931). "The modern radio Meteorograph," *Nature*, vol. 130, pp. 1006-1007; December, (1932). These papers<sup>1,2</sup> give descriptions of the first radio meteorograph utilizing the Olland principle; this instrument was developed by Moltchanoff and manufactured by the Askania Werke, Germany.

<sup>3</sup> W. H. Wenstrom, "Radiometeorography as applied to unmanned balloons," *PROC. I.R.E.*, vol. 23, pp. 1345-1355; November, (1935).

<sup>4</sup> K. O. Lange, "Radiometeographs," *Bull. Amer. Meteorological Soc.*, vol. 16, pp. 233-236, October; 267-271, November; 297-300, December, (1935). These papers<sup>3,4</sup> represent reviews of the prior art.

<sup>5</sup> L. F. Curtis and A. V. Astin, "A practical system for radio-meteorography," *Jour. Aero. Sci.*, vol. 3, pp. 35-39; November, (1935). An Olland-type radio

contactor, propelled by a clock or other drive, makes contact as it passes pointers which are controlled by changes in pressure, temperature, and humidity, and thereby keys the radio transmitter. The time intervals between these contacts and others which the rotating contactor makes regularly with fixed points may be interpreted as definite values of pressure, temperature, and humidity. A special case of this class consists in converting electrical impulses into the operation of a relay for keying the balloon transmitter, the frequency of keying being a measure of the intensity of the phenomenon producing the impulses. This method has been applied to the study of cosmic rays.<sup>9</sup>

In a second class, the deflections of the pointers are interpreted in terms of some measuring scale independent of time. The radio meteorographs developed by Moltchanoff<sup>10</sup> and Bureau<sup>11</sup> and the pressure indications employed by Duckert<sup>12</sup> are representative of this class. In the Moltchanoff arrangement, the pointer deflections are interpreted in terms of coded signals repeated in distinctive groupings. In Bureau's arrangement, the pointers are grouped as in the Olland method; however, the rotating contactor carries with it a means for mechanically modulating the transmitter so that the angular deflection of a given pointer from its zero reference is interpreted in terms of the number of cycles of the modulation occurring between the corresponding contacts rather than in terms of the intervening time. In the Duckert instrument, the barometer serves to interrupt the transmitter at fixed pressure levels; by keeping track of the number of interruptions occurring from the beginning of an ascension, the pressure level corresponding to a given interruption may be determined.

In the third class, the deflections of mechanical instruments or the

---

meteorograph similar to the Askania-Werke model, but employing ultra-short waves.

<sup>6</sup> K. O. Lange, "The 1935 radio meteorograph of Blue Hill Observatory," *Bull. Amer. Meteorological Soc.*, vol. 17, pp. 136-147; May, (1936). An Olland-type radio meteorograph employing ultra-short waves and having an expanded scale to reduce errors due to the pulsating motion of the clock arm.

<sup>7</sup> O. C. Maier and L. E. Wood, "The Galciet radio meteorograph," *Jour. Aero. Sci.*, vol. 4, pp. 417-422; August, (1937). An Olland-type radio meteorograph on 200 megacycles.

<sup>8</sup> L. F. Curtis and A. V. Astin, "An electric motor for radio meteorographs," *Rev. Sci. Instr.*, vol. 7, pp. 358-359; September, (1936).

<sup>9</sup> L. F. Curtis, A. V. Astin, L. L. Stockman, B. W. Brown, S. A. Korff, "Cosmic ray observations in the stratosphere," *Phys. Rev.*, vol. 53, pp. 23-29; January, (1938).

<sup>10</sup> P. Moltchanoff, "On the accuracy of the atmosphere investigations by means of radio meteorographs," (In Russian—title in English). *Meteorologia i Hydrologia*, vol. 2, pp. 30-41, (1936).

<sup>11</sup> R. Bureau, "Les Radiosondages meteorologiques," *L'Onde Elec.*, vol. 14, pp. 10-26; January, 87-96; February, (1935).

<sup>12</sup> P. Duckert, "Das Radiosondemodell Telefunken und seine Anwendung," *Beiträge zur Physik der freien Atmosphäre*, vol. 20, pp. 303-311, (1933).

changes in properties of electrical devices are caused to vary either the carrier frequency or the modulating frequency of the balloon transmitter and the values of the effects studied are interpreted in terms of the frequency. In the radio meteorograph developed by Väisälä,<sup>13,14</sup> three condensers, controlled respectively by mechanical instruments responsive to pressure, temperature, and humidity, and two additional calibrating condensers are successively switched into the carrier oscillator circuit. The values of pressure, temperature, and humidity are interpreted in terms of the carrier frequency. Similarly, in the Duckert radio meteorograph, a bimetal thermometer controls a condenser which varies the carrier frequency. Feige<sup>15</sup> devised a modification of the Duckert radio meteorograph for measuring cloud height and vertical thickness. He substituted a photoelectric cell for the bimetal thermometer and employed a special milliammeter, carrying a variable condenser, for controlling the carrier frequency as a function of the current through the photocell, and, hence, as a function of light brightness.

Consideration of the several means described for translating variations in the phenomena under investigation into interpretable characteristics of the emitted signals reveals that they are more suited to the use of mechanical instruments than to electrical devices. In the two cases<sup>9,15</sup> discussed in this section where electrical devices are employed, their variations are first converted into mechanical deflections before they are caused to control a characteristic of the radio emission.

### III. BASIS OF OUR METHOD

In our experimental work, a method was sought which would not be restricted to the use of mechanical devices. The basis for this search is the fact that a number of the upper-air phenomena which it was desired to study are best measured by means of electrical devices. In particular, there appeared to be possibilities in such a method for eliminating the operational difficulties involved in the use of the several radio meteorographs described in the previous section. A study of such devices revealed that a considerable number of them were characterized by changes in electrical resistance as a function of the

<sup>13</sup> Vilho Väisälä, "Eine Neue Radiosonde," *Mitteilungen des Meteorologischen Instituts der Universität Helsingfors*, vol. 29, pp. 1012-1029, (1935).

<sup>14</sup> Vilho Väisälä, "The Finnish radio-sound," *Mitteilungen des Meteorologischen Instituts der Universität Helsingfors*, vol. 35, pp. 1-28, (1937).

<sup>15</sup> R. Feige, "Zur Messung der oberen Wolken- und Nebelgrenze auf drahtlichem und drahtlosen Wege," *Zeit. für Instrumentenkunde*, vol. 54, pp. 23-26, (1934).

phenomena to which they were responsive. For example, the temperature coefficient of resistance of certain electrolytes is quite high so that their variation in resistance may be used as a measure of temperature; the surface-leakage resistance of certain glasses may be used as a measure of humidity; the resistance of an air gap ionized by a radioactive substance varies as a function of the barometric pressure, the equivalent resistance of a photoelectric cell varies as a function of light intensity or brightness, etc. Accordingly, a translating means was desired wherein the variation of electrical resistance was caused to vary a characteristic of the radio emission from the balloon, *viz*, the modulating frequency.

The negative transconductance circuit described by Herold,<sup>16</sup> (of the voltage-controlled type), was adapted to this purpose since it provided a lightweight audio-frequency oscillator in which the generated frequency is approximately inversely proportional to the grid-circuit resistance. With this translating means, electrical devices having inherent resistance variation as a function of some phenomenon may be connected directly in the grid circuit while the deflection of a mechanical instrument responsive to some phenomenon is readily converted into the variation of a grid-circuit resistor.

An added advantage of the negative-transconductance circuit is that the generated audio frequency is also a function of the bias voltage on the control grid so that electrical devices producing a variable current through a constant grid-circuit resistor may also be made to vary the modulating frequency of the emitted radio wave. For example, a Geiger counter may be connected in a suitable resistance-capacitance network to supply a variable current to the grid-circuit resistor, the average value of this current being directly proportional to the frequency of the counter breakdown. The generated audio frequency, varying in accordance with the resultant variations in the grid bias voltage, will then be a measure of the cosmic-ray intensity. Similarly, the variation in electrical charge on collecting conductors may be used to produce a proportional variation in the grid bias voltage, and, hence, the generated audio frequency of the modulating oscillator may be made a function of atmospheric potential gradient or conductivity.

A particular advantage of the translating means just described is that the continuous emission from the balloon on a constant carrier frequency facilitates the application of direction-finding methods at the ground station.

<sup>16</sup> E. W. Herold, "Negative resistance and devices for obtaining it," Proc. I.R.E., vol. 23, pp. 1201-1223; October, (1935).

#### IV. THE TRANSMITTING CIRCUIT ARRANGEMENT

A circuit diagram of the radio transmitting equipment used on the balloon is given in Fig. 1.\* The transmitter employs a type 1A6 tube for the audio-frequency oscillator, a type 32 tube as an audio-frequency amplifier, and a type 30 tube as a radio-frequency oscillator. The audio-frequency oscillator operates on the negative characteristic produced between grids 2 and 4 of the 1A6 tube. Its frequency-determining circuit consists primarily of the charging condenser  $C$  and of the total resistance of the control-grid circuit. In this circuit,  $V$  is the device whose electrical resistance varies as a function of the phenomenon to be measured and  $R$  and  $R_2$  are limiting resistors to fix, respectively, the lower and upper limits of the frequency range covered. (A range of from 20 to 200 cycles has been employed in practically all of our ex-

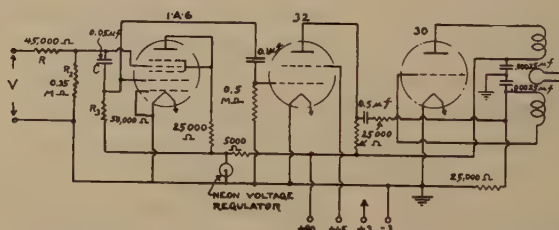


Fig. 1—Electrical circuit arrangement of the radio transmitter used on the balloon.

periments.) The generated frequency is, however, also dependent to a considerable extent upon the value of the charging resistor  $R_3$ , upon the plate-battery voltage, the internal battery resistance (which adds to the charging resistance), and, to a lesser degree, upon the filament-battery voltage. The frequency is also affected by radio-frequency feedback into the grid circuit which operates to change the effective control-grid bias. The voltage-regulating neon tube in Fig. 1 is employed to minimize the effect of variations in the plate-battery voltage and in its internal resistance. The audio-frequency amplifier serves to reduce the radio-frequency feedback and at the same time presents a

\* In recent application of our method to radio meteorographs, a simplified transmitting circuit arrangement has been devised which employs a single type 19 (double-triode) electron tube in order to reduce cost. This arrangement, based on suggestions of RCA Radiotron, Inc., utilizes one triode as a modulating oscillator and the other as the carrier-frequency oscillator. The modulating oscillator operates at 1 megacycle per second in short pulses occurring at an audio-frequency rate, controlled by the time constant of a resistance-capacitance network connected in the grid circuit. The carrier-oscillator output is interrupted during the pulses. The carrier wave sent out by the transmitter is thus modulated at an audio rate which is substantially inversely proportional to the value of resistance in the resistance-capacitance network.

high-impedance load to the output circuit of the audio-frequency oscillator.

Grid modulation of the radio-frequency oscillator is employed, nearly complete modulation of the emitted carrier being obtained. In our experiments we have used carrier frequencies ranging from 50 to 200 megacycles, the upper frequencies in this range being generated by means of a special type 955 acorn tube having low filament-power consumption.

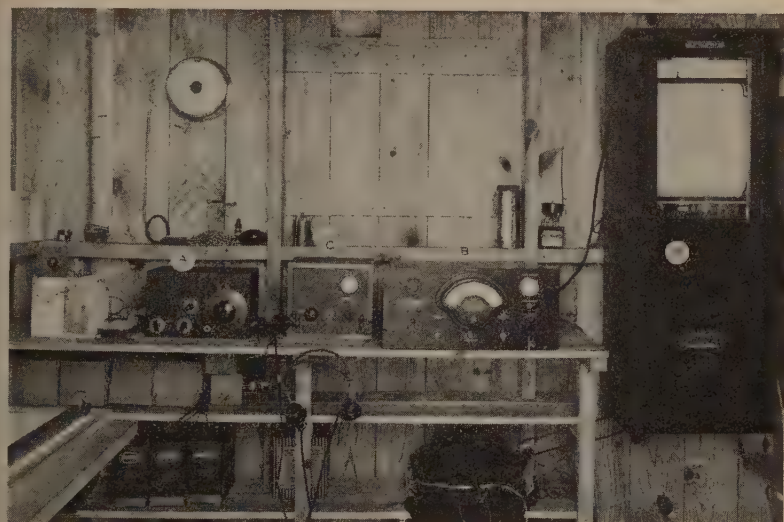


Fig. 2—Ground-station receiving and recording equipment.

With the various precautions used for increasing the frequency stability of the audio-frequency oscillator, as indicated, the generated frequency corresponding to a given grid-circuit resistance remains constant within  $\pm 3$  per cent for changes in the filament-battery voltage of from 3 to 2 volts, for changes in the plate-battery voltage of from 90 to 65 volts, in the plate-battery resistance of from 100 to 1500 ohms, in the transmitter temperature of from +40 to -60 degrees centigrade, and in the antenna load of from 100 to 20 per cent. These variations represent the extreme limits encountered in the usual upper-air studies.

#### V. THE GROUND-STATION RECEIVING EQUIPMENT

A photograph of the ground-station receiving and recording equipment used with this method is shown in Fig. 2. The superregenerative receiving set *A* feeds an electronic frequency meter *B* through a suitable amplifier and electrical filter unit *C*. The electronic frequency

meter operates to deliver a series of direct-current pulses to its indicating meter the average value of which ranges from 0 to 500 microamperes as the frequency varies from 0 to 200 cycles. This current is filtered to an average value and the voltage drop obtained by passing it through a resistor is applied to the input terminals of a high-speed recording millivoltmeter *D*. The complete setup is essentially a recorder which converts the audio-frequency notes received in the radio-receiver output into a graphical chart. The abscissa scale of the chart may obviously be calibrated directly in terms of the phenomenon measured, provided the generated audio frequency in the balloon transmitter is a known function of the phenomenon.

In the first use of the receiving setup, considerable difficulty was experienced due to the varying wave form of the received audio-frequency note. The frequency meter responds to the predominant harmonic of the voltage applied to its input terminals. The wave form produced by the audio-frequency oscillator in the balloon transmitter departs considerably from a sine wave. This wave form is further distorted during modulation of the radio-frequency oscillator and during demodulation by the superregenerative detector. The audio-frequency system of the radio receiver also modifies the wave form of the received signal. As a result, the frequency meter did not always respond to the fundamental (first harmonic) but, particularly for the lower frequencies, would frequently indicate in accordance with the second, third, or even fourth harmonic. This difficulty was overcome through adoption of a filter unit which rejected all frequencies above 300 cycles and by modifying the audio-frequency system of the radio receiver so that maximum amplification occurred at 20 cycles with progressively decreasing amplification for increasing frequencies. At 200 cycles, the voltage amplification is only one third that at 20 cycles.

The limited frequency response of the audio-frequency circuits, coupled with the operation of the frequency meter to respond only to the predominant note of a signal renders the receiving system quite free from interference. An interfering signal must have a single note below 300 cycles which is of greater intensity than the desired signal before it can take over the operation of the frequency meter and recorder.

The receiving setup is practically automatic in its operation. There is little need for retuning except just after the transmitter has left the ground. Two separate automatic-volume-control features take care of the large variation in received voltage as the distance of the balloon transmitter from the receiving station increases. The first is inherent in the operation of the superregenerative detector while the second is provided by the frequency meter which operates accurately for a range of input voltages of from 2 to 150 volts.

## VI. APPLICATIONS OF OUR METHOD IN SIMPLIFIED FORMS

The operation of our method is best illustrated by means of several simplified applications. In Figs. 3 and 4 are shown experimental models of electrical devices designed to respond to temperature and humidity,



Fig. 3—Capillary electrolytic thermometer.



Fig. 4—Electrical hygrometer.

respectively. The temperature device consists of a glass capillary tube filled with an electrolyte having a high temperature coefficient of resistance so that its resistance is a function of temperature. The humidity device consists of a bifilar winding wound on the etched surface of a glass tube, the surface-leakage resistance as measured between the two wires being a function of humidity. Further description of the two devices will be given in later sections. Figs. 5 and 6 show typical charts obtained at the ground receiving station from ascension tests in which the temperature and humidity tubes, previously calibrated, were respectively connected in the grid circuit of the audio-frequency oscillator. The abscissas give the values of the received audio fre-

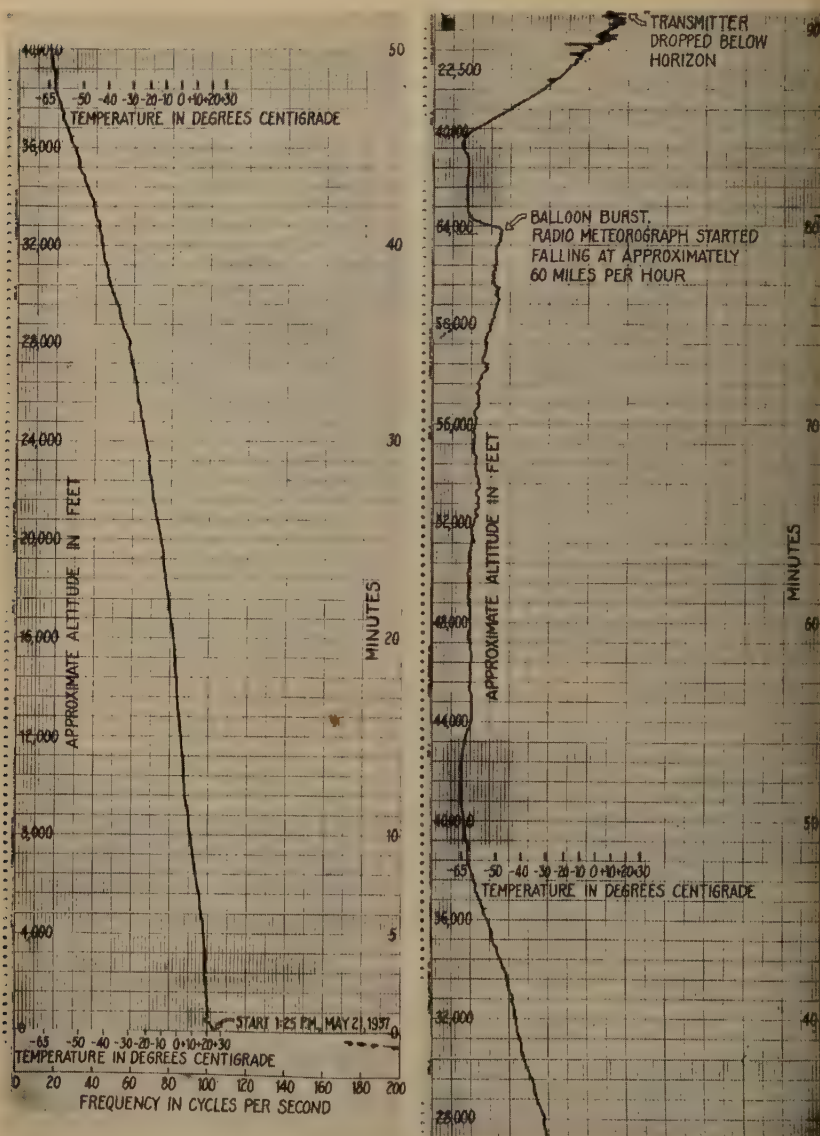


Fig. 5—Ascension record illustrating operation of electrolytic thermometer.

quency and also the corresponding values of the functions measured. The ordinates show the estimated altitude of the balloon based on the amount of balloon inflation at the surface altitude. The balloon rate of ascent is approximately constant (except when the balloon is s

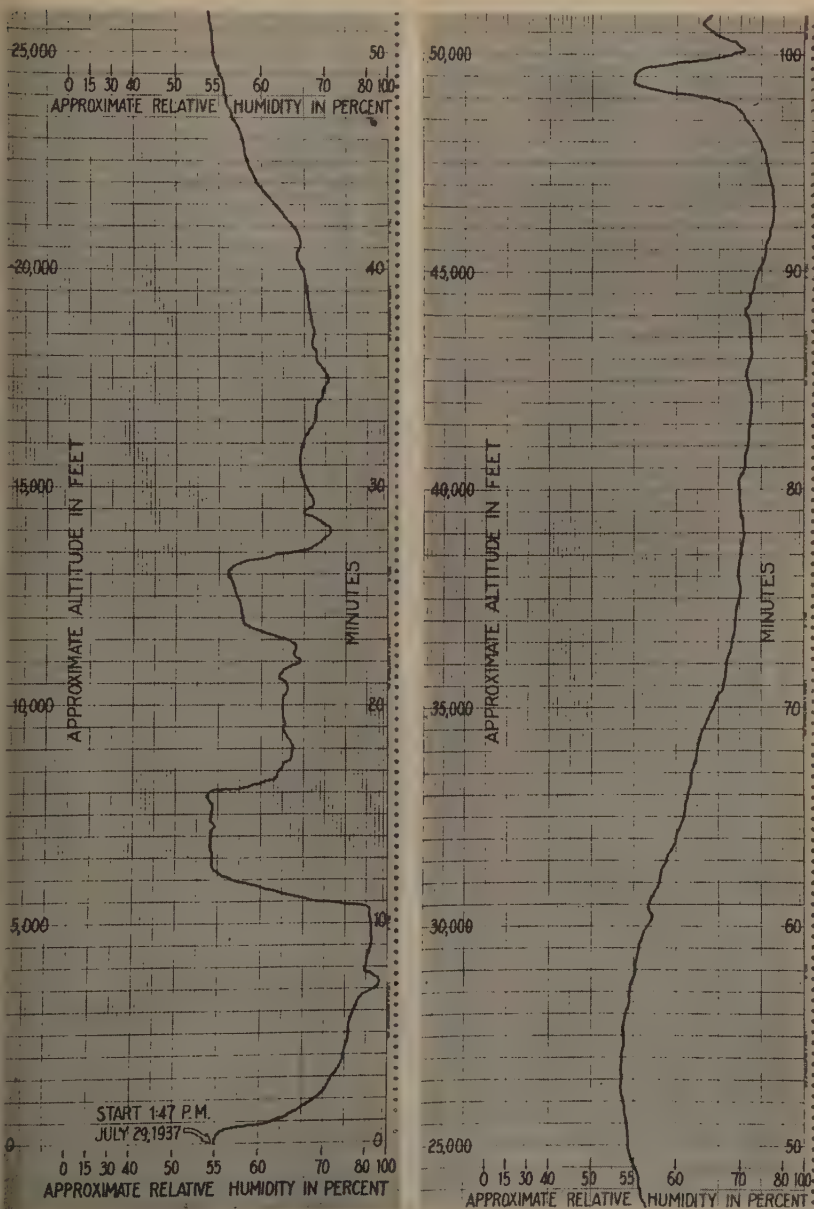


Fig. 6—Ascension record illustrating operation of electrical hygrometer.

close to the bursting point) and, hence, the altitude is directly proportional to the elapsed time from the beginning of the ascent.

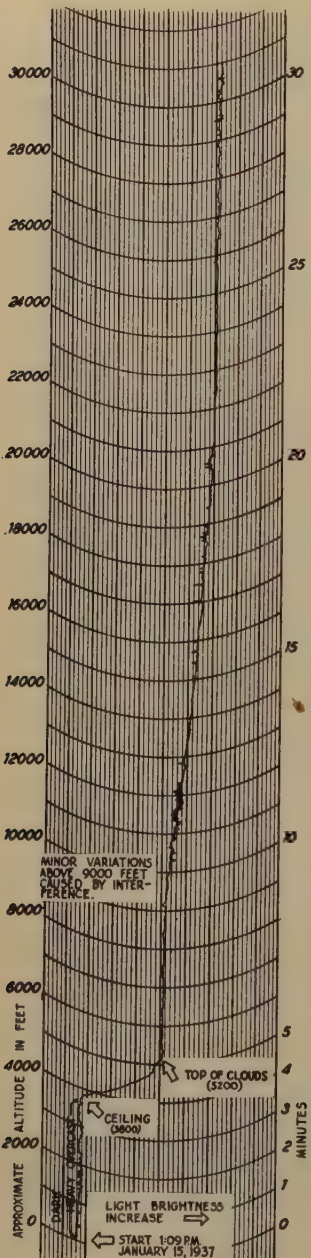


Fig. 7—Ascension record illustrating use of the photoelectric cell in measuring the ceiling and height of top of clouds.

## VII. MEASUREMENT OF CLOUD HEIGHT AND THICKNESS

A record obtained from an ascension test in which a photoelectric cell was connected in the grid circuit of the audio-frequency oscillator to give information on the variation of light brightness with altitude is shown in Fig. 7. Such data give a direct measure of the height to the tops of existing clouds and the visibility conditions above each cloud. The window of the photoelectric cell was pointed downward to eliminate the effect of direct sunlight upon emergence from the clouds. Heavy overcast with intermittent rain occurred on the day of the test.

Referring to the record, the abscissas represent brightness, the reference mark DARK corresponding to complete absence of light. The ordinates represent altitude or elapsed time. As the balloon ascended it will be noted that the brightness was quite low and steady except for minor fluctuations, until the balloon reached approximately 3800 feet. In the altitude range of from 3800 to 5200 feet, the increase in brightness with height indicates the presence of a cloud layer some 1400 feet thick. The balloon, penetrating the light-absorbing layer, is moving toward the region of higher brightness. The chart clearly shows the height of the "ceiling" (3800 feet) and the height to the top of the cloud layer (5200 feet). At 5200 feet the balloon emerged from the cloud and the light brightness remained substantially constant at the increased value until about 9000 feet. The gradual increase in brightness from 9000 to 20,000 feet probably indicates the presence of haze in this altitude region. Above 20,000 feet the brightness reached a constant value.

### VIII. ALTITUDE DETERMINATION

While the measurement of altitude in terms of elapsed time and a predetermined rate of balloon ascent may be sufficiently accurate for some applications, many studies require considerably more precise altitude determination. This requires that the barometric pressure be measured and, in more rigorous applications, also the temperature and humidity. (The altitude correction for temperature may be up to 10 per cent and for humidity up to about 0.5 per cent.) An obvious extension of our method to include the measurement of any number of upper-air phenomena, of which the barometric pressure may be one, consists of the use of a rotary switch which connects into the audio-frequency oscillator grid circuit, in any desired succession, resistors responsive to the various phenomena to be measured. As previously indicated, certain of the resistors may vary inherently with the phenomena or may be controlled mechanically by instruments responsive to the phenomena. The switch may be driven by a spring or electric motor or by an air fan which operates by virtue of the upward motion of the balloon. The switch may also connect into the circuit, at desired intervals, one or more fixed calibrating resistors which may serve as checks on the frequency stability of the audio-frequency oscillator. If frequency drift should occur, the reference frequencies provide means for correcting the various measurements on a proportional basis.

In an early radio-meteorograph model, we employed a fan-driven rotary switch which successively connected into the circuit three variable resistors, controlled respectively by a barometer of the diaphragm type, a bimetal thermometer, and a hair hygrometer, and a fourth, fixed resistor, for reference purposes. This arrangement was found deficient in one respect because of the unusual precision of pressure measurement required in radio meteorography. The Bureau of Aeronautics, United States Navy Department, had formulated the following minimum requirements for radio-meteorograph operation: pressure indications are required in the range of from 1050 to 150 millibars or lower to an accuracy of 1 millibar, temperature indications in the range of from +40 to -75 degrees centigrade to an accuracy of one degree, and humidity indications in the range of from 0 to 100 per cent relative humidity accurate to within 3 per cent. It will be seen that the required accuracy is greatest for the pressure indications. Experiments with the method described showed that accuracies in the frequency measurements of the order of 0.5 per cent could be expected under carefully controlled conditions and of the order of 1 per cent in routine operation. The chief difficulty arose from the fact that the

frequency-resistance characteristic of the audio-frequency oscillator altered somewhat under operating conditions so that, even after correction for drift on the basis of the reference frequency, a residual error of about 0.5 per cent remained. While this error was not sufficient to affect the required accuracy of temperature and humidity indication it was much too large for the pressure measurements.

To increase the accuracy of pressure measurement, we adopted a novel method<sup>17</sup> of indication which at the same time introduced several additional operating improvements. This method makes use of the

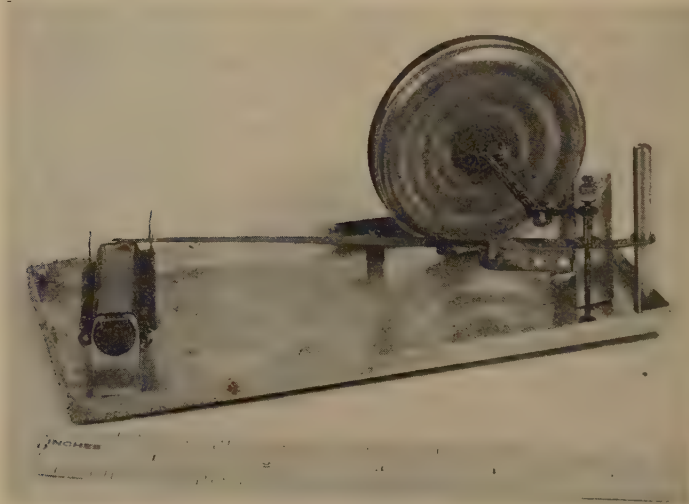


Fig. 8—An experimental model of one form of the pressure-switching unit.

fact that the pressure element deflects continuously in one direction as the balloon ascends, and employs this motion for carrying out the switching operation in the balloon transmitter. The sequence of switching operations serves for absolute indication of the barometric pressure in discrete steps thereby obviating the need for interpreting pressure in terms of either time or frequency. A greater accuracy of indication is inherent in this arrangement. At the same time, the need for any other form of motive power for carrying out the switching operations is eliminated. Other advantages of this type of pressure indication will be considered in the following section.

<sup>17</sup> Some months ago there came to the attention of the authors a description of a temperature-switching arrangement<sup>18</sup> applied to the switching of lights for use of meteorographs at night, somewhat similar to the pressure-switching method which we have developed.

<sup>18</sup> J. Patterson, "A visual signalling meteorograph," *Trans. Royal Soc. (Canada)*, vol. 25, section III, pp. 115-120, (1931).

## Pressure Switching

An experimental model of one form of pressure switching with which we experimented is shown in Fig. 8, and the corresponding electrical circuit arrangement in Fig. 9. The pressure diaphragm operates a pointer which moves over a simple switching element consisting of electrical conducting strips separated by insulating strips. The face of the switching element is polished so that friction opposing the arm movement is negligible. Contact of the pressure arm with a given conducting strip is therefore a direct measure of the barometric pressure to which the diaphragm is subjected. It is necessary only to provide means for identifying the particular conducting strip being contacted to secure an absolute pressure scale. This is accomplished by the se-

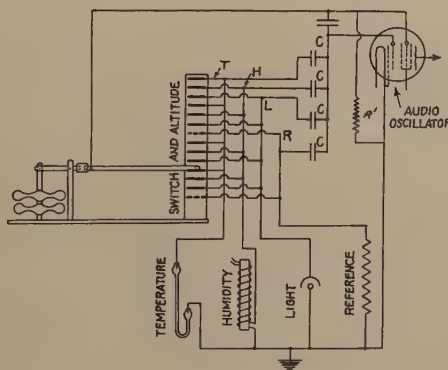


Fig. 9—Schematic of pressure-switching circuit arrangement as employed in the measurement of three properties of the atmosphere in addition to altitude (barometric pressure).

quence of switching into the circuit the several devices employed and by the regular spacing of the conducting strips to which the reference resistor is connected. In Fig. 9 we show elements responsive to temperature, humidity, light brightness, and the reference resistor. The symbols *T*, *H*, *L*, and *R* refer to the conducting strips on the switching element to which they are connected. The pressure arm moving over the conducting strips of the switching element successively connects into the circuit the three devices in the order named and then repeats the sequence. After each two groups, the reference resistor is switched into the circuit. Since it produces a substantially fixed frequency which occurs every seventh contact, the occurrence of this frequency may serve as an index mark on the pressure scale. If desired, successive seventh contacts may switch in different reference resistors to distinguish between index marks. However, since the purpose of the index marks is to eliminate the need for keeping close touch of the number of

contacts from the beginning of an ascent, and since the elapsed time is of considerable assistance in this respect, distinguishing between index marks is not considered essential in this application.

Because of the widely different resistance ranges of the devices shown in Fig. 9, the pressure arm switches in suitable condensers  $C$  (in parallel with the charging condenser) simultaneously with the resistors in order that the generated audio frequencies may remain in the same range, 20 to 200 cycles. This is desirable for convenience in recording. The resistor  $R'$  in Fig. 9 serves as the frequency-limiting resistor for the lower part of the range. It is the frequency-determining resistor when the pressure arm passes over the insulating strips of the switching element.

A second variation of the method of pressure switching shows its adaptability to particular requirements. In routine radio-meteorograph operation, it is desirable that the balloon equipment be as simple as possible in order to reduce weight and to keep the unit price within the cost of the present airplane ascensions made for upper-air soundings. Also, the readings of temperature and humidity should be made at as many altitude levels as possible in order to obtain a nearly continuous picture of their variations. Accordingly, the radio meteorograph designed for use by the Navy Department<sup>19,20</sup> does not include the photoelectric cell; also, the electrical circuit of the pressure-switching unit is arranged so that temperature readings are obtained when the pressure arm is on an insulating segment and humidity readings when the pressure arm is on a conducting segment (exclusive of the index contacts).

A description of this instrument will form the chief subject matter of the remaining portions of this paper. However, before entering into this description, a brief outline will be given of the advantages of pressure switching in combination with the frequency scale for measuring the upper-air phenomena investigated. The advantages are:

(1) The method provides for great flexibility in the measurement of upper-air phenomena, a large class of mechanical and electrical devices being readily employed.

(2) Readings of the phenomena being measured are obtained directly as a function of pressure, which may be readily converted into height. The record obtained at the ground station is plotted in this form and is easy to interpret.

<sup>19</sup> H. Diamond, W. S. Hinman, Jr., and F. W. Dunmore, "Development of a radio meteorograph system for the Navy Department, *Bull. Amer. Meteorological Soc.*, vol. 18, pp. 73-99; March, (1937).

<sup>20</sup> H. Diamond, W. S. Hinman, Jr., and F. W. Dunmore, "A radio meteorograph system with special aeronautical applications," *Jour. Inst. Aero. Sci.*, vol. 4, pp. 241-248; April, (1937).

(3) Observations are obtained at predetermined pressure levels, independent of the rate of ascent of the balloon. This permits using any practicable rate of ascent, thereby reducing the time required for a given set of observations. The use of electrical devices is of particular value in this respect since they are inherently faster in response than mechanical instruments.

(4) The possibility of higher rates of ascent provides other important advantages: (a) since the balloon will not drift so far, there is a greater chance for recovery of the instruments, particularly in near-coastal regions; (b) the shorter range permits taking check observations during the descent of the equipment; (c) battery requirements may be reduced appreciably; (d) better ventilation may be had of instruments requiring ventilation, such as the temperature and humidity devices.

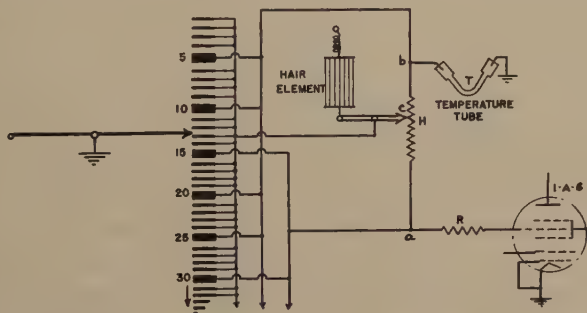


Fig. 10—Electrical circuit arrangement of the pressure-switching unit employed in the Navy radio meteorograph.

(5) The accuracy of pressure indication is practically equal to the accuracy of the instrument itself and does not depend upon any translatory means.

## IX. THE NAVY RADIO METEOROGRAPH

### *Pressure-Switching Circuit Arrangement*

The electrical circuit arrangement of the pressure-switching unit used in the Navy radio meteorograph is shown in Fig. 10. The grid circuit of the audio-frequency oscillator includes three resistors in series,  $R$ ,  $H$ , and  $T$ . The resistor  $R$  is of fixed value.  $H$  is a special resistor which is controlled by a hair hygrometer so that the position of the contact point  $c$  varies in accordance with the relative humidity, being at the point  $a$  for 100 per cent value, at the point  $b$  for 0 per cent, and at intermediate positions for intermediate values of the relative humidity.  $T$  is a special resistor which varies inherently with the temperature. (See Fig. 3.) The switching element consists of 75 conducting strips separated by insulating strips. The conducting strips are

arranged in groups of four adjacent intermediate contacts, the adjacent groups being separated by wider index contacts. The intermediate conducting strips are all connected together while the index contacts are connected in two sets. In Fig. 10, the three resistors are electrically connected to the switching element as shown. The point *a* is connected to one set of index contacts, (numbers 15, 30, 45, etc.); the point *b* is connected to the second set of index contacts, (numbers 5, 10, 20, 25, etc.); and the variable contact point *c* is connected to the intermediate conducting strips of the switching element. The pressure arm *P*, which moves over the switching element, is electrically connected to ground as is also the lower end of the resistor *T*.

It will be seen that so long as the pressure arm rests on one of the insulating strips of the switching element, the series circuit formed by *R*, *T*, and *H* is undisturbed. Since *R* is fixed and the full value of *H* is in circuit, the frequency of the audio-frequency oscillator is controlled by the value of the resistor *T* and hence by the temperature. Assume now that the pressure arm contacts one of the intermediate conducting strips. The contact *c* is thereby connected to ground shorting out a portion of the resistor *H* (*c* to *b*) together with the variable resistor *T*. The value of resistance remaining in circuit consists of *R* and a variable portion of *H* depending upon the position of point *c* and hence on the value of the relative humidity. The frequency of the audio-frequency oscillator is now dependent on the relative humidity. When the pressure arm contacts one of the index segments, it connects either the point *a* or the point *b* to ground, shorting out *H* and *T* together or *T* alone. In the former case, the frequency of the audio-frequency oscillator is determined by the resistor *R* and in the latter case by the resistor *R* in series with the full value of the resistor *H*. Hence two fixed identifying frequencies are produced corresponding to the two sets of index contacts. It will be observed that the identifying frequencies coincide exactly with the frequencies corresponding to 100 and 0 per cent relative humidity. The use made of this feature will appear later.

The complete operation of the system now becomes apparent. The pressure arm, moving continuously in one direction as the balloon ascends, switches the frequency of the audio-frequency oscillator to correspond alternately to the values of the temperature and of the humidity encountered. The alternate change-overs from one set of frequencies to the other indicate that the pressure arm is just reaching or is just leaving one of the intermediate contacts and has attained definite deflection positions which may be determined. When the pressure arm reaches successive fifth conducting segments, the fre-

quency of the audio-frequency oscillator attains predetermined fixed values which positively identify these contacts so that they may serve as index marks for the absolute pressure scale. The two identifying frequencies used serve an additional purpose in that they provide periodic checks during the progress of a flight on the degree of frequency stability of the audio-frequency oscillator. If any accidental variation should occur, for example, due to varying battery conditions, the recorded value of temperature may be corrected for the indicated variations. Corrections to the humidity readings need not be applied even in such event. Upon completion of a record, two lines may be drawn in on the chart to connect the recorded values of the two sets of identifying frequencies. These two lines frame the scale of humidity indications, thereby automatically transferring the plot of humidity indications to a corrected frequency scale.

### *The Temperature Capillary Tube*

A description of the temperature capillary tube is of interest at this point. A photograph of a practical form of this device was shown in Fig. 3. The glass capillary tube has an over-all length of 8 centimeters, a bore diameter of 0.75 millimeter, and a wall thickness of 0.4 millimeter. The dimensions were chosen on the basis of practical considerations, such as mechanical sturdiness, facility of manufacture, and rapidity of response to varying ambient temperatures. The time-lag constant of the device in an air stream of 10 miles per hour is of the order of 2 to 5 seconds.

The electrolyte employed (chosen to give a resistance of 30,000 ohms at +30 degrees centigrade) consists of 24 per cent (by volume) concentrated hydrochloric acid, 76 per cent of ethyl alcohol, and 2.7 grams of cuprous chloride for each 100 cubic centimeters of the resultant combination. This solution has several important advantages for the radio-meteorograph application. It does not freeze at any normal stratosphere temperature reported (down to -80 degrees centigrade). The use of the cuprous chloride minimizes the polarizing action attendant to the passing of a current through the electrolyte; hence, the electrical resistance corresponding to a given temperature is independent of the current and the tube may be calibrated independently of the audio-frequency oscillator with which it is used. Use of predetermined ratios of the ingredients permits a wide choice of resistivity and some control of the temperature coefficient. A detailed account of the properties of this electrolyte is given by Craig.<sup>21</sup>

<sup>21</sup> D. N. Craig, "An electrolytic resistor," *Nat. Bur. Stand. Jour. Res.*, vol. 21, pp. 225-233; August, (1938).

The variation of resistance with temperature for a typical capillary tube is given by curve (a) of Fig. 11 while curve (b) shows the resistance-frequency characteristic of a typical audio-frequency oscillator. The corresponding variation of modulation frequency with temperature when the capillary thermometer is connected in the grid circuit of the audio-frequency oscillator may be evaluated from these two curves, as indicated in Fig. 11.

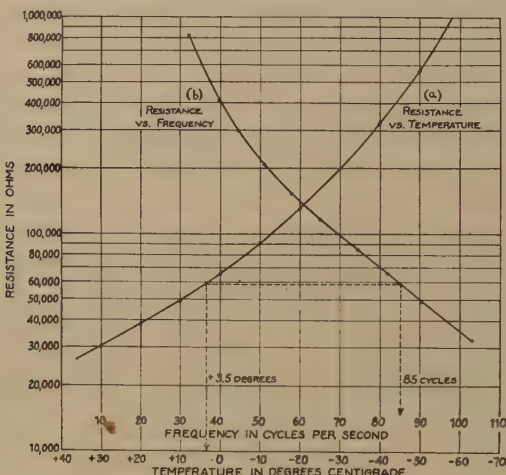


Fig. 11—Graphs showing the variation of electrical resistance with temperature of the electrolytic thermometer and the variation of the generated audio frequency with resistance for a sample audio-frequency oscillator. Together they determine the temperature-frequency scale of the radio meteorograph.

### *The Meteorograph Unit*

Figs. 12 and 13 show two views of the meteorograph which incorporates the pressure-switching unit, the temperature tube, and the hair-controlled hygrometer. In Fig. 12 the pressure diaphragm, linkage, and arm are clearly shown. The end of the pressure arm carries a platinum tip which slides over the polished surface of the switching element. The conducting segments of the switching element stand out in the photograph as white lines, particularly the index contacts, which are of greater thickness.

At *a* in Fig. 12 a small metal cam is shown which is swung about its shaft by two hair elements operating in series (on the other side of the base plate). A wire-wound resistor mounted to pivot at the point *b* is held in contact with the cam by a spring. As the cam moves under the action of the hair hygrometer, the resistor is forced to follow it due to

the spring. A rolling contact is thereby obtained between the metal cam and the resistor. This contact moves from one end of the resistor to the other as the relative humidity varies from 0 to 100 per cent. The arrangement is therefore ideally suited to serve for the resistor  $H$  shown in Fig. 10. This satisfactory arrangement was developed for us by Julien P. Friez and Sons, Inc.

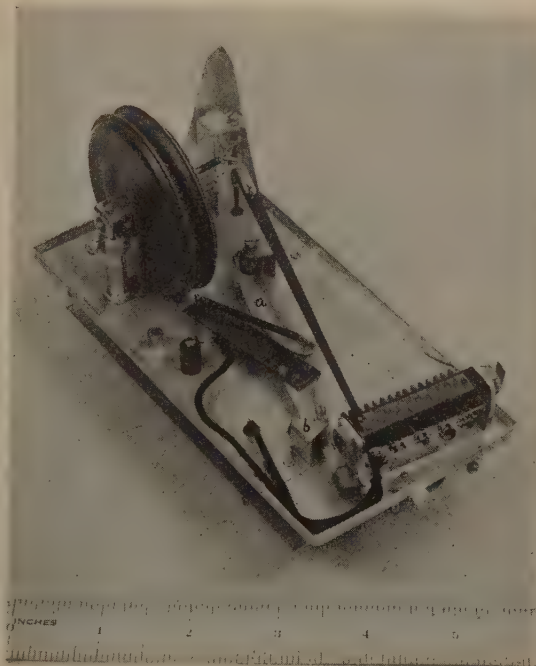


Fig. 12—Front view of the meteorograph unit.

Fig. 13 shows the other side of the meteorograph unit with the radiation shields removed. The hair drive for the metal cam and the temperature capillary tube are seen in this view. The thin metal plate normally mounted between the hair elements and the temperature tube is cut away to permit a view of the hair elements. This plate serves as a shield against the radiation of heat from the base plate to the temperature tube. The ventilated outer radiation shield protects the temperature tube from direct solar radiation.

#### *The Complete Radio-Meteorograph Assembly*

The complete radio meteorograph consists of a radio transmitting unit (operating on a carrier frequency of 65 megacycles), a battery

unit, and a meteorograph. The entire assembly of the three units is contained in a balsa-wood box,  $6 \times 6 \times 4\frac{1}{2}$  inches. (See top view in Fig. 14.) The total weight is two pounds in the current design and is capable of considerable reduction through refinement of the component units. In its present design, the transmitter is capable of over four hours of efficient operation under ground conditions.



Fig. 13—Rear view of the meteorograph unit, with radiation shield removed.

The battery unit consists of two 45-volt batteries for the plate supply and a 3-volt dry-battery unit for the filament supply. The plate batteries weigh slightly over 4 ounces each and have a capacity of 75 milliampere-hours. The filament battery weighs 2 ounces and has a capacity of 750 milliampere-hours. The total plate current required by the transmitter is 15 milliamperes and the filament current is 180 milliamperes. The battery unit is packed in rock-wool insulation in order that it may retain its original heat as long as possible during an ascent. In the course of an ascent, the ambient temperature may drop to -75 degrees centigrade, while the batteries cease to operate when they drop to -20 degrees centigrade. Because of the effect of the

low ambient temperatures upon the battery capacity, the operation of the transmitter during an actual ascent is limited to an average of two hours.

#### Sample Record of an Ascension

Some 75 ascensions have been made using the radio meteorograph described. These have shown the system to be practicable and have provided gratifying records. Fifty of these ascents were made at the

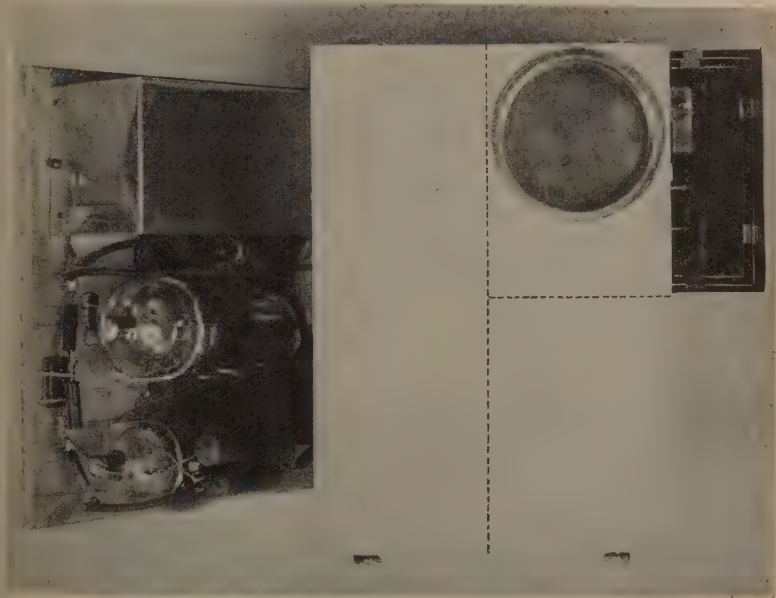
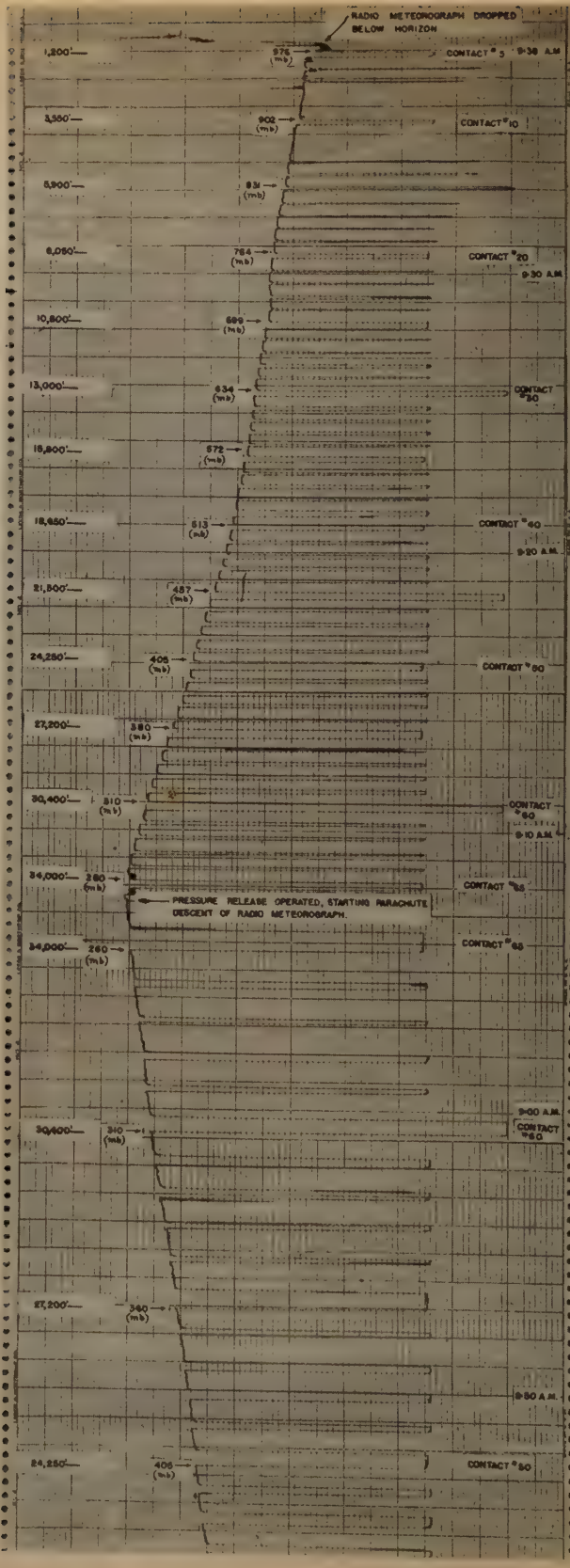


Fig. 14—Complete radio-meteorograph assembly.

Naval Air Station, Anacostia, D. C., under service conditions, and the records obtained were compared with aerograph observations obtained simultaneously in a Navy airplane. The results of these comparisons are described in separate papers.<sup>22,23</sup> The excellent agreement obtained indicates that the accuracy of indication of pressure, temperature, and humidity, while not quite within the requirements set forth in Section VIII, is sufficient to warrant the use of the instrument to replace the present airplane soundings.

<sup>22</sup> H. Diamond, W. S. Hinman, Jr., and E. G. Lapham, "Performance tests of the Navy radio meteorograph system," *Jour. Aero. Sci.*, to be published (1938).

<sup>23</sup> H. Diamond, W. S. Hinman, Jr., and E. G. Lapham, "Comparisons of aerograph, meteorograph and radio meteorograph soundings," *Bull. Amer. Meteorological Soc.*, vol. 19, pp. 129-141; April, (1938).



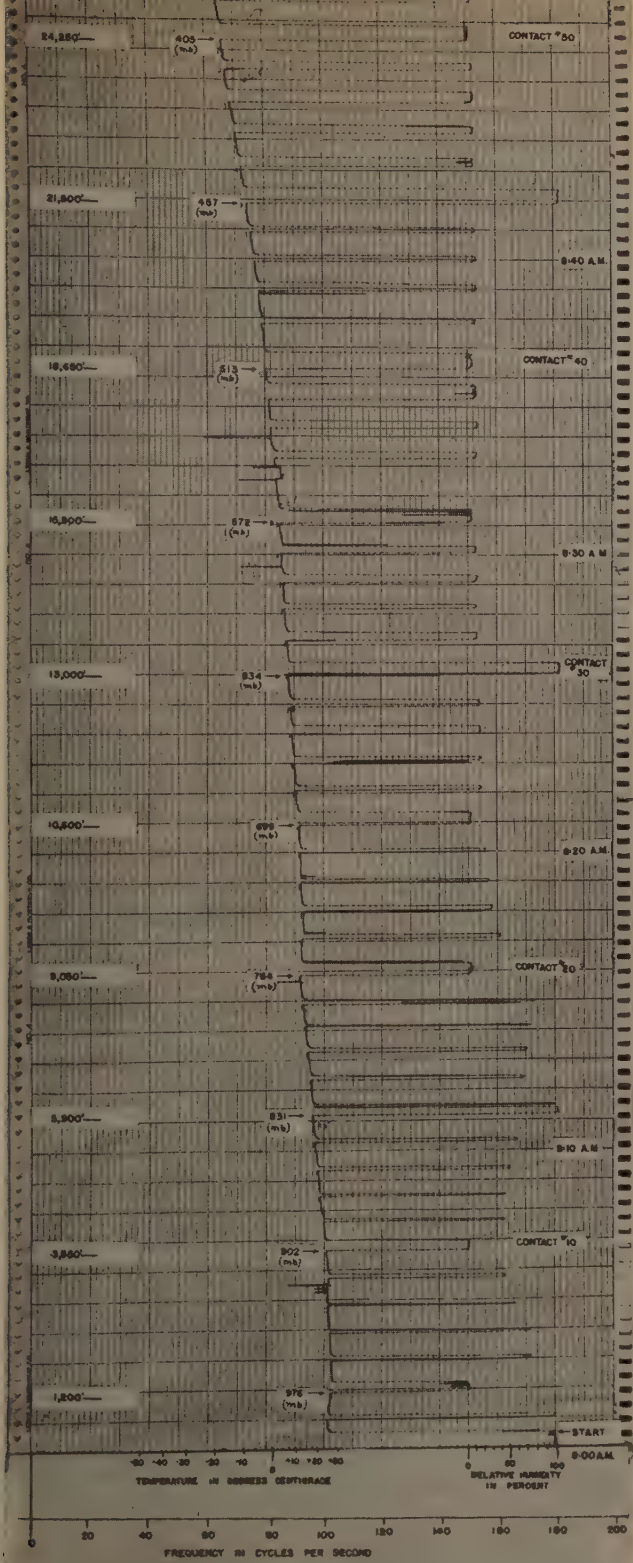


Fig. 15—Sample radio-meteorograph ascension record.

A sample record is shown in Fig. 15. The scale of abscissas on the chart is on a frequency basis, 0 to 200 cycles (left to right). For ease in interpretation, the corresponding temperature and humidity scales are also marked on the chart. The start of the run, corresponding to the release of the balloon, is at the bottom of the chart.

It is convenient to consider the recorder pen as producing a temperature plot which is a function of time and hence of the ascent of the balloon. This plot, represented by the vertical traces at the left of the record, is not continuous, being interrupted at predetermined altitude levels of the balloon by contact of the pressure arm with the conducting strips of the switching element. The modulating frequency of the emitted wave then changes to either the humidity or the reference values. At each interruption, the recorder pen sweeps laterally to the right to record these values, returning again to the left when the pressure arm leaves the corresponding conducting strip and the modulating frequency is again proportional to temperature. A line drawn through the frequency traces (at the right of the chart) which relate to the intermediate or humidity contacts will, therefore, represent the variation of humidity as the balloon ascends. Similarly, vertical lines through the two sets of reference-frequency traces represent the 0 and 100 per cent points of the scale of humidity values. The horizontal traces of the record made by the recorder pen in sweeping from the temperature traces to the humidity (and index) traces, and vice versa, show that the pressure arm has reached definite points of deflection and may be evaluated in terms of pressure, based on previous calibration. Note that the humidity readings occur in groups of four while the index traces define the 5th, 10th, 15th, 20th, etc., contacts. On the record, the values of the barometric pressure corresponding to the beginning of contact of the pressure arm with the index conducting strips are shown, forming an ordinate scale of pressure values. The balloon altitude at these points, corrected for the indicated temperature and humidity, are also shown. Similar data are not inserted for the other contacts for the sake of clarity of the record.

When the balloon reached an altitude of 34,000 feet, a special pressure-operated releasing device opened the string connection between the balloon and a small parachute to which the radio meteorograph was attached. The parachute then opened and the equipment descended back to the earth's surface. This releasing device was employed in certain of our tests to prevent the equipment from reaching the normal ceiling heights of 65,000 to 75,000 feet, since it was desired to obtain check temperature readings during the descent of the equipment while the batteries were still in good condition and the balloon

not too far away from the receiving station. Referring to Fig. 15, check readings were obtained down to the 5th contact, the equipment being then within 1200 feet of the ground.

The temperature readings during the descent agreed with the corresponding readings during the ascent within less than 1 degree centigrade, testifying to the accuracy of the frequency-translating means and the independence of the temperature tube to the rate of motion through the air. The humidity readings, while indicating changes at the same altitude levels, did not check the ascending values because of the inherent lag in the hairs after exposure to low temperatures.

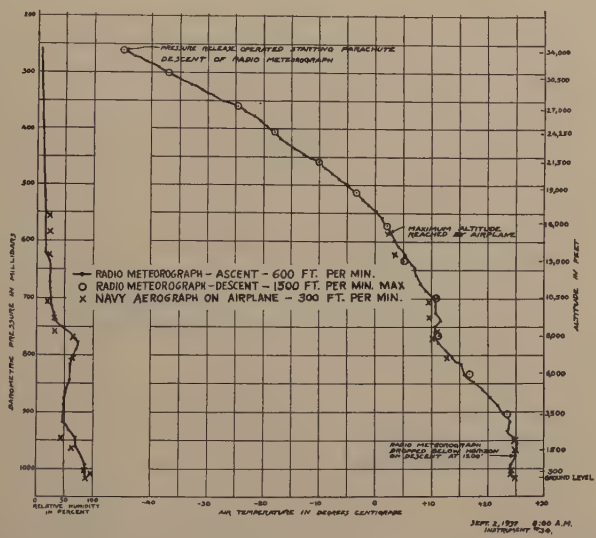


Fig. 16—Chart showing agreement of radio-meteorograph and aerograph observations.

The meteorologist examining the record of Fig. 15 would be interested chiefly in the points where the temperature variation with increasing altitude departs from a normal cooling rate and either ceases to decrease or actually increases. These are termed temperature-inversion points. Information is required on the extent of the inversions, the altitudes at which they occur and of the corresponding values of relative humidity. These data are plotted on an adiabatic chart for further computation. An advantage of the type of record shown in Fig. 15 is that the significant data required may be used without consideration of the remaining data.

An indication of the order of agreement obtained between the radio-meteorograph and aerograph observations may be had from the chart

shown in Fig. 16. In this chart the ordinates represent values of the barometric pressure in millibars and the abscissas values of the temperature in degrees centigrade and of relative humidity in per cent. The full lines represent the radio-meteorograph data corresponding to the record of Fig. 15. The crosses represent the aerograph data obtained simultaneously. It will be seen that the temperature readings agreed within 1 degree centigrade and the humidity readings within 5 per cent relative humidity except at abrupt changes. The close agreement of the temperature and humidity plots testify to the agreement of the pressure readings.

#### *Calibrating Procedure*

The procedure followed in calibrating the complete radio meteorograph in preparation for an upper-air sounding has been outlined in detail.<sup>22</sup> Since the pressure indications are on an absolute basis, the pressure calibration consists simply in subjecting the pressure unit to a variable pressure and noting the values at which the arm just contacts the various conducting strips of the switching element. The temperature and humidity elements are calibrated on a resistance basis. Special scales, used in conjunction with the frequency-resistance characteristic of the audio-frequency oscillator, are employed for converting the resistance values into corresponding frequency values.

With the calibrating procedure adopted, a radio meteorograph may be taken off the shelf, completely calibrated and prepared for an ascent within 90 minutes. If the instrument has been previously calibrated by the manufacturer, the check calibrations necessary to insure its accurate operation, together with the preparation of the instrument, balloon, parachute, etc., for ascent, take about 45 minutes. The record can be evaluated and plotted on the standard adiabatic chart used by meteorologists within a few minutes of the time the signals corresponding to the highest altitude of interest have been recorded.

#### X. THE ELECTRICAL HYGROMETER

In Section VI, a brief description was given of a resistance device which varied inherently with the moisture content of the air. A photograph of the device was shown in Fig. 4 and a record obtained in an ascension flight in Fig. 6. The development of an electrical hygrometer was undertaken to find a substitute for the hair hygrometer universally employed in upper-air soundings. Complete details of this development are given in a separate paper.<sup>24</sup> A serious defect of the hair-type

<sup>24</sup> F. W. Dunmore, "An electric hygrometer and its application to radio meteorography," *Nat. Bur. Stand. Jour. Res.*, vol. 20, pp. 723-744; June, (1938) (RP 1102).

hygrometer is its inability to respond to abrupt change in humidities encountered by rapidly ascending balloons. This lag in response increases rapidly with decreasing temperature. Hence the hair hygrometer gives only a qualitative measurement of the variation of humidity with altitude. It was believed that an electrical device for measuring humidity would provide much more rapid response to humidity variations, especially at the low temperatures.

The development of the unit shown in Fig. 4 was based on an observation that the resistance between the two wires of a bifilar winding wound on a glass tube was influenced markedly by humidity. An extensive investigation of this phenomenon was undertaken, the work including the study of the effect of different types of glass, roughness of the glass surface, coatings over the glass, binders over the coatings, spacing of the wires, and wire size and composition. Over 150 samples were made up and tested. All of the units were found to vary in electrical resistance with relative humidity, and, in lesser degree, with temperature. A simple graphical arrangement permits applying the appropriate temperature correction factor on the basis of the observed temperatures and relative humidities obtained during an ascent.

The record of Fig. 6 shows the rapidity of response obtained with the electrical hygrometer. In comparative laboratory tests at room temperatures in an air stream of 10 miles per hour, the time-lag constant for this device was found to be 3 seconds compared with 40 seconds for the hair hygrometer. The indicated variations in humidity at the higher altitudes in the record of Fig. 6 shows the operation of this device when exposed to low temperatures at which the hair hygrometer could not possibly respond. As previously indicated, the altitude scale of Fig. 6 is only approximate.

## XI. OTHER APPLICATIONS OF THE GENERAL METHOD

In the foregoing text, we have limited our description to arrangements wherein the device for pressure indication is also utilized to carry out all of the switching operations of the balloon transmitter. In certain applications it is convenient to employ auxiliary means for accomplishing the switching. An example of this class is the investigation of Stair and Coblenz<sup>25,26</sup> on the measurement of ultraviolet solar intensities in the stratosphere. In this application, based on our method,

<sup>25</sup> W. W. Coblenz and R. Stair, "A radiometric method of measuring ultraviolet solar radiation intensities in the stratosphere," *Radiologica*, vol. 1, pp. 12-20; November, (1937).

<sup>26</sup> R. Stair and W. W. Coblenz, "Radiometric measurements of ultraviolet solar intensities in the stratosphere," *Nat. Bur. Stand. Jour. Res.*, vol. 20, pp. 185-215; February, (1938) (R.P1075).

the variation in resistance of a photoelectric cell equipped with several light filters is converted into a variable modulation of the emitted carrier. At predetermined altitudes, the pressure-switching unit introduces fixed resistors in the grid circuit of the audio-frequency oscillators for the purpose of altitude determination. Between the altitude measurements, a motor-driven wheel successively interposes the several filters over the photocell to determine the spectral quality of ultraviolet in the solar radiation.

A second example of this class is shown in Fig. 17. In this arrangement, a miniature motor-driven switch connects into the grid circuit of the audio-frequency oscillator a number of devices. In the illustra-

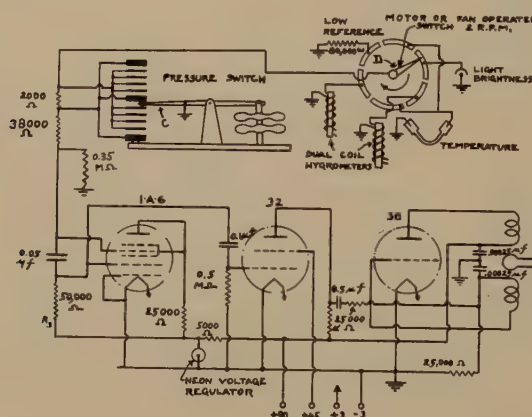


Fig. 17—Electrical circuit arrangement illustrating the use of the method of pressure indication in combination with an auxiliary switching device.

tion a capillary thermometer, a photoelectric cell, two electrical hygrometers (covering different portions of the humidity scale), and a fixed calibrating resistor are shown. These may be connected into the circuit as rapidly as the response of the recording equipment will permit, of the order of a few seconds. The arm of the pressure-switching unit, upon reaching a conducting strip, short-circuits whatever device happens to be in circuit, giving a fixed frequency. The latter represents a point on the altitude scale. For the purpose of providing index marks on the altitude scale, only a portion of resistor  $R$  is left in the grid circuit when the pressure arm reaches the index contacts. An advantage of this arrangement over the one shown in Fig. 8 is the possibility of its extension to the measurement of a large number of phenomena without requiring an unduly complicated pressure-switching element.

## XII. ACKNOWLEDGMENTS

The writers wish to express their appreciation to L. L. Hughes of the Radio Section of the National Bureau of Standards for his skillful construction and contributions to the mechanical design of numerous experimental models; to D. N. Craig of the Battery Section for co-operation in the design of the temperature capillary thermometer; to J. P. Schrodt and C. L. Snyder of the Battery Section for assistance in determining battery requirements; and to W. G. Brombacher of the Aeronautic Instrument Section for advice and data on meteorological instruments and calibration procedure and equipment. Special acknowledgment is due Commanders J. B. Anderson and W. M. Lockhart of the Bureau of Aeronautics, United States Navy Department, for advice on the meteorological aspects involved in the development of the radio meteorograph, and to Julien P. Friez and Sons, Inc., for co-operation in the mechanical design of the instruments.



## TRANSIENTS OF RESISTANCE-TERMINATED DISSIPATIVE LOW-PASS AND HIGH-PASS ELECTRIC WAVE FILTERS\*

By

WENTWORTH CHU AND CHUNG-KWEI CHANG

(Physics Department, National University of Peking, Peiping, China)

**Summary**—Formulas are derived for the solution of the transient receiving-end currents of resistance-terminated dissipative T- and  $\pi$ -type low-pass and high-pass electric wave filters. Oscillograms taken with a cathode-ray oscilloscope for direct- and alternating-current cases are found to agree with the results calculated from these formulas. From these calculations the following conclusions are derived: (1) When the terminating resistance is gradually increased from zero, the damping constants of the damped sine terms begin to differ greatly from each other, ranging in decreasing amplitudes from the first damped sine term to the last term of (approximately) cutoff frequency. Hence, the transient is ultimately of the cutoff frequency. At the last frequency, this constant is greater than the corresponding constant (approximately equal to  $R/2L$ ), when the termination is absent. (2) For each increase of one section, there is introduced an additional damped sine term with a smaller damping constant. Therefore transients die out faster in filters of a small number of sections. (3) The last resonant frequency of the filters varies with the number of sections used. It approaches the cutoff frequency as the number of sections is increased.

This paper deals with the receiving-end transient currents of resistance-terminated dissipative low-pass and high-pass electric wave filters of T- and  $\pi$ -types. Transients of nondissipative electric wave filters were first treated by John R. Carson and Otto J. Zobel,<sup>1</sup> who considered primarily an infinite succession of similar T-sections and obtained formulas for the current at any section. In 1935, E. Weber and M. J. Di Toro<sup>2</sup> calculated the transient currents of resistance-terminated non-dissipative low-pass electric wave filters of finite number of sections. Therefore it is now worth while to solve for the transient currents for dissipative electric wave filters.

### DERIVATION OF FORMULAS AND CALCULATION OF TRANSIENT CURRENTS

Let  $P$  = generalized angular velocity,

$$\lambda = \sqrt{LCP},$$

$$\tau = 57.3t/\sqrt{LC},$$

$$\tau' = t/\sqrt{LC},$$

$2Z_1$  = total series impedance per section of T- or  $\pi$ -type filter, and

$Z_2$  = total shunt impedance per section, where  $t$  is the time in seconds, and  $L$  and  $C$  are to be defined later. Then

\* Decimal classification: R386. Original manuscript received by the Institute, September 10, 1936; revised manuscript received by the Institute, November 9, 1937.

<sup>1</sup> "Transient oscillations in electric wave-filters," *Bell. Sys. Tech. Jour.*, vol. 2, pp. 1-52; July, (1923).

<sup>2</sup> E. Weber and M. J. Di Toro, "Transients in the Finite Artificial Line," *Elect. Eng.*, pp. 661-663; June, (1935).

$\theta$  = hyperbolic angle per section =  $2 \sinh^{-1}(\sqrt{Z_1/Z_2})$ , for both  $T$ - and  $\pi$ -type filters,

$Z_0$  = image impedance =  $\sqrt{Z_1^2 + 2Z_1Z_2}$ , for  $T$ -type filter,

$Z_0 = 2Z_2\sqrt{Z_1/(Z_1+2Z_2)}$ , for  $\pi$ -type filter, and

$\theta'$  = hyperbolic angle subtended by the terminating resistance  $R_0$  =  $\tanh^{-1}(R_0/Z_0)$ , for both types of filters.

### T-TYPE LOW-PASS FILTER

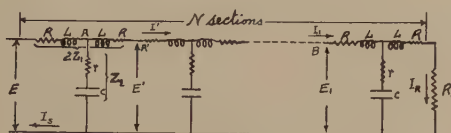


Fig. 1

In Fig. 1, let

$$2L = \text{total inductance per section},$$

$$C = \text{total capacitance per section},$$

$$2R = \text{resistance of } 2L = 2K_R \sqrt{L/C},$$

$$r = \text{resistance of } C = K_r \sqrt{L/C},$$

$$R_0 = \text{terminating resistance} = K_{R_0} \sqrt{L/C}$$

where  $K_R$ ,  $K_r$ , and  $K_{R_0}$  are any constants. Now

$$Z_1 - R = LP,$$

$$Z_2 - r = 1/CP, \quad \text{and}$$

$$L/C = (Z_1 - K_R \sqrt{L/C})(Z_2 - K_r \sqrt{L/C}).$$

Substituting the values of hyperbolic functions and the value of  $\sqrt{L/C}$  from the last equation into the equation for  $\theta'$  and neglecting the terms containing  $K_R^2$  and  $K_r^2$ ,

$$\begin{aligned} \tanh \theta' &= [K_{R_0}/2(1 - K_R K_r)][-\tanh(\theta/2) - K_R \operatorname{csch} \theta \\ &\quad + \sqrt{2 - K_R K_r} \operatorname{sech}(\theta/2)]. \end{aligned} \quad (1)$$

Now  $I_R$  = receiving-end current =  $E \cosh \theta'/Z_0 \sinh(N\theta + \theta')$ , where  $E$  is equal to the sending-end voltage and  $N$  is equal to the number of sections of the filter.

To factor the denominator of the last expression, let

$$\begin{aligned} \sinh(N\theta + \theta') &= 0, \\ N\theta + \theta' &= j\kappa\pi, \\ \kappa &= 0, 1, 2, \dots, N, \\ \tanh N\theta &= -\tanh \theta'. \end{aligned} \quad (2)$$

then

where

and

Let  $\theta = a + jb$ , and substitute (1) into (2), and separate the real and imaginary parts

$$\begin{aligned} & (1 + F_1) \cosh (N - 1)a \cos (N - 1)b \\ & \quad - (1 - F_1) \cosh (N + 1)a \cos (N + 1)b + G_1 \cosh Na \cos Nb \\ & = H_1 [\sinh (N + 0.5)a \cos (N + 0.5)b \\ & \quad - \sinh (N - 0.5)a \cos (N - 0.5)b] \end{aligned} \quad (3)$$

and

$$\begin{aligned} & (1 + F_1) \sinh (N - 1)a \sin (N - 1)b \\ & \quad - (1 - F_1) \sinh (N + 1)a \sin (N + 1)b + G_1 \sinh Na \sin Nb \\ & = H_1 [\cosh (N + 0.5)a \sin (N + 0.5)b \\ & \quad - \cosh (N - 0.5)a \sin (N - 0.5)b] \end{aligned} \quad (4)$$

where

$$\begin{aligned} F_1 &= K_{R_0}K_r/2(1 - K_RK_r), \\ G_1 &= K_{R_0}(K_R - K_r)/(1 - K_RK_r), \text{ and} \\ H_1 &= K_{R_0}\sqrt{2 - K_RK_r}/(1 - K_RK_r). \end{aligned}$$

From these two equations,  $N+1$  values of  $\theta$  can be found by the cut-and-try method, of which one is a negative number, and the rest are complex numbers with real parts negative.

Now  $\theta = 2 \sinh^{-1} \sqrt{(\lambda^2 + K_R\lambda)/2(K_R\lambda + 1)}$ , and  $\lambda$  can be solved; let  $\lambda_\kappa = -X_\kappa \pm jY_\kappa$ , then the factors of  $Z_0 \sinh(N\theta + \theta')$  are of the types  $(\lambda + X_0)$  and  $\lambda^2 + 2X_\kappa\lambda + (X_\kappa^2 + Y_\kappa^2)$ , or,  $A_0\lambda + 1$  and  $A_\kappa\lambda^2 + B_\kappa\lambda + 1$ , where  $A_\kappa = 1/(X_\kappa^2 + Y_\kappa^2)$ .

It is shown in the Appendix that

$$I_R = \sqrt{C/L} (K_r\lambda + 1)^N / (2NK_R + K_{R_0})(A_0\lambda + 1)(A_1\lambda^2 + B_1\lambda + 1) \cdots (A_n\lambda^2 + B_n\lambda + 1). \quad (5)$$

From this, the transients under impressed direct and alternating voltages can be easily calculated, and the results are shown in the table and the accompanying figures.

### $\pi$ -TYPE LOW-PASS FILTER

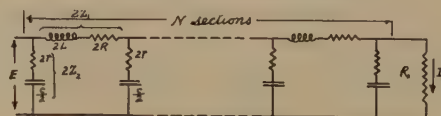


Fig. 2

In Fig. 2, the constants are the same as in Fig. 1. This case is the same as before except that the formula for  $Z_0$  is different. By the same method,

$$\tanh \theta' = [K_{R_0}/4(K_R K_r - 1)][K_r \sinh \theta + K_R \coth (\theta/2) - 2\sqrt{2 - K_R K_r} \cosh (\theta/2)]$$

and the formulas for the determination of  $\theta$  are as follows:

$$\begin{aligned} F_2 & [\cosh (N + 1.5)a \cos (N + 1.5)b + \cosh (N - 1.5)a \cos (N - 1.5)b] \\ & - (1 - G_2) \cosh (N + 0.5)a \cos (N + 0.5)b \\ & + (1 + G_2) \cosh (N - 0.5)a \cos (N - 0.5)b \\ & = H_2 [\sinh (N + 1)a \cos (N + 1)b - \sinh (N - 1)a \cos (N - 1)b] \quad (6) \end{aligned}$$

and

$$\begin{aligned} F_2 & [\sinh (N + 1.5)a \sin (N + 1.5)b + \sinh (N - 1.5)a \sin (N - 1.5)b] \\ & - (1 - G_2) \sinh (N + 0.5)a \sin (N + 0.5)b \\ & + (1 + G_2) \sinh (N - 0.5)a \sin (N - 0.5)b \\ & = H_2 [\cosh (N + 1)a \sin (N + 1)b - \cosh (N - 1)a \sin (N - 1)b] \quad (7) \end{aligned}$$

where

$$\begin{aligned} F_2 & = K_{R_0} K_r / 8(1 - K_R K_r), \\ G_2 & = K_{R_0} (K_R - 0.5 K_r) / 4(1 - K_R K_r), \text{ and} \\ H_2 & = K_{R_0} \sqrt{2 - K_R K_r} / 4(1 - K_R K_r). \end{aligned}$$

From (6) and (7),  $N$  values of  $\theta$  can be found, and in a similar way, the factors of  $Z_0 \sinh(N\theta + \theta')$  are found to be of the type  $A_n \lambda^2 + B_n \lambda + 1$ , and

$$I_R = \sqrt{C/L} (K_r \lambda + 1)^N / (2N K_R + K_{R_0}) (A_1 \lambda^2 + B_1 \lambda + 1) \cdots (A_n \lambda^2 + B_n \lambda + 1). \quad (8)$$

### T-TYPE HIGH-PASS FILTER

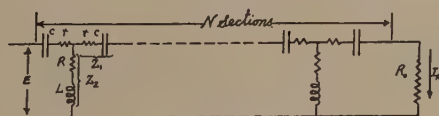


Fig. 3

In Fig. 3, let

$$C/2 = \text{capacitance per section},$$

$$2r = \text{resistance of } C/2 = 2K_r \sqrt{L/C}$$

$$L = \text{inductance per section},$$

$$R = \text{resistance of } L = K_R \sqrt{L/C}, \text{ and}$$

$$R_0 = \text{terminating resistance} = K_{R_0} \sqrt{L/C},$$

where  $K_r, K_R$ , and  $K_{R_0}$  are any constants.

In this case  $L/C = (Z_1 - K_r \sqrt{L/C}) (Z_2 - K_R \sqrt{L/C})$ .

By comparing with the case of a *T*-type low-pass filter, the expression is the same except that  $K_R$  and  $K_r$  are interchanged. Therefore the formulas for the determination of the values of  $\theta$  are the same as (3) and (4) with  $K_R$  and  $K_r$  interchanged. With  $\theta$  known, the factors are found to be of the types  $\lambda + X_0$  and  $\lambda^2 + A_s\lambda + B_s$ ; and in this case

$$I_R = \sqrt{C/L} \lambda (\lambda^2 + K_R \lambda)^N / (2NK_r + K_{R_0})(\lambda + X_0)(\lambda^2 + A_1 \lambda + B_1) \cdots (\lambda^2 + A_n \lambda + B_n). \quad (9)$$

### $\pi$ -TYPE HIGH-PASS FILTER

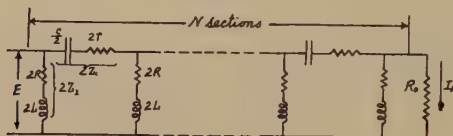


Fig. 4

The formulas for the determination of the values of  $\theta$  are the same as (6) and (7) except that  $K_R$  and  $K_r$  are interchanged. The factors are of the type  $\lambda^2 + A_s\lambda + B_s$ , and in this case

$$I_R = \sqrt{C/L} (\lambda^2 + K_R \lambda)^N / (2NK_r + K_{R_0})(\lambda^2 + A_1 \lambda + B_1) \cdots (\lambda^2 + A_n \lambda + B_n). \quad (10)$$

### RESULTS OF *T*-TYPE LOW-PASS FILTERS

In Table I

$$I_0 = \sqrt{C/L},$$

$A_R(t)$  = receiving-end indicial admittance, and

$I_R(t)$  = receiving-end current under an impressed alternating voltage of the form  $\sin(W\tau + \alpha)$

The filters tested have the following constants:

For *T*- and  $\pi$ -type low-pass filters

$$L = 0.64 \text{ henry},$$

$$C = 0.503 \text{ microfarad},$$

$$R = 52.5 \text{ ohms} = 0.04653 \sqrt{L/C},$$

$$r = 8.11 \text{ ohms} = 0.00717 \sqrt{L/C},$$

$$R_0 = 1596 \text{ ohms} = \sqrt{2} \sqrt{L/C}.$$

For *T*- and  $\pi$ -type high-pass filters

$$L = 0.32 \text{ henry},$$

$$C = 0.504 \text{ microfarad},$$

$$R = 24.46 \text{ ohms} = 0.0307\sqrt{L/C},$$

$$r = 10.676 \text{ ohms} = 0.0134\sqrt{L/C},$$

$$R_0 = 1127 \text{ ohms} = \sqrt{2}\sqrt{L/C}.$$

The expression of the current is of the general form

$$A_R(t), \text{ or } I_R(t), = I_0[a, \text{ or } a \sin(W\tau + \theta), + a_0 \exp(-D_0\tau') \\ + \sum_{K=1}^{K=N} a_K \exp(-D_K\tau') \sin(W_K\tau + \theta_K)],$$

when the impressed voltage  $E$  is either unit direct or alternating voltage of the form  $\sin(W\tau + \alpha)$ .

TABLE I

SECTIONS $E$	ONE	TWO	FIVE	FIVE $\sin(1.747\tau)$	FIVE	FIVE
	Direct current	Direct current	Direct current		Direct current	Direct current
$a$	0.6637	0.551	0.5262	- 0.00182 -10.9°	2.152	0.7114
$\theta$				0.0732	-2.152	- 1.01
$a_0$	- 0.518	- 0.442	- 0.298	0.499	0.0465	0.315
$D_0$	0.9745	0.762	0.499	0.2688	- 0.458	- 1.284
$a_1$	- 0.471	- 0.7413	- 1.277	0.237	0.024	0.264
$D_1$	0.2664	0.38	0.237	0.296	0.44	0.326
$W_1$	1.214	0.7282	0.296	0.44		
$\theta_1$	17.92°	17.64°	20.14°	-25°	0	- 2.64°
$a_2$		0.1394	0.429	- 0.2143	0.241	0.49
$D_2$		0.0958	0.181	0.181	0.0257	0.166
$W_2$		1.326	0.688	0.688	0.832	0.683
$\theta_2$		55.89°	48.49°	-20.27°	0	46.61°
$a_3$			- 0.1836	0.1604	- 0.175	- 0.187
$D_3$			0.11	0.11	0.028	0.085
$W_3$			1.012	1.012	1.145	1.017
$\theta_3$			66.43°	-11°	0	67.6°
$a_4$			0.08	- 0.1632	0.149	0.79
$D_4$			0.0593	0.0593	0.03	0.031
$W_4$			1.263	1.263	1.345	1.263
$\theta_4$			78.52°	- 2.14°	0	75.35°
$a_5$			- 0.022	0.0486	- 0.0707	- 0.0225
$D_5$			0.0384	0.0384	0.0304	0.00343
$W_5$			1.397	1.397	1.4142	1.4
$\theta_5$			73.9°	- 9.86°	0	78.3°

In Table I, for the first four cases,  $K_R = 0.04653$ ,  $K_r = 0.00717$ , and  $K_{R_0} = \sqrt{2}$ ; for the fifth case,  $K_R$  and  $K_r$  are the same, but  $K_{R_0} = 0$ ; and for the sixth case,  $K_R = K_r = 0$  and  $K_{R_0} = \sqrt{2}$ .

#### EXPERIMENTS FOR CHECKING SOME OF THE FORMULAS DERIVED

The transients are taken by a cathode-ray oscilloscope with a moving-film camera. The circuit for taking alternating-current transients is shown in Fig. 5, where  $G$  represents the horizontal deflecting plates of the oscilloscope, and  $H$  and  $K$  are switches fastened to a rigid and vertical frame and controlled by means of a dropped weight. The power capacity of the usual low-frequency oscillator is found inadequate, for the voltage drops considerably as the load is suddenly

taken by the filter. To eliminate this voltage transient, there are interposed between the oscillator and the filter tested an audio-frequency amplifier and a resonant circuit whose inductance could be adjusted and short-circuited for any convenient portion. Switch  $K$  is arranged so that it connects the filter to the source and short-circuits a portion of the inductance simultaneously. The source is first loaded with the resonant circuit, and by short-circuiting a portion of the inductance, the circuit is nonresonant, and the load is thus decreased. When this decrease of the load is made equal to the increase of the load due to the parallel insertion of the filter, the oscillator voltage remains unchanged when switch  $K$  to the filter is suddenly closed. To minimize the effect of harmonics in the output wave of the source, a low-pass filter is inserted between the amplifier and the resonant circuit as shown in Fig. 5.

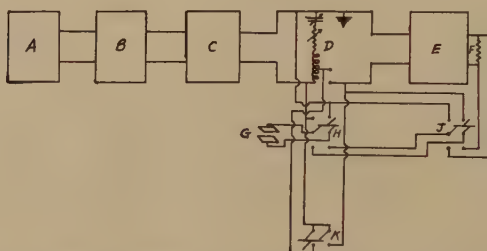


Fig. 5—Audio-frequency oscillator.  $B$  = audio-frequency amplifier,  $C$  = low-pass filter to eliminate harmonics,  $D$  = resonant circuit,  $E$  = filter under test,  $F$  = terminating resistance  $R_0$ .  $G$  = deflecting plate of cathode-ray oscilloscope,  $H$  and  $K$  = switches operated by a dropped weight.

The characteristics of the transients depend on the phase of the impressed voltage at the instant when switch  $K$  is closed. To evaluate this angle, switch  $J$  is closed to the lower side. A weight dropped from a definite height disconnects switch  $H$  from the upper side, and connects it to the lower side, and then closes switch  $K$ . When  $K$  is closed, voltage is impressed on the filter tested. When  $H$  is disconnected from the upper side, the deflecting plates  $G$  are disconnected from the oscillator voltage, and when  $K$  is closed, the plates are reconnected to oscillator voltage. Hence the picture taken has two steady-state waves with a dash between them, and the angle  $\alpha'$  in electrical degrees, occupied by the time from the disconnection of  $H$  from the upper side to the closing of  $K$ , is equal to the length of the dash. To take alternating-current transients,  $J$  is closed to the upper side. Then the weight falling from the same height first disconnects the plates from oscillator voltage and then connects them across the terminating resistance, when  $H$  is closed to the lower side. The picture taken is a steady-state impressed

voltage wave and the transient receiving-end voltage wave with a dash between them. Then the angle at which the stationery impressed voltage wave stops plus the angle  $\alpha'$  is equal to the angle  $\alpha$  of the impressed voltage when  $K$  is closed.

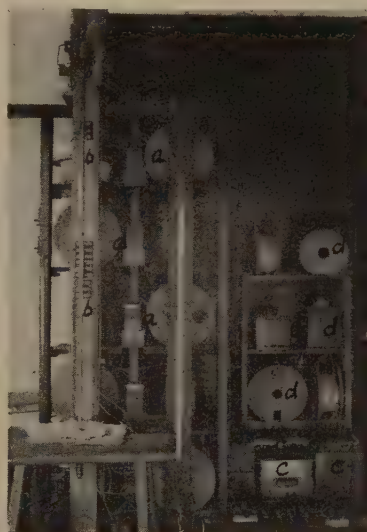


Fig. 6



Fig. 7

Photographs of the whole apparatus are shown in Figs. 6 and 7, where  $a$  is the filter tested;  $b$  is the frame containing the dropped weight and switches;  $c$ , the resonant circuit;  $d$ , the low-pass filter to eliminate the harmonics;  $e$ , the cathode-ray oscilloscope tube and camera; and  $f$ , the power-supply unit of the oscilloscope.

Some of the oscillograms taken are shown in the accompanying figures. In Figs. 8 through 16,  $t' = 57.3t$ , where  $t$  is the time in seconds.



Fig. 8—Indicial admittance of the receiving end of a 2-section, low-pass, T-type filter.

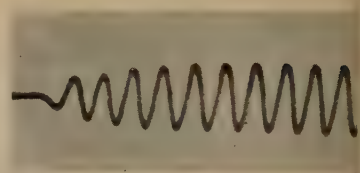


Fig. 9— $I_R(t)$  of a 2-section, low-pass T-type filter under an impressed voltage.  $\sin(2316t' + 207.2^\circ)$



Fig. 10— $I_R(t)$  of a 2-section, low-pass, T-type filter under an impressed voltage.  $\sin(2701.8t' + 118.18^\circ)$

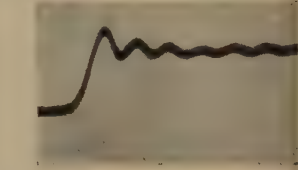


Fig. 11—Indicial admittance for the receiving end of a 5-section, low-pass T-type filter.

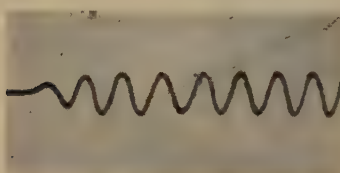


Fig. 12— $I_R(t)$  of a 5-section, low-pass, T-type filter under an impressed voltage.  $\sin(1787.6t' + 68.3^\circ)$

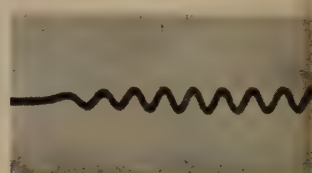


Fig. 13— $I_R(t)$  of a 5-section, low-pass T-type filter under an impressed voltage.  $\sin(2463t' + 48.93^\circ)$



Fig. 14— $I_R(t)$  of a 5-section, low-pass, T-type filter under an impressed voltage.  $\sin(2525.8t' + 141.7^\circ)$



Fig. 15—Indicial admittance of the receiving end of a 2-section, low-pass  $\pi$ -type filter.



Fig. 16—Indicial admittance for the receiving end of a 1-section, high-pass, T-type filter.

The readings are taken from these oscillograms by a microscope capable of traveling along two dimensions. The calculated and experimental results are plotted side by side, and the discrepancies are found to be small, as illustrated in Figs. 17 and 18, where the calculated results are represented by solid curves, and the experimental results by dotted curves;  $t' = 57.3 t$ .

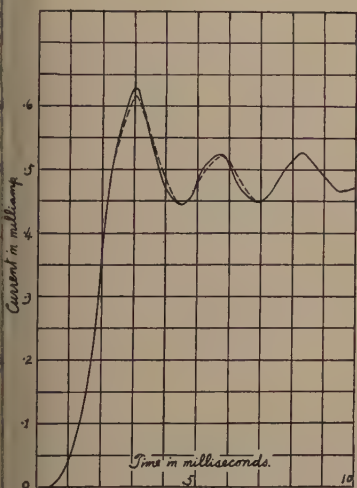


Fig. 17—Indicial admittance of the receiving end of a 2-section, low-pass,  $T$ -type filter. Steady-state amplitude = 0.4884 milliampere.

Steady-state amplitude = 0.79 milliampere.

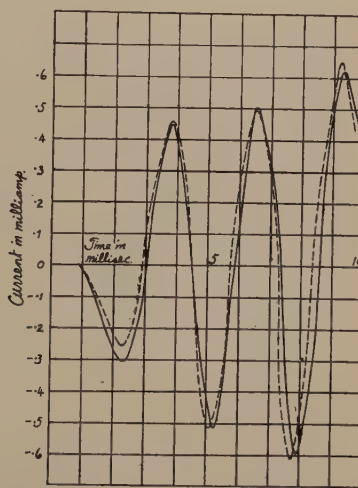


Fig. 18— $I_R(t)$  of a 2-section, low-pass,  $T$ -type filter under an impressed voltage.  $\sin(2316t' + 207.2^\circ)$

### CONCLUSIONS

The formulas give results which compare well with experimental values. From the results, the effect of terminating resistance is to make the damping constants of the damped sine terms differ greatly from each other. Without termination, the damping constants for all the damped sine terms are nearly equal to but greater than  $R/2L$ , and as a result the transients die out very slowly, and in the transient state there is no definite frequency. With terminating resistance, the damping constants all increase and differ greatly from each other, ranging in decreasing magnitudes from the first damped sine term to the last damped sine term of nearly cutoff frequency. No matter what the external frequency is, the transient is ultimately of the cutoff frequency, because the last term has the lowest damping constant. Since this constant is always much greater than  $R/2L$ , the transients die

out much faster than in the case where the termination is absent. As the terminating resistance is increased, the deviations of the damping constants from  $R/2L$  are increased, and the transients die out faster.

The effect of  $R$  is very large on the damping constants, as their deviations due to termination are all based on  $R/2L$ . Thus with  $R=0$ , the smallest damping constant is only  $0.00343/\sqrt{LC}$ , and the transients die out very slowly.

The effect of the number of sections can be seen easily. For the same  $R$  and  $R_0$ , the damped sine terms increase with the number of sections. With each increase of one section, there is an increase of one transient term with a smaller damping constant. Hence the transients die out faster in a filter of a small number of sections. While  $R$ ,  $R_0$  and the number of sections affect the damping constants considerably, they do not have much effect on the transient amplitudes.

The last resonant frequency of each filter is different from the ideal cutoff frequency. This difference is larger in  $\pi$ -type filters than in the corresponding  $T$ -type filters. With either type, this difference decreases as the number of sections is increased.

#### APPENDIX

Referring to Fig. 1, when one section of the  $T$ -type filter is terminated by  $R_0$ , the impedance to the right of  $B$  is given by

$$Z_B = \sqrt{L/C} \left[ \frac{K_R + \lambda + (K_r\lambda + 1)(\lambda + K_R + K_{R_0})}{\{\lambda^2 + (K_R + K_r + K_{R_0})\lambda + 1\}} \right]$$

and

$$I_1 = \frac{E_1 \sqrt{C/L} [\lambda^2 + (K_R + K_r + K_{R_0})\lambda + 1]}{(2K_R + K_{R_0})(1 + C_1'\lambda + C_2'\lambda^2 + C_3'\lambda^3)}$$

where  $C_1'$ , etc., are constants involving  $K_R$ ,  $K_r$ , and  $K_{R_0}$ .

$$\begin{aligned} I_R &= \frac{I_1(K_r\lambda + 1)}{[1 + (K_R + K_r + K_{R_0})\lambda + \lambda^2]} \\ &= \frac{E_1 \sqrt{C/L} (K_r\lambda + 1)}{(2K_R + K_{R_0})(1 + \dots + C_3'\lambda^3)}. \end{aligned}$$

Assume that, at  $A'$ , where there are  $N-1$  sections,

$$\begin{aligned} I' &= \frac{E' \sqrt{C/L} [1 + \dots + \lambda^{2(N-1)}]}{[2(N-1)K_R + K_{R_0}][1 + \dots + C_{2N-1}\lambda^{2N-1}]} \\ \text{and} \\ I_R &= \frac{E' \sqrt{C/L} (K_r\lambda + 1)^{N-1}}{[2(N-1)K_R + K_{R_0}][1 + \dots + C_{2N-1}\lambda^{2N-1}]} \end{aligned} \quad (11)$$

so that

$$I_R = \frac{I'(K_r\lambda + 1)^{N-1}}{[1 + \dots + \lambda^{2(N-1)}]}$$

where  $C_{2N-1}$ , etc., are constants.

Then the impedance at  $A$ , excluding the parallel impedance of  $C$  and  $r$ , is

$$\begin{aligned} Z_A &= \frac{\sqrt{L/C}(\lambda + K_R) + \sqrt{L/C}[2(N-1)K_R + K_{R_0}][1 + \dots + C_{2N-1}\lambda^{2N-1}]}{[1 + \dots + \lambda^{2(N-1)}]} \\ &= \frac{\sqrt{L/C}[(2N-1)K_R + K_{R_0} + \lambda][1 + \dots + C_{2N-1}\lambda^{2N-1}]}{[1 + \dots + \lambda^{2(N-1)}]}; \end{aligned}$$

and the impedance at  $A$ , including the parallel impedance, is

$$\begin{aligned} Z_A' &= \frac{\sqrt{L/C}(K_r\lambda + 1)Z_A}{(1 + K_r\lambda + Z_A\lambda)} \\ &= \frac{\sqrt{L/C}[(2N-1)K_R + K_{R_0}][1 + \dots + C_{2N}\lambda^{2N}]}{(1 + \dots + C_{2N}'\lambda^{2N})}. \end{aligned}$$

The impedance of  $N$  sections is given by

$$\begin{aligned} Z_s &= Z_A' + \sqrt{L/C}(\lambda + K_R) \\ &= \frac{\sqrt{L/C}[2NK_R + K_{R_0}][1 + \dots + C_{2N+1}\lambda^{2N+1}]}{[1 + \dots + C_{2N}'\lambda^{2N}]} \end{aligned}$$

and the sending-end current  $I_s$  is

$$I_s = \frac{E}{Z_s}.$$

Now

$$I' = \frac{I_s(K_r\lambda + 1)[1 + \dots + \lambda^{2(N-1)}]}{[1 + \dots + C_{2N}'\lambda^{2N}]}$$

therefore

$$I_R = \frac{E\sqrt{C/L}(K_r\lambda + 1)^N}{(2NK_R + K_{R_0})[1 + \dots + C_{2N+1}\lambda^{2N+1}]} \quad (12)$$

Hence if (11) is true, then (12) is also. Since for one section, (12) holds, so it holds for any number of sections. In a similar way, the formulas for other filters can be derived.

## THE BRIDGE-STABILIZED OSCILLATOR\*

BY

L. A. MEACHAM

(Bell Telephone Laboratories, Inc., New York, N. Y.)

**Summary**—A new type of constant-frequency oscillator of very high stability is presented. The frequency-controlling resonant element is used as one arm of Wheatstone resistance bridge. Kept in balance automatically by a thermally controlled arm, this bridge provides constancy of output amplitude, purity of wave form and stabilization against fluctuations in power supply or changes in circuit elements. A simple one-tube circuit has operated consistently with no short-time frequency variations greater than  $\pm 2$  parts in  $10^8$ . Convenient means are provided for making precision adjustments over a narrow range of frequencies to compensate for long-time aging effects.

Description of the circuit is followed by a brief linear analysis and an account of experimental results. Operating records are given for a 100-kilocycle oscillator.

### INTRODUCTION

THE problem of improving the stability of constant-frequency oscillators may be divided conveniently into two parts, one relating to the frequency-controlling resonant element or circuitry and the other to the means for supplying energy to sustain oscillations. The ideal control element would be a high-*Q* electrical resonant circuit or a mechanical resonator such as a tuning fork or crystal, whose properties were exactly constant, unaffected by atmospheric conditions, jar amplitude of oscillation, age or any other possible parameter. The ideal driving circuit would take full advantage of the resonator's constancy by causing it to oscillate at a stable amplitude and at a frequency determined completely by the resonator itself, regardless of power-supply variations, aging of vacuum tubes or other circuit elements, or the changing of any other operating condition.

This paper, concerning itself principally with the second part of the problem, describes an oscillator circuit which attains a very close approximation to the latter objective. The "bridge-stabilized oscillator" provides both frequency and amplitude stabilization, and as it operates with no tube overloading, it has the added merit of delivering a very pure sinusoidal output.

### OSCILLATOR CIRCUIT

The bridge-stabilized oscillator circuit, shown schematically in Fig. 1, consists of an amplifier and a Wheatstone bridge. The ampli-

\* Decimal classification: R355.9×R214. Original manuscript received by the Institute, April 6, 1938. Presented before Thirteenth Annual Convention, New York, N. Y., June 16, 1938.

ier output is impressed across one of the diagonals of the bridge, and he unbalance potential, appearing across the conjugate diagonal, is applied to the amplifier input terminals. One of the four bridge arms,  $R_1$ , is a thermally controlled resistance; two others,  $R_2$  and  $R_3$ , are fixed resistances, and the fourth,  $Z_4 = R_4 + jX_4$ , is the frequency-controlling resonant element.

In this discussion  $Z_4$  is assumed to represent a crystal suitable for operation at its low-impedance or series resonance. A coil and condenser in series could be substituted, and even a parallel-resonant control element might be used by exchanging its position in the bridge with  $R_2$  or  $R_3$ . Operating a crystal at series resonance has the advantage of minimizing effects of stray capacitance.

The bridge is kept as nearly in exact balance as possible. Assuming that  $R_1$ ,  $R_2$ , and  $R_3$  are pure resistances, we may write for exact reactive balance

$$X_4 = 0$$

and for exact resistive balance

$$\frac{R_1}{R_2} = \frac{R_3}{R_4} .$$

In order that the circuit may oscillate, a slight unbalance is required. Accordingly  $R_1$  must be given a value slightly smaller than  $(R_2R_3)/R_4$ , so that the attenuation through the bridge is just equal to the gain of the amplifier.

It is evident that if all the bridge arms had fixed values of resistance, the attenuation of the bridge would be very critical with slight changes in any arm. This would obviously be undesirable, for the circuit would either fail to oscillate, or else build up in amplitude until tube overloading occurred. The thermally controlled resistance  $R_1$  eliminates this difficulty. This arm has a large positive temperature coefficient of resistance, and is so designed that the portion of the amplifier output which reaches it in the bridge circuit is great enough to raise its temperature and increase its resistance materially. A small tungsten-filament lamp of low wattage rating has been found suitable. It functions as follows:

When a battery is first applied to the amplifier, the lamp  $R_1$  is cold and its resistance is considerably smaller than the balance value. Thus the attenuation of the bridge is relatively small, and oscillation builds up rapidly. As the lamp filament warms, its resistance approaches the value for which the loss through the bridge equals the gain of the ampli-

fier. If for some reason  $R_1$  acquires too large a resistance, the unbalance potential  $e$  becomes too small or possibly even inverted in phase, so that the amplitude decreases until the proper equilibrium is reached.

This automatic adjustment stabilizes the amplitude, for the amount of power needed to give  $R_1$  a value closely approaching  $(R_2 R_3)/R_4$  is always very nearly the same. A change in the amplifier gain would cause a readjustment of the bridge balance, but the resulting variation in  $R_1$  or in the amplifier output would be extremely small. The operating temperature of the lamp filament is made high enough so that variations in the ambient temperature do not affect the adjustment appreciably.

No overloading occurs in the amplifier, which operates on a strictly class A basis, nor is any nonlinearity necessary in the system other than

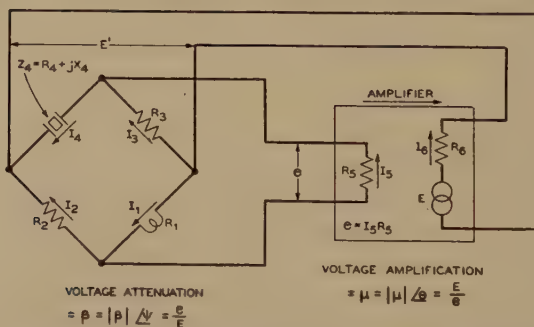


Fig. 1—Schematic circuit diagram of a bridge-stabilized oscillator.

the thermal nonlinearity of  $R_1$ . As the lamp resistance does not vary appreciably during a high-frequency cycle, it is not a source of harmonics (or of their intermodulation, which Llewellyn<sup>1</sup> has shown to be one of the factors contributing to frequency instability).

In contrast to the lamp, an ordinary nonlinear resistance, of copper oxide for example, would not be suitable for  $R_1$ . A resistance of the thermally controlled type having a negative temperature coefficient could be used by merely exchanging its position in the bridge with  $R_2$  or  $R_3$ .

The frequency control exerted by the crystal depends upon the fact that the phase shift of the amplifier must be equal and opposite to that through the bridge. In the notation of Black,<sup>2</sup> applied to the circuit of Fig. 1,

<sup>1</sup> F. B. Llewellyn, "Constant frequency oscillators," Proc. I.R.E., vol. 19, pp. 2063-2094; December, (1931).

<sup>2</sup> H. S. Black, "Stabilized feedback amplifiers," Bell. Sys. Tech. Jour., vol. 13, pp. 1-18; January, (1934).

$$\mu = \frac{E}{e} = |\mu| \angle \theta,$$

and

$$\beta = \frac{e}{E} = |\beta| \angle \psi,$$

The condition for oscillation is

$$\mu\beta = 1 \angle 0,$$

which implies that  $|\mu\beta| = 1$  and  $\theta = -\psi$ .

The vector diagrams of Fig. 2 illustrate the frequency-stabilizing

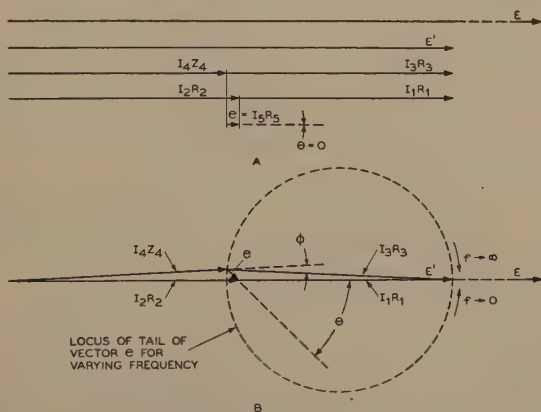


Fig. 2.—Vector diagrams illustrating the operation of a bridge oscillator, with simplifying assumptions that  $R_5$  is large and that  $E$  and  $E'$  are strictly in phase.

A—at resonance

$$Z_4 = R_4 + j0$$

$$\theta = 0$$

$$R_1 < R_2 = R_3 = R_4$$

B—above resonance

$$Z_4 = R_4 + jX_4$$

$$X_4, \text{ inductive}$$

$$\theta = +45^\circ$$

$$R_1 < R_2 = R_3 = R_4 \ll R_5$$

action of the bridge by showing the voltage relations therein for two values of amplifier phase shift  $\theta$ . When  $\theta$  is zero, as in diagram A, the unbalance vector  $e$  is in phase with the generated voltage  $E$  applied to the bridge input, and thus all the vectors shown are parallel. They are displaced vertically from each other merely to clarify the drawing. The crystal is here constrained to operate at exact resonance.

In diagram B, the amplifier is assumed to have changed its phase for some reason by an amount far in excess of what would be anticipated in practice,  $\theta$  here having a value of +45 degrees. The important point to be observed is that the ratio of  $\theta$  to the resulting change in the

phase angle  $\phi$  of the crystal impedance  $Z_4$  is very large. That is, the crystal is still operating close to resonance in spite of the exaggerated change in the driving circuit. If the gain of the amplifier were greater, the action of the thermally controlled resistance would keep the amplifier output vector  $E$  practically the same in length, making the unbalance vector  $e$  correspondingly shorter. The angle  $\phi$  would therefore have to be more acute for the same value of  $\theta$ , and it follows that with increased gain the crystal is held closer to true resonance and the stability is improved.

When  $\theta$  equals zero, changes in  $|\mu|$  do not affect the crystal operating phase, but for any other small value of  $\theta$ , gain variations cause slight readjustments of the angles between vectors. The amplifier should accordingly be designed for zero phase shift, and also, of course, should have as much phase stability as possible.

In this discussion the input and output impedances of the amplifier,  $R_5$  and  $R_6$ , are assumed to be constant pure resistances. Actually, changes in the tube parameters or in certain circuit elements are likely to affect both the magnitude and the phase of these impedances. It may be shown, however, that such changes have the same effect upon the bridge and upon the frequency as do changes of about the same percentage in  $|\mu|$  or  $\theta$ ; therefore all variations in the driving circuit external to the bridge may be assumed for convenience to be represented by variations in its gain and phase.

This leniency with regard to  $R_5$  and  $R_6$  does not apply to the other bridge resistances, however.  $R_1$ ,  $R_2$ , and  $R_3$  are directly responsible for the crystal's operating phase and amplitude; they should be made as stable and as free from stray reactance as possible.

The effect of the bridge upon harmonics of the oscillation frequency is of interest. Harmonics, being far from the resonant frequency of the crystal, are passed through the bridge with little attenuation but with a phase reversal approximating 180 degrees, as illustrated by the dotted locus in Fig. 2. Thus if the amplifier were designed to cover a band broad enough to include one or more harmonics and if care were taken to avoid singing at some unwanted frequency, a considerable amount of negative feedback could be applied to the suppression of the harmonics in question.

### CIRCUIT ANALYSIS

In the following section, expressions are derived for the frequency of oscillation in terms of the gain and phase shift of the amplifier, the  $Q$  of the crystal, and values of the bridge resistances. It is assumed that the latter are constant and nonreactive, and therefore, as explained previously, that all sources of frequency fluctuations apart from

changes in the crystal itself appear as variations in  $|\mu|$  or  $\theta$ . Because the bridge oscillator does not rely upon nonlinearity in the ordinary sense to limit its amplitude, the analysis can be based reasonably on simple linear theory.

In the near vicinity of series resonance the crystal may be represented accurately by a resistance  $R_4$ , inductance  $L$ , and capacitance  $C$ , connected in series. The reactive component of the crystal's impedance is accordingly

$$X_4 = \omega L - \frac{1}{\omega C} = \frac{\omega^2 LC - 1}{\omega C}. \quad (1)$$

Solving for the frequency,

$$\begin{aligned} \omega &= \frac{X_4}{2L} + \sqrt{\left(\frac{X_4}{2L}\right)^2 + \frac{1}{LC}} \\ &= \frac{1}{\sqrt{LC}} \left[ \frac{X_4}{2} \sqrt{\frac{C}{L}} + \sqrt{1 + \left(\frac{X_4}{2} \sqrt{\frac{C}{L}}\right)^2} \right] \\ &= \frac{1}{\sqrt{LC}} \left[ 1 + \frac{X_4}{2} \sqrt{\frac{C}{L}} + \frac{1}{2} \left( \frac{X_4}{2} \sqrt{\frac{C}{L}} \right)^2 \right. \\ &\quad \left. - \frac{1}{2} \cdot \frac{1}{4} \left( \frac{X_4}{2} \sqrt{\frac{C}{L}} \right)^4 + \dots \right]. \end{aligned} \quad (2)$$

Near series resonance,  $(X_4/2) \sqrt{(C/L)} \ll 1$ . We therefore disregard powers higher than the first in the series expansion above and obtain the close approximation

$$\omega \doteq \frac{1}{\sqrt{LC}} \left[ 1 + \frac{X_4}{2} \sqrt{\frac{C}{L}} \right]. \quad (3)$$

The frequency deviation from resonance, expressed as a fraction of the resonant frequency  $f_0$ , is thus

$$\frac{f - f_0}{f_0} = \frac{\omega - \omega_0}{\omega_0} \doteq \frac{X_4}{2} \sqrt{\frac{C}{L}}, \quad (4)$$

and in the region of interest, where  $\omega L$  and  $1/\omega C$  are approximately equal,

$$\frac{f - f_0}{f_0} \doteq \frac{X_4}{2\omega L} = \frac{X_4}{2QR_4}. \quad (5)$$

Considering now the bridge circuit, and applying well-known equations,<sup>8</sup> we obtain

$$\beta = \frac{I_5 R_5}{E} = \frac{A R_4 - j B X_4}{M R_4 + j N X_4}, \quad (6)$$

in which

$$\left. \begin{aligned} A &= R_5(R_2 R_3 - R_1 R_4), \\ B &= R_1 R_4 R_5, \\ M &= (R_1 + R_2)(R_3 R_4 + R_5 R_6) + (R_3 + R_4)(R_1 R_2 + R_5 R_6) \\ &\quad + (R_5 + R_6)(R_1 R_4 + R_2 R_3) + R_5(R_1 R_3 + R_2 R_4) \\ &\quad + R_6(R_1 R_2 + R_3 R_4), \\ \text{and } N &= R_4(R_1 + R_3 + R_5)(R_2 + R_6) + R_1 R_4(R_3 + R_5). \end{aligned} \right\} \quad (7)$$

The condition for oscillation, as mentioned previously, is  $\mu\beta = 1 \angle 0$ . Putting  $\mu = \mu_1 + j\mu_2$ , we may write

$$(\mu_1 + j\mu_2) \left( \frac{A R_4 - j B X_4}{M R_4 + j N X_4} \right) = 1, \quad (8)$$

which gives the pair of equations

$$\mu_1 A R_4 + \mu_2 B X_4 - M R_4 = 0 \quad (9)$$

and

$$\mu_2 A R_4 - (\mu_1 B + N) X_4 = 0. \quad (10)$$

For the special case in which the amplifier phase shift is zero ( $\mu_2 = 0$ ), these become

$$\mu_1 = \frac{M}{A} = |\mu| \quad (11)$$

and

$$X_4 = 0. \quad (12)$$

The latter equation indicates that the frequency is then independent of changes in any of the circuit parameters except the crystal, which must operate exactly at resonance.

If the phase of  $\mu$  differs only slightly from zero, so that  $\mu_2$  is very small, then it may be inferred from continuity considerations that the frequency is still very nearly independent of all circuit parameters,

<sup>8</sup> K. S. Johnson, "Transmission Circuits for Telephonic Communication," pp. 284-285. D. Van Nostrand Company, (1925).

except of course variations in  $\theta$ , the phase of  $\mu$ . When  $\theta$  is limited to values for which  $\mu_2 BX_4 \ll \mu_1 AR_4$ , (11) still applies closely. Substitution into (10) gives

$$X_4 \doteq \frac{MR_4}{B\mu_1 + N} \cdot \frac{\mu_2}{\mu_1} \doteq \frac{MR_4\theta}{B|\mu| + N}, \quad (13)$$

and finally from (5) and (13) we obtain the frequency deviation in the form

$$\left[ \frac{f - f_0}{f_0} \right] \doteq \frac{M\theta}{2Q(B|\mu| + N)}. \quad (14)$$

As noted above, this expression applies accurately only when  $\theta$  is small, as it should be in a well-designed bridge oscillator.

The effect of variations in the amplifier may be examined by differentiating (14). For changes in  $\theta$  only,

$$\left[ \frac{df}{f_0} \right]_{\theta} \doteq \frac{M}{2Q(B|\mu| + N)} d\theta, \quad (15)$$

and for those of  $|\mu|$ ,

$$\left[ \frac{df}{f_0} \right]_{|\mu|} \doteq -\frac{BM\theta}{2Q(B|\mu| + N)^2} d|\mu|. \quad (16)$$

Equations (15) and (16) have been found to be closely in accord with experiment, although the differentiation is not rigorously allowable ( $B$ ,  $M$ , and  $N$  being only approximately constant).

In the special case where all the fixed bridge resistances ( $R_2$  to  $R_6$  inclusive) are equal, and  $|\mu|$  is large enough so that  $R_1$  has nearly the same value, (14), (15), and (16) reduce to the following:

$$\left[ \frac{f - f_0}{f_0} \right] \doteq \frac{8\theta}{Q(|\mu| + 8)}, \quad (17)$$

$$\left[ \frac{df}{f_0} \right]_{\theta} \doteq \frac{8}{Q(|\mu| + 8)} d\theta, \quad (18)$$

$$\left[ \frac{df}{f_0} \right]_{|\mu|} \doteq -\frac{8\theta}{Q(|\mu| + 8)^2} d|\mu|. \quad (19)$$

These expressions show, as did the vector diagrams, that for optimum stability the amplifier phase shift should be made approximately zero, the crystal should have as large a value of  $Q$  (as low a decrement) as possible, and the amplifier should have high gain. Linearity in the

amplifier is also desirable, to minimize the modulation effects described by Llewellyn.<sup>1</sup> When present, these effects appear as variations in  $|\mu|$  and  $\theta$ .

One of the significant differences between the bridge oscillator and other oscillator circuits is the fact that its frequency stability is roughly proportional to  $|\mu|$ . This relationship holds at least for amounts of gain that can be dealt with conveniently. Although increased gain is generally accompanied by larger variations in phase, the two are not necessarily proportional. For example, if greater stability were required for some precision application than could be achieved with a single-tube bridge oscillator, and if the constancy of the crystal itself warranted further circuit stabilization, it could be obtained by adding another stage. The phase fluctuations in the amplifier might possibly be doubled, but the value of  $|\mu|$  would be multiplied by the amplification of the added tube, giving an over-all improvement.

To illustrate the high order of stability provided by a bridge oscillator, let us consider a model composed of a single-tube amplifier and a bridge in which all the fixed resistances are made equal to that of the crystal. We shall assume the crystal to have a reasonably high<sup>4</sup>  $Q$ , of 100,000. The amplifier phase, let us say, is normally zero, but may possibly vary  $\pm 0.1$  radian ( $\pm 6$  degrees), and the value of  $|\mu|$ , nominally 400, may change  $\pm 10$  per cent. From (18) and (19) we find

$$\left[ \frac{\Delta f}{f_0} \right]_{\theta} = \pm \frac{(8)(0.1)}{(100,000)(360 + 8)} = \pm 2.17 \times 10^{-8},$$

and (when  $\theta$  has its maximum value of 0.1 radian)

$$\left[ \frac{\Delta f}{f_0} \right]_{|\mu|} = \pm \frac{(8)(0.1)(40)}{(100,000)(360 + 8)^2} = \pm 2.36 \times 10^{-9}.$$

This example represents the degree of stabilization against circuit fluctuations than can be obtained with a simple form of the oscillator operating under poorly controlled conditions. By stabilizing the power supply and other factors affecting  $|\mu|$  and  $\theta$ , and by increasing the gain, the frequency variations arising in the driving circuit may be made negligible compared to the variations found at present in the properties even of the best mounted crystals.

## EXPERIMENT

The circuit diagram of an experimental bridge-stabilized oscillator is shown in Fig. 3, and its photograph in Fig. 4. The amplifier unit

<sup>4</sup> For crystals in vacuum, values of  $Q$  as great as 300,000 have been obtained.

consists of a single high- $\mu$  tube  $V_1$  with tuned input and output transformers  $T_1$  and  $T_2$  and the usual power supply and biasing arrangements. The crystal, mounted in the cylindrical container at the left end of the panel, is one having a very low temperature coefficient of frequency at ordinary ambient temperatures. In Fig. 4 it is shown without provisions for temperature control. A high  $Q$  is obtained by clamping

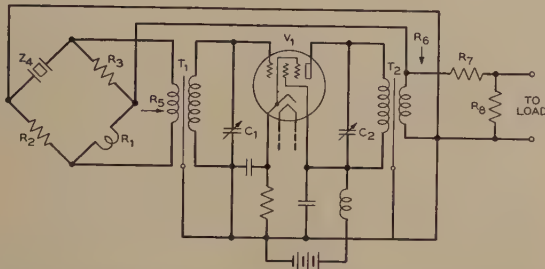


Fig. 3—Circuit of an experimental bridge oscillator.

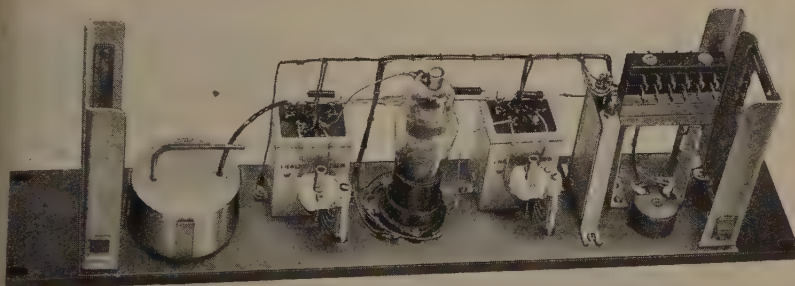


Fig. 4—Experimental bridge-stabilized oscillator without provision for temperature control.

the crystal firmly at the center of its aluminum-coated major faces between small metal electrodes ground to fit, and by evacuating the container.

Some of the circuit parameters are listed below.

$$R_1 = \text{tungsten-filament lamp}$$

$$R_2 = 100 \text{ ohms}$$

$$R_3 = 150 \text{ ohms}$$

$$Z_4 = 100\text{-kilocycle crystal}$$

$$R_4 = 114 \text{ ohms}$$

$$X_L = X_C = 11,900,000 \text{ ohms (at resonance)}$$

$$Q = 104,000$$

$R_5 = R_6 = 150$  ohms (approximately)

$R_7 = 500$  ohms

$R_8 = 200$  ohms

$|\mu| = 422$  (52.5-decibel voltage gain from  $e$  to  $E$ ).

Fig. 5 shows the resistance of the lamp  $R_1$  plotted against the power dissipated in its filament. The large rise in resistance for small amounts of power is due to the effective thermal insulation provided by the vacuum surrounding the filament and to low heat loss by radiation. The lamp operates at temperatures below its glow point, assuring an extremely long life for the filament.

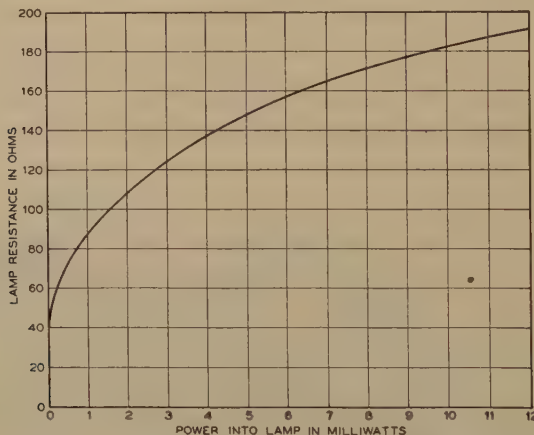


Fig. 5—Characteristic of the lamp used for  $R_1$ .

The particular value assumed by  $R_1$  in the circuit of Fig. 4 is approximately  $(R_2 R_3)/R_4 = [(100)(150)]/114 = 131.6$  ohms, and hence from Fig. 6 it follows that the power supplied to the lamp is about 3.7 milliwatts. The root-mean-square voltage across the lamp is computed to be 0.70 volt, and across the entire bridge, 1.23 volts. The power supplied to a load of 150 ohms through the pad composed of  $R_7$  and  $R_8$  is accordingly 0.22 milliwatt, or 6.6 decibels below 1 milliwatt, which is in agreement with measurements shown in Figs. 8 and 9, described below. These quantities are given to illustrate the fact that currents and voltages in this type of oscillator may be calculated readily from the values of the circuit elements, and without reference to the power-supply voltages or the tube characteristics except to assume that they give the amplifier sufficient gain to operate the bridge near balance, and that tube overloading does not occur at the operating level.

Experimental performance curves for the circuit of Fig. 4 are presented in Figs. 6 to 11 inclusive. Fig. 6 shows frequency deviation plot-

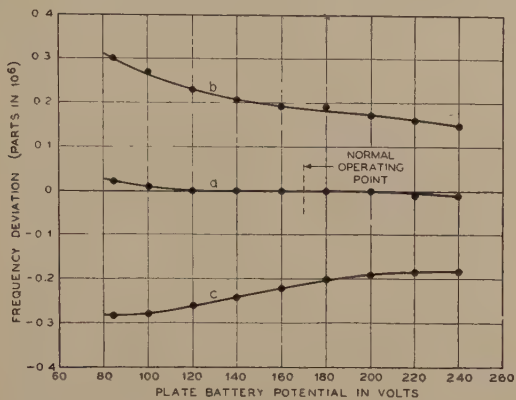


Fig. 6—Oscillator frequency versus plate-battery potential.  
 a— $C_1$  and  $C_2$  tuned for maximum amplifier gain.  
 b— $C_1$  and  $C_2$  decreased 5 per cent.  
 c— $C_1$  and  $C_2$  increased 5 per cent.

ted against plate-battery voltage for several settings of the grid- and plate-tuning condensers. For curve *a* the amplifier was adjusted at

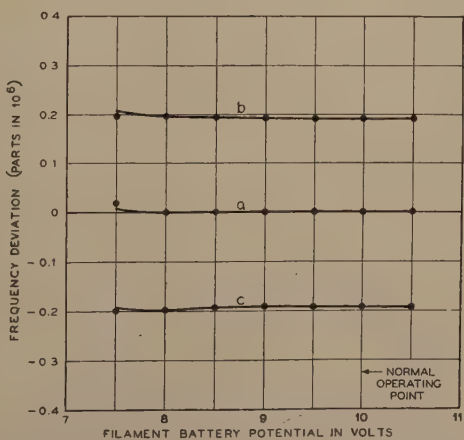


Fig. 7—Oscillator frequency versus filament-battery potential.  
 a— $C_1$  and  $C_2$  tuned for maximum amplifier gain.  
 b— $C_1$  and  $C_2$  decreased 5 per cent.  
 c— $C_1$  and  $C_2$  increased 5 per cent.

maximum gain, corresponding approximately to zero phase shift as well. Here the frequency varied not more than one part in one hundred million for a voltage range from 120 to 240 volts. Curve *b* was taken

with the two tuning capacitances  $C_1$  and  $C_2$  decreased 5 per cent from their optimum settings, and curve *c* with both capacitances increased 5 per cent. These detunings introduced phase shifts of about  $\pm 40$  degrees ( $\pm 0.70$  radian), decreased  $|\mu|$  by 0.8 decibel and changed the frequency, as shown in Fig. 6, approximately  $\pm 2$  parts in ten million.

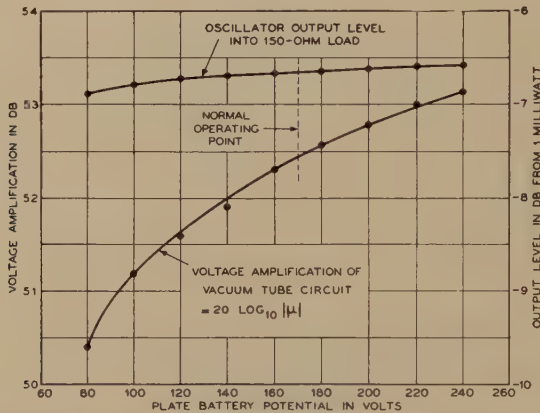


Fig. 8—Amplifier gain and oscillator output level versus plate-battery potential.

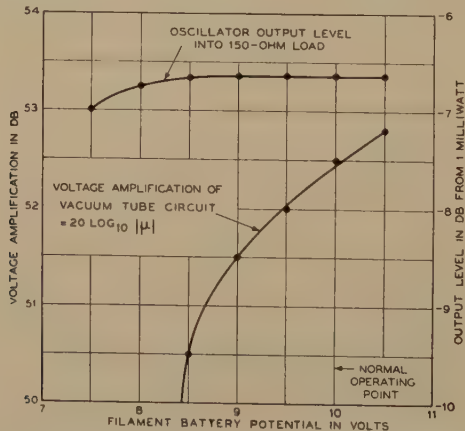


Fig. 9—Amplifier gain and oscillator output level versus filament-battery potential.

Although the analysis should not be expected to apply accurately for such large phase shifts, calculation of the frequency deviations by means of (18) gives  $\pm 1.4$  parts in ten million—in fair agreement with the experimental results. As might be expected, curves *b* and *c* show somewhat less stability with battery-voltage changes than does curve *a*.

Fig. 7 presents a similar set of curves for variations of filament voltage. Here, for the "maximum-gain" tuning adjustment, a drop from 10 volts, the normal value, to 8 volts caused less than one part in one hundred million change of frequency, as shown in curve *a*.

In Fig. 8, the gain of the amplifier and the output level of the oscillator are plotted against plate-battery voltage, while in Fig. 9 the same quantities are related to the filament potential. These curves show that although power-supply variations change the amplifier gain, they have but slight effect upon the amplitude of oscillation. This stabilization is produced, as explained heretofore, by the action of the lamp.

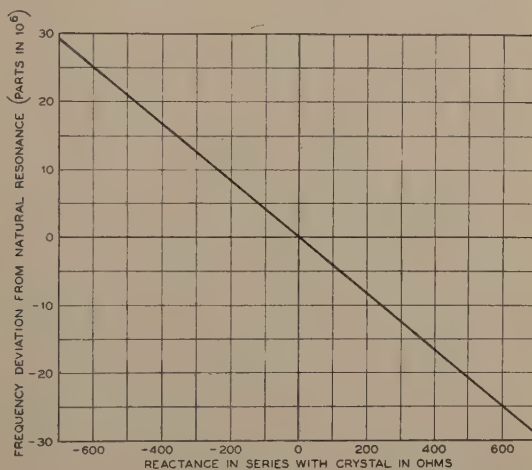


Fig. 10—Frequency of oscillator versus adjusting reactance.

The oscillator was designed to work into a load of 150 ohms, its output impedance approximately matching this value. It might be expected that variations in the magnitude or phase angle of the load would affect the frequency materially even though a certain amount of isolation is provided by  $R_7$  and  $R_8$ . However, measurements made with (1) a series of load impedances having a constant absolute magnitude of 150 ohms but with phase angles varying between -90 degrees and +90 degrees and (2) a series of resistive loads varying between 30 ohms and open circuit, showed less than one part in a hundred million frequency variation. Graphs of these results have not been included, since they practically coincide with the axis of zero frequency deviation.

The tuned transformers  $T_1$  and  $T_2$  in this experimental model precluded the suppression of harmonics by negative feedback,  $|\mu|$  being small at the harmonic frequencies. The tuning itself provided sup-

pression, however, so that the measured levels of the second and third harmonics in the output current were, respectively, 67 and 80 decibels below that of the fundamental. This purity of wave form is of course largely dependent upon the absence of overloading.

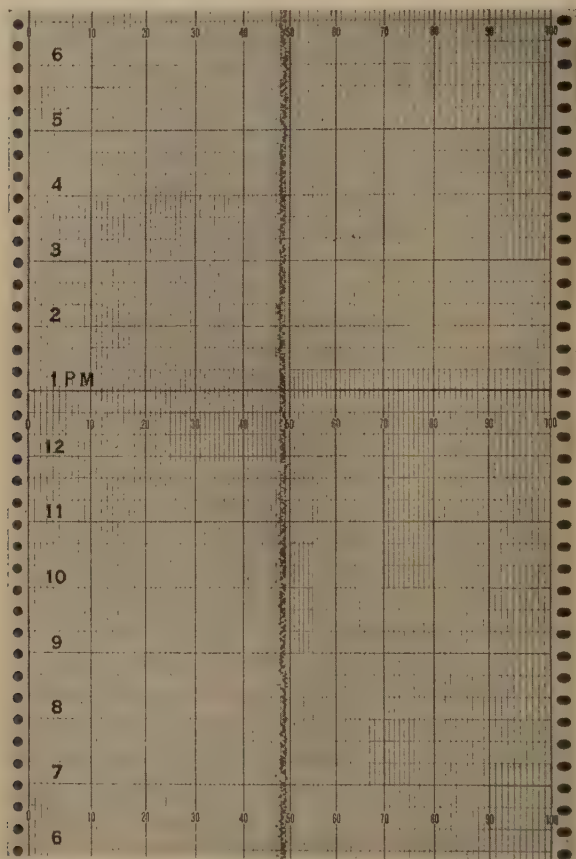


Fig. 11—Record of frequency comparison between two bridge-stabilized oscillators. Full scale one part in a million. Variations less than  $\pm 2$  parts in one hundred million.

To correct any small initial frequency error of the crystal and to allow for subsequent aging, a small reactance connected directly in series with the crystal provides a convenient means of adjusting the frequency as precisely as it is known. This added reactance may be considered as modifying either of the reactances in the equivalent series-resonant circuit of the crystal. Fig. 10 shows that for a small range of frequencies the change introduced in this manner is accurately

proportional to the added reactance. Series inductance, of course, lowers the frequency, while series capacitance raises it. The stability requirement imposed on the adjusting reactance is only moderate, for its total effect upon the frequency should not be more than a few parts in a million.

The frequency measurements here presented were obtained using apparatus similar in principle to the frequency-comparison equipment of the National Bureau of Standards.<sup>5</sup> Frequency differences between the oscillator under test and a reference bridge oscillator were read upon a linear scale calibrated directly in terms of frequency deviation. Full scale could be made one part in  $10^4$ ,  $10^5$ ,  $10^6$ , or  $10^7$  by means of a simple switching operation. For most of the measurements in this paper the full-scale reading was one part in a million, and the resolution about  $\pm 0.005$  part in a million.

By using a recording meter with this measuring set, continuous frequency comparisons between two independent bridge oscillators were obtained over a period of several months. Fig. 11 is a photograph of a section of this record. It shows the short-time variations of both oscillators plus a small amount of scattering caused by the measuring equipment itself. The crystals were temperature controlled in separate ovens, and the power was supplied from separate sets of laboratory batteries controlled to about  $\pm 2$  per cent in voltage. Shielding was ample to avoid any tendency to lock in step.

In addition to these small short-time variations, the oscillators exhibited a very slow upward drift in frequency, attributed to aging of the mounted crystals. This aging decreased in a regular manner with time, the mean drift of one of the crystals being less than one part in ten million per month after three months of continuous operation, and about a third of this amount after seven months. In most applications, gradual frequency drift is not objectionable even though the required accuracy is very high, for readjustment is merely a matter of setting a calibrated dial.

#### APPLICATION

The bridge-stabilized oscillator promises to become a useful tool in many commercial fields as well as in certain purely scientific problems, such as time determination and physical and astronomical measurement. It may be used either to increase the frequency precision in applications where operating conditions are accurately controlled, or

<sup>5</sup> E. G. Lapham, "A harmonic method of intercomparing the oscillators of the national standard of radio frequency," *Nat. Bur. Stand. Jour. Res.*, vol. 17, pp. 491-496; October, (1936); *PROC. I.R.E.*, vol. 24, pp. 1495-1500; November, (1936).

else to make such control unnecessary, affording high stability in spite of unfavorable conditions.

An interesting application in the field of geophysics has already been made in the form of a "crystal chronometer." This chronometer consists of a single-tube bridge oscillator, a frequency-dividing circuit, and a synchronous timing motor. It was recently loaned by the Bell Telephone Laboratories to the American Geophysical Union and was used with the Meinesz gravity-measuring equipment on a submarine gravity-survey expedition in the West Indies. Although operating under somewhat adverse conditions of power supply, temperature, and vibration, it was reported<sup>6,7</sup> to be more stable than any timing device previously available, errors in the gravity measurements introduced by the chronometer being negligibly small.

<sup>6</sup> M. Ewing, "Gravity measurements on the U. S. S. Barracuda," *Trans. Amer. Geophys. Union*, part I, pp. 66-69, (1937).

<sup>7</sup> A. J. Hoskinson, "Crystal chronometer time in gravity surveys," *Trans. Amer. Geophys. Union*, part I, pp. 77-79, (1937).

## CHARACTERISTICS OF THE IONOSPHERE AT WASHINGTON, D. C., AUGUST, 1938\*

BY

T. R. GILLILAND, S. S. KIRBY, AND N. SMITH

(National Bureau of Standards, Washington, D. C.)

**G**RAPHS of the critical frequencies and virtual heights of the ionosphere layers during August, 1938, are given in Fig. 1.

Fig. 2 shows the maximum frequencies which could be used for radio sky-wave communication by way of the F, F<sub>2</sub>, F<sub>1</sub>, and normal E

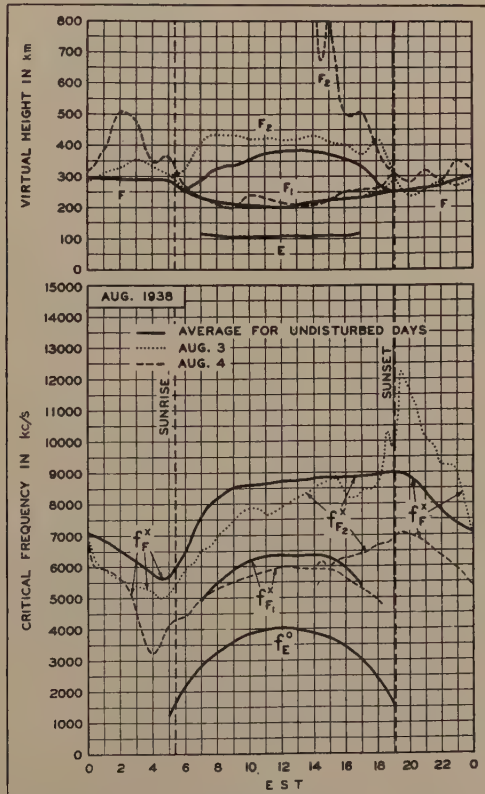


Fig. 1—Virtual heights and critical frequencies of the ionosphere layers, August, 1938.

\* Decimal classification: R113.61. Original manuscript received by the Institute, September 13, 1938. These reports have appeared monthly starting in vol. 25, September, (1937). See also vol. 25, pp. 823-840, July, (1937). Publication approved by the Director of the National Bureau of Standards of the U. S. Department of Commerce.

layers, at the latitude of Washington. As in June and July, the flatness of the graphs indicates very little change in maximum usable frequencies from day to night. The curves of critical frequency and maximum usable frequency were still of the summer type, and resembled those for June and July, although slightly higher.

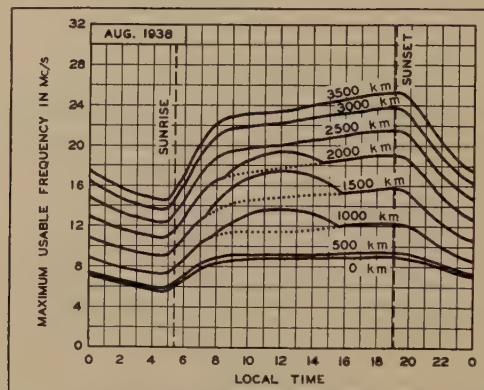


Fig. 2—Maximum usable frequencies for radio sky-wave transmission, averages for August, 1938, for undisturbed days, for dependable transmission by the regular ionosphere layers. The values shown were considerably exceeded during irregular periods by reflections from patches of sporadic E layer. For distances of 1000, 1500, and 2000 kilometers, the dotted portions of the graphs represent maximum usable frequencies for F<sub>2</sub>-layer transmission, when these were less than those determined by the E layer.

Sporadic-E reflections were still observed on many occasions at irregular intervals, but were not nearly as prevalent as during June and July. These reflections often caused the maximum usable frequency,

TABLE I  
IONOSPHERE STORMS (APPROXIMATELY IN ORDER OF SEVERITY)

Date and hour, E.S.T.	$h_F$ before sunrise, km	Minimum $f_F^S$ before sunrise, kc	Noon $f_F^S$ , kc	Magnetic character <sup>1</sup>		Iono- sphere character <sup>2</sup>
				00-12 G.M.T.	12-24 G.M.T.	
August						
{ 3 (after 1700)	—	—	—	0.3	1.3	2
4	406	3300	<5900	1.6	0.9	2
5	360	4600	6500	0.9	0.7	1
6 (until 0900)	314	4600	—	0.5	0.1	½
{ 11 (after 0200)	322	4600	about 6000	1.2	1.3	1½
{ 12 (until 0600)	344	4300	—	0.7	0.5	1½
{ 23 (after 0400)	—	4400	6100	1.1	0.7	1
{ 24 (until 0500)	296	4900	—	0.2	0.6	½
{ 2 (after 0200)	314	4800	6300	0.9	0.5	½
{ 3 (until 0800)	326	5000	—	0.3	1.3	½
Average for un- disturbed days	293	5710	8740	0.2	0.2	0

<sup>1</sup> American magnetic character figure, based on observations of seven observatories.

<sup>2</sup> An estimate of the severity of the ionosphere storm at Washington on an arbitrary scale of 0, 1, 1½, and 2, the character 2 representing the most severe disturbance.

for distances up to 2000 kilometers, to exceed greatly the values given in Fig. 2. Because of their erratic occurrence they could not be included in the graphs; data are given in Table IV.

While there were a fair number of ionosphere storms (Table I) in August, there were unusually few sudden ionosphere disturbances or fade-outs (Table II). This lends weight to the idea that ionosphere

TABLE II  
SUDDEN IONOSPHERE DISTURBANCES

Date	G.M.T.			Location of transmitter	Remarks	Minimum <sup>1</sup> relative intensity
	Beginning of fade-out	Beginning of recovery	Recovery complete			
Aug. 14	1748	1800	1820	Ontario, Mass., D. C.	Terr. mag. pulse	0.0
Aug. 15	1410	—	1420	Ontario, Mass.	—	0.1
Aug. 31	1719	1750	1820	Ontario, Mass., D. C.	Terr. mag. pulse	0.0

<sup>1</sup> Ratio of received intensity during fade-out to average intensity before and after, for station CFRS, 6070 kilocycles, 600 kilometers distant.

storms and sudden ionosphere disturbances are not closely related except that both are manifestations of a general irregular solar activity.

Data on the degree of departure of values on individual days from

TABLE III  
CRITICAL-FREQUENCY VARIATION FOR 744 HOURS OF OBSERVATION

Per cent	-40	-30	-20	-10	-0	+0	+10	+20
Number of hours	1	23	78	187	432	312	64	4
Disturbed hours	1	23	78	122	139	8	5	3
Undisturbed hours	0	0	0	65	293	304	59	1

TABLE IV

SPORADIC E. APPROXIMATE UPPER LIMIT OF FREQUENCY OF THE STRONGER SPORADIC-E REFLECTIONS AT VERTICAL INCIDENCE  
Midnight to Noon

Date	Hour, E.S.T.											
	00	01	02	03	04	05	06	07	08	09	10	11
August 1	8	4.5			8	6		4.5	6	8	4.5	4.5
3								4.5	4.5	6	6	6
8	4.5	4.5	4.5		8	4.5	8	6	6	6	8	4.5
9	8	4.5	4.5		8	4.5		4.5	4.5	(10)	4.5	4.5
13								4.5	6	4.5	8	6
20					6	6	4.5	4.5	6	4.5	6	6

Noon to Midnight

Date	Hour, E.S.T.											
	12	13	14	15	16	17	18	19	20	21	22	23
August 8								4.5	4.5	8	8	8
9								8	8	6	8	8
11								8	8	4.5	8	8
12								8	8	8	8	8
13	4.5	4.5					4.5	4.5	8	8	4.5	
20							4.5	4.5	8	8	4.5	

the averages in Figs. 1 and 2 are given in Table III. It gives the number of hours the  $f_F^x$  and  $f_{F_2}^x$  differed from the average for undisturbed days by more than the percentage indicated.

The days during which sporadic E-layer reflections were most prevalent at Washington are listed in Table IV. The table shows the approximate upper limits of frequency at which strong sporadic E-layer reflections were observed at the hours listed. The observations were nearly continuous at 4.5, 6, 8, and 10 megacycles. When the frequency is given as (10), this value may have been considerably exceeded.

**DISCUSSION ON "SINGLE-SIDE-BAND TELEPHONY APPLIED TO THE  
RADIO-LINK BETWEEN THE NETHERLANDS AND THE  
NETHERLANDS EAST INDIES"\***

N. KOOMANS

**H. J. J. M. de Bellescize:**<sup>1</sup> Mr. Koomans discloses a method for controlling at the receiver the frequency relation of the heterodyne and carrier (or pilot) waves, whereby the final carrier frequency is fixed at ten kilocycles.

As explained in the paper, a single frequency correcting influence, directed to neutralize both Doppler effect and large frequency drifts, would, when momentarily disappearing through fading, expose the heterodyne and final carrier frequencies to undue variations; moreover, the tuning of the heterodyne oscillators ought to be readjusted every time the regulating voltage returns.

These drawbacks are partly nullified by permanently keeping the regulation voltage as small as possible; for this purpose, two frequency correcting influences are applied together to the local oscillators, one of them being exclusively intended for the more rapid variations, and the other for the variations of longer duration. The rapid influence is performed through purely electrical means, whereas the progressive influence is effected mechanically, thus preventing going off frequency in case fading should affect the pilot signal.

All the above explanations and means may be read in my previous patents and publications, for instance:

"La Synchronisation des Courants de Haute Fréquence," *Bulletin de la Société Francaise des Electriciens*, no. 31, p. 709-713; July, (1933).

"Les Communications Radio-Electriques," *Gauthier-Villars, Editors*, pp. 28-136; Chap. III; copyright by H. de Bellescize, (1936).

U. S. A. patent No. 1,990,428.

Discussion sur "La Transmission radiotéléphonique à Ondes courtes à bande latérale unique," of *Bulletin de la Société Francaise des Electriciens*, no. 27, p. 313-315, March, (1933). As in the present case, this discussion related to single-band telephony with, at the receiver, a regulating voltage derived through the same means from a pilot wave.

As told by Mr. Koomans, the maximum speed allowable to the rapid controlling influence is limited by the band width of the filter selecting the carrier or pilot wave, and by requirements concerning the quality and hunting. But I think that a speed of 50 cycles per second (maximum correction:  $7000 = 2 \times 3500$  cycles; time constant: 70 seconds) would be considerably too large in the case of broadcasting, where the filter selecting the carrier wave must eliminate closely adjacent components, for instance those of the organ or violoncello. My own practice, disclosed in my publications and grounded on several years of homodyne reception, consists in relying on the perfect drift neutralization ensured by the slower acting influence for limiting the frequency correction of the relatively rapid influence to the value strictly required by the Doppler effect and other small frequency fluctuations; it is needless and even harmful to supply this rapid influence with a speed enabling it to follow closely the very quick steps frequently caused in the phase of the carrier or pilot wave by the selective

\* Proc. I.R.E., vol. 26, pp. 182-206; February, (1938).

<sup>1</sup> Neuilly, Seine, France.

fading. Thus, the synchronizing system is freed from the pendular oscillations which could proceed from the side components and, moreover, it enjoys the best protection against static; the importance of this last result is linked to the necessity of weakening the carrier or pilot wave at the transmitter to save energy.

*Comparative Analysis of the systems disclosed by H. de Bellescize and N. Koomans.*

N. Koomans: PROCEEDINGS OF THE INSTITUTE OF RADIO ENGINEERS, pp. 196-197 and 202-203; February, (1938).

- de Bellescize: I. *Onde Electrique*, pp. 240-245; June and July, (1932).  
 II. *Bulletin de la Société Française des Electriciens*, no. 27, pp. 313-315; March, (1933).  
 III. *Bulletin de la Société Française des Electriciens*, no. 31, pp. 710-713; July, (1933).  
 IV. *Les Communications Radio-Electriques*, pp. 128-136; (copyright 1936).  
 V. U.S.A. patent No. 1,990,428.

Koo-mans	de Bellescize				
	I	II	III	IV	V
With a single controlling influence:					
(a) If the pilot wave disappears through fading, the heterodyne frequency will undergo undue variations.	p. 196	p. 313-314	p.	p. 128	
(b) The heterodyne must be readjusted every time the regulating voltage returns.	196	240		128	
These drawbacks may be nullified by keeping the regulating voltage as small as possible.	197	244	314	713	132
This is obtained by the co-operative action of two frequency controlling influences, the one exclusively directed to neutralize the more rapid variations, the other to neutralize the variations of larger duration.	197	243-244	315	710-713	130-131
The more rapid influence is performed through purely electrical means; the slower one is effected mechanically, which prevents the going off frequency in case fading should affect the pilot signal.	197, 202	243-244	314	710-713	130, 132
The mechanical device of de Bellescize is equivalent to the readjustment of a tuning condenser, as performed by Koomans.	202-203			712-713	
The slower influence is applied to the heterodyne oscillator of higher frequency.	197				Fig. 7

N. Koomans:<sup>2</sup> The remarks of Mr. de Bellescize, concerning the drawbacks of a frequency correction with too high a speed correspond completely with our own experience expressed on page 196. There is not the least difference in opinion on this point. The trouble caused by the absence of the pilot signal through fading, is overcome for a good deal by amplifying and limiting the pilot signal.

<sup>2</sup> Netherlands Telegraph Administration, s'Gravenhage, The Netherlands.

The figure of fifty cycles per second, given by Mr. de Bellescize for the speed of frequency correction should only occur in the case that the second heterodyne is detuned 3500 cycles by the regulating voltage. The figure  $7000 = 2 \times 3500$  is only given in our paper to show the maximum adjusting range of the second heterodyne. In practice, that is to say, operating with the mechanically adjusted first heterodyne switched on, or with a crystal oscillator, the detuning of the second heterodyne, caused by the regulating voltage never exceeds fifty cycles, so the speed of frequency regulation is always less than one cycle per second. The mid-zero instrument showing the strength and sign of the regulating voltage (Fig. 5) has full-scale deflection for a voltage corresponding to a detuning of fifty cycles and the meter normally shows a deflection of no more than approximately one fifth of the scale.

## BOOKLETS, CATALOGS, AND PAMPHLETS RECEIVED

The following commercial publications of radio engineering interest have been received by the Institute. You can obtain a copy of any item without charge by addressing the issuing company and mentioning your affiliation with the Institute of Radio Engineers.

**ANTENNA COUPLING UNITS** • • • *Victor J. Andrew, 6429 S. Laverne Avenue, Chicago, Ill.* Bulletin 87, 2 pages,  $8\frac{1}{2} \times 11$  inches. Describes units for coupling a coaxial transmission line to a vertical radiator in a point between 500 and 3000 cycles, series or shunt excitation.

**INSTRUMENTS** • • • *General Radio Company, 30 State Street, Cambridge, Mass.* *Experimenter for August-September*, 8 pages,  $6 \times 9\frac{1}{2}$  inches, printed. Uses of a vacuum tube voltmeter for R-F current measurement and application of variable condensers with logarithmic angle frequency characteristics are described.

**INSTRUMENTS** • • • *H. W. Sullivan, Ltd., Leo Street, London, S.E. 15, England*. 1938 Catalog, 196 pages + cover,  $7\frac{1}{4} \times 9\frac{1}{2}$  inches, printed. Complete descriptions of the Sullivan Line of testing and measuring apparatus for communication engineering.

**MOLDING MATERIAL** • • • *Bakelite Corporation, 247 Park Avenue, New York, N.Y.* Bulletin 1513-B, 4 pages,  $8\frac{1}{2} \times 11$  inches, printed. Electrical, physical and chemical characteristics of a new thermo plastic material for injection and compression molding is described.

**NICKEL ALLOY** • • • *International Nickel Company, 67 Wall Street, New York, N.Y.* Nickelsworth for the third quarter of 1938, 8 pages,  $8\frac{1}{2} \times 11$  inches, printed. Summarizes mechanical characteristics of "Z" nickel which combines corrosion resisting properties of nickel with mechanical properties of heat-treated steel.

**PARTS** • • • *Wholesale Radio Service Company, Inc., 100 Sixth Avenue, New York, N.Y.* Catalog No. 78, 184 pages + cover,  $7 \times 10$  inches, printed. The 1939 edition of this company's general catalog.

**PHOTOC CELLS** • • • *G-M Laboratories, Inc., 1731-M Belmont Avenue, Chicago, Ill.* Bulletin No. CS604, 2 pages,  $8\frac{1}{2} \times 11$  inches, lithographed. Electrical, mechanical and optical characteristics of two new photoelectric cells of the barrier-layer type are given.

**ROTARY SWITCHES** • • • *Roller-Smith Company, 233 Broadway, New York, N.Y.* Catalog No. 9, 12 pages,  $8\frac{1}{2} \times 11$  inches, lithographed. This catalog lists and gives mechanical and electrical specifications on the Type R-2 instrument and control switches.

**SERVICE INSTRUMENTS** • • • *Service Instruments, Inc., 404 Fourth Avenue, New York, N.Y.* Bulletin,  $6 \times 9$  inches, 16 pages, printed. Describes the operation and use of the Rider chanalyst, a new instrument for running down faults in radio receivers.

**TUBE DATA** • • • *RCA Manufacturing Company, Inc., Harrison, N.J.* Application Notes,  $8\frac{1}{2} \times 10\frac{1}{2}$ . No. 95, "On Operating Positions of Receiving Tubes," and No. 96, "On a Voltage Regulator for D-C Power Supplies."

CONTRIBUTORS TO THIS ISSUE

**Chu, Wentworth:** Born 1901 at Kiangsu, China. Graduated National Chiao Tung University, Shanghai, 1923; received Ph.D. degree, Harvard University, 1926. Professor of physics and electrical engineering, National Chung San University, Canton, 1926-1930; professor of physics and electrical engineering, National Chiao Tung University, Tong San Branch, 1930-1933; professor of physics, National Peking University 1933 to date. Nonmember, Institute of Radio Engineers.

**Chang, Chung-Kuei:** Born 1901 at Hopei, China. Received B.S. degree, National Peking University, 1924. Instructor in physics, National Peking University, 1928-1937. Graduate student, Stanford University, 1937 to date. Nonmember, Institute of Radio Engineers.

**Diamond, H.:** Born 1900 at Quincy, Massachusetts. Received B.S. degree, Massachusetts Institute of Technology, 1922; M.S. degree, Lehigh University, 1925. Engaged in research work in mechanical engineering, General Electric Company, 1922-1923; instructor in electrical engineering, Lehigh University, 1923-1927; associate radio engineer, National Bureau of Standards, 1927-1928; radio engineer, 1929; senior radio engineer, 1930-1935; principal radio physicist, 1936 to date. In charge of development of radio aids to aviation, 1928-1934, and of ultra-high-frequency research, including radio meteorography, 1934 to date. Member, Washington Academy of Sciences and Washington Philosophical Society. Associate member, Institute of Radio Engineers, 1926; Member, 1930.

**Dunmore, F. W.:** Born January 24, 1891, at Haverhill, Massachusetts. Commercial radio operator, summers, 1911-1913. Received B.S. degree, Pennsylvania State College, 1915. Student engineering course, General Electric Company, 1915-1917; research department, American Radio and Research Corporation, 1918. Member of staff, National Bureau of Standards, specializing in research work on direction finders, directional transmission, ultra-high-radio-frequency transmitters and receivers, radio aids to air navigation, and radio meteorographs, 1918 to date, senior radio engineer, radio section, National Bureau of Standards, 1936 to date. Nonmember, Institute of Radio Engineers.

**Hinman, Wilbur S., Jr.:** Received B.S. degree in electrical engineering, Virginia Military Institute, 1926. Westinghouse Electric and Manufacturing Company, 1926-1928; radio engineering, National Bureau of Standards, 1928 to date, aeronautical radio research, 1928-1935; radio meteorograph development, 1935 to date. Nonmember, Institute of Radio Engineers.

**Gilliland, T. R.:** See PROCEEDINGS for January, 1938.

**Kirby, S. S.:** See PROCEEDINGS for January, 1938.

**Meacham, Larned A.**: Born September 3, 1908, at Denver, Colorado. Received B.S. degree in electrical engineering, University of Washington, 1929. Certificate of Research, Cambridge University, England, 1930. Member of technical staff, Bell Telephone Laboratories, Inc., 1930 to date. Associate member, Sigma Xi; Member, Tau Beta Pi and Phi Beta Kappa. Associate member Institute of Radio Engineers, 1938.

**Smith, N.**: See PROCEEDINGS for January, 1938.

